Salt marshes: habitat suitability and flood hazard reduction effectiveness

MSc. Thesis

M.A. (Marco) Mendoza Viteri

Technische Universiteit Delft

TU Delft

Salt marshes: habitat suitability and flood hazard reduction effectiveness

MSc. Thesis

by

M.A. (Marco) Mendoza Viteri

to obtain the degree of Master of Science

at the Delft University of Technology

to be defended publicly on Wednesday January 27, 2021 at 14:30 PM.

Student number:	4726073	
Thesis committee:	Prof. dr. ir. S.G.J. Aarninkhof	TU Delft (chairman)
	Dr. ir. V. Vuik	TU Delft (supervisor)
	Dr. ir. A.P. Luijendijk	TU Delft/Deltares
	Dr. ir. B.C. van Prooijen	TU Delft

An electronic version of this thesis is available at `http://repository.tudelft.nl/`.

Cover: Salt marsh edge subjected to a flooding event. Photo retrieved from www.nioz.nl and captured by Zhenchang Zhu.

TU Delft Delft University of Technology

Preface

This document represents the final milestone to finalize the Master of Science program in Hydraulic Engineering at the Delft University of Technology, as well as the end of a personal journey that started some five years ago.

I would like to thank my graduation committee for all the input they gave me throughout the execution of this thesis. Vincent, you have been incredibly supportive and enthusiastic from the first day until the last one. Your constant (weekly, actually) guidance and advise during these unusual times were invaluable to me, and I am truly grateful to have had you as my supervisor. Arjen, your early input and questioning of the topic helped steer the scope of this research into what it eventually became. I'll never forget your highly critical comments given during our first meetings. Bram, even though you 'jumped in' as the last piece of this committee in a later stage of the process, the knowledge you brought along shed the necessary light onto one of the main topics of this topic. Hopefully this document serves you for future in-depth MSc's, just as you have suggested. And Stefan, in all of our meetings you have presented a broader perspective than the one I was bringing forward, which helped me address the final aim of this research.

This thesis, and the overall journey over the past two years, would have not been possible without people who I can very proudly call my friends. I have been lucky to count with them for several - and very much necessary - study breaks, whether from a close distance (over a drink) here in the Netherlands, or from afar (still over a drink) in Ecuador through a video call. Mayra, Tess, Vesna, Noor, Haisam, Fernando, Chris, Andrés, Sebastián, Carlos, Jeroen, and Marnix: thank you all.

Last, but certainly not the least, I'd like to thank my family who has been a never-ending source of encouragement, support and joy some 9800 km away from what has been my home since August 2018. Sergio and Isabel, thank you for your constant content sharing, without which I could not laugh as much. And to my parents, Julio and Josa, I will be forever grateful to you for always encouraging me to pursue my personal and professional goals. This journey would have been a completely different one without our countless hour-lasting conversations over the phone. I am forever grateful to all, and the best is yet to come.

M.A. (Marco) Mendoza Viteri
Delft, January 2021

Summary

In recent years, nature-based solutions have gained recognition for their capacity to reduce flood hazard on coastal communities. These coastal threats range from waves and tides, to future storm variability and predicted sea level rise. Vegetated foreshores are one of the measures that fall under this palette of solutions, and are the focus of this thesis. While vegetated foreshores can be colonized by several plant species (mainly mangroves or marshes), this thesis presents the study of phenomena occurring at salt marshes in an attempt to determine which are relevant indicators that can predict the presence or absence of this ecosystem at a given location. Moreover, the wave height attenuation capacity of such vegetated foreshores under different conditions is also assessed for different effectiveness indicators, in a way the provides insight into whether this habitat is not just feasible, but also effective as a coastal protection measure, with respect to wave height attenuation.

The study is divided into two main sections, characterized by different methodologies: one treating the habitat suitability and one addressing the effectiveness with respect to wave height attenuation rates. The habitat suitability chapter evaluated daily conditions occurring during the months of Aprl-July (2020) at 28 different sites located within two water systems in The Netherlands: the Western Scheldt and the Wadden Sea. Locations were characterized by mature salt marshes, emerging salt marshes (patches of vegetation), bare intertidal fringing flats, and intertidal shoals. The assessment was performed through numerical modelling of occurring water levels (inundation-free periods), flow velocities, waves, and excess wave-induced bed-shear stresses. Additionally, boundary conditions were affected in the model used to determine flow velocities in the Western Scheldt in order to simulate storm conditions.

Results from the habitat suitability analysis suggest that within a water system with similar sediment composition, inundation-free period and daily-occurring hydrodynamics, such as flow velocities and wave height, can explain the presence/absence of vegetation at most sites, while storm conditions can be the determining condition for vegetation absence in other locations. However, a generalization of these findings was not possible between the two water systems, which was likely due to the several differences found between them. This occurrence led to the introduction of the dimensionless wave-induced excess bed-shear stress factor, where positive values indicate sediment re-suspension (erosion). Final results suggest that at sites across both water systems where this dimensionless factor exceeded the 2.5, 4.2 and 5.3 values at 10%, 1%, and 0.1% of the assessed time, respectively, were indeed non-vegetated sites. Furthermore, these conclusions indicate the occurrence of sediment re-suspension during approximately 20% of the assessed time, at the most, in the most energetic vegetated sites (Western Scheldt), and as little as 1% in the least energetic locations (Wadden Sea). This analysis shows that a generalization of habitat suitability indicators has to include both external loading and bed resistance, providing initial values for excess bed-shear stress occurrence.

The wave attenuation effectiveness assessment was likewise performed by numerical modelling of waves propagating over a vegetated field, under different imposed boundary conditions. This assessment, assisted by the spectral wave model SWAN, covered indicators such as relative vegetation height (h_v/h), wave height to water depth ratio (H/h) and tidal regime. Imposed boundary conditions consisted of deep ($kh > 3.0$) to shallow water ($kh > 0.3$) conditions, as well as characteristic values described as 'Exposed coast, local wind waves' ($H_s = 1.0m$; $T_p = 4.0s$); 'Exposed coast, swell waves' ($H_s = 1.0m$; $T_p = 12.0s$); and 'Sheltered coast, local wind waves' ($H_s = 0.5m$; $T_p = 4.0s$). Moreover, different surge levels and tidal regimes with characteristic amplitudes were included so as to account for different water depths over the foreshore (micro = 0.5 m; meso = 1.5 m; and macro = 2.5 m).

From this assessment, considerations for tidal regime, surge height, and type of wave forcing were used to determine the degree of effectiveness of salt marshes in the studied water systems, while defining effectiveness in terms relative to a mudflat located at MSL. Output of the simulations suggests that salt marshes that develop in macro tidal sites, like in the Western Scheldt, can dissipate more wave energy than habitats located in micro or meso tidal areas, such as the Wadden Sea. This is due to the fact that foreshores accrete at higher

elevations with respect to MSL, due to sediment deposition on higher levels occurring during MHWS. On the other hand, results treating the different wave loads (swell waves, sheltered locally wind-generated waves, and exposed wind-generated waves) further indicates that greater wave height attenuation may be achieved in sheltered coastal locations such as the Western Scheldt estuary; which is is due to the fact that longer swell waves are dissipated by other mechanisms (such as wave breaking and bottom friction), while shorter waves can be largely be dissipated by the vegetated foreshore itself. This observation suggests that introduction of this system as a flood protection measure may be more effective in sheltered than in exposed coastal areas.

Finally, the set of conclusions provided by both sections proposed generally applicable indicators that may serve to determine whether an arbitrary location is capable of hosting salt marsh vegetation as a flood defense measure, as well as the effectiveness of such nature-based solution with respect to wave height attenuation. The elaboration of an assessment tool was not achieved in this thesis; however, in order to perform a quick check for salt marsh introduction as an effective flood defense measure at a given site, results indicate the gathering of necessary data such as bed level elevations - for inundation-free period analysis - as well as occurring hydrodynamic forcing and sediment properties at such arbitrary site (excess bed shear stress determination, evaluated with the previously proposed limits). With respect to the degree of wave height reduction effectiveness, the determination of the occurring tidal regime, design surge heights, and considerations of sheltered/exposed coastal conditions may serve as a first estimate for this purpose.

Contents

List of Figures

List of Tables

1 Introduction

1.1. Problem description

Coastal populations are constantly exposed to the risk of flooding due to their proximity to the sea and hence to permanent hydrodynamic forcing exerted by waves, storm surge, and tides. In addition, future storm variability, sea-level rise and shoreline change are factors that enhance these coastal hazards (Woodruff et al., 2013). For instance, it has been determined that 24% of the world's sandy beaches are experiencing erosion, either by natural processes or by human activity (Luijendijk et al., 2018).

Due to these coastal threats, many different types of measures have been undertaken in order to reduce the risk of flooding, while defining flood risk as a function of the hazard, the exposure, and vulnerability of the exposed community (UNDRR, 2016). Flood hazard is typically characterized by the aforementioned (daily or future) phenomena; whereas exposure and vulnerability are more related to socio-economical factors (assets exposed to likely damage and the capacity of society to deal with the event). Civil engineering practices largely target the reduction - or elimination - of the hazard itself. In general terms, flood hazard reduction measures can be summarized into structural and non-structural (Dodo et al., 1985). Typical structural measures include rouble mound breakwaters, seawalls, groynes, and other similar so-called 'hard' interventions; while non-structural measures include land use zoning, evacuation strategies, the use of green infrastructure, and nature-based coastal defenses, also referred to as 'soft' interventions.

Amongst such 'soft' interventions, nature-based coastal defenses have proven to be an appealing alternative. When compared with traditional 'hard' coastal defenses, they can be more cost-effective under certain conditions (Narayan et al., 2016), improve the surrounding ecosystem's functioning, and are generally more adaptable to changing conditions i.e. sea level rise (van der Nat et al., 2016). Ecosystems that fall under this category of nature-based defenses, are e.g. coral reefs, salt marshes, mangrove forests, sand dunes, beach nourishments, and several others. Studies regarding the behavior of these ecosystems have made it possible to better understand their response under daily and extreme conditions, as well as to determine their effectiveness as flood hazard reduction measures.

Even though the flood hazard mitigation characteristics of these 'soft' interventions have been researched and established in several previous studies, as gathered by Narayan et al. (2016), there exists a knowledge gap regarding which site-specific conditions can determine the introduction of these measures as an effective flood protection solution. There is the need to establish general feasibility indicators that are able to predict to what extent these measures are viable and effective at an arbitrary location. With such indicators - both for habitat suitability and flood hazard reduction effectiveness - at hand, they may serve as an effective tool at a decision-making level, where a coastal protection solution is required.

However diverse these nature-based solutions are, this thesis is focused exclusively on salt marsh-vegetated foreshores. Furthermore, the physical feasibility (habitat suitability) of the salt marshes will be assessed, leaving a cost-benefit feasibility analysis for further research.

1.2. Aim of research

The aim of this thesis is to quantitatively determine limit values of various habitat suitability indicators for salt marsh ecosystems, as well as the degree of effectiveness, regarding the flood hazard reduction capacity, of salt marsh-foreshore systems under varying conditions. The method is based on numerical modelling of phenomena occurring at observation sites located in salt marsh-rich water systems, through readily available open source data providing hydrodynamic and atmospheric conditions in the proximity of such sites. In some cases, numerical modelling is performed for idealized scenarios (next section).

The following research questions will address the previously described purpose of this thesis:

1. Based on site-specific conditions, can general threshold values be given to salt marsh habitat suitability indicators?
2. To which degree are different characteristics of salt marsh-foreshore systems effective regarding their flood hazard reduction capacity?
3. Can the previously assessed indicators and limit values serve as an assessment tool for salt marsh habitat introduction as a flood hazard reduction measure?

1.3. Methodology

This thesis is divided into two sections: i) habitat suitability for salt marsh habitats; and ii) flood hazard reduction effectiveness of salt marsh-vegetated foreshores. Therefore, different methodologies are used for each of the thesis' sections; however, they both start with consultation of existing literature to compile a first estimate of habitat suitability and wave height attenuation effectiveness indicators, along with their approximate limit values.

For the habitat suitability analysis, readily available open source data (e.g. hydrodynamic, bathymetric, atmospheric) will be used to generate local hydrodynamic conditions at different locations of interest in two salt marsh-rich water systems in The Netherlands (the Western Scheldt and the Wadden Sea), selecting both vegetated and non vegetated sites within them. These generated conditions will be assessed in order to determine fundamental differences between all selected sites in order to gather limit values that would enable habitat establishment and survival.

Likewise, the wave height reduction effectiveness indicators compiled from literature will be assessed for their likely degree of effectiveness under several imposed boundary conditions, which would attempt to recreate conditions found in nature. This evaluation will be done initially on the effect of vegetation alone, while latter adding the effect of the changing bathymetry itself, caused by the presence of the foreshore. For the vegetation assessment, a sensitivity analysis on existing formulae describing wave propagation over vegetated fields will be used. The vegetated foreshore system analysis will be done with the spectral wave model SWAN (Simulating WAves Nearshore) under the previously explained boundary conditions. Various simulations with varying boundary conditions will aid in this step, after which the results will be compared to the water systems previously introduced.

Once the proposed habitat suitability and effectiveness indicators are determined, a link between the two will be proposed as an assessment tool for a quick scan at an arbitrary site, with the assumption that a salt-marsh vegetated foreshores is a desired solution for coastal protection.

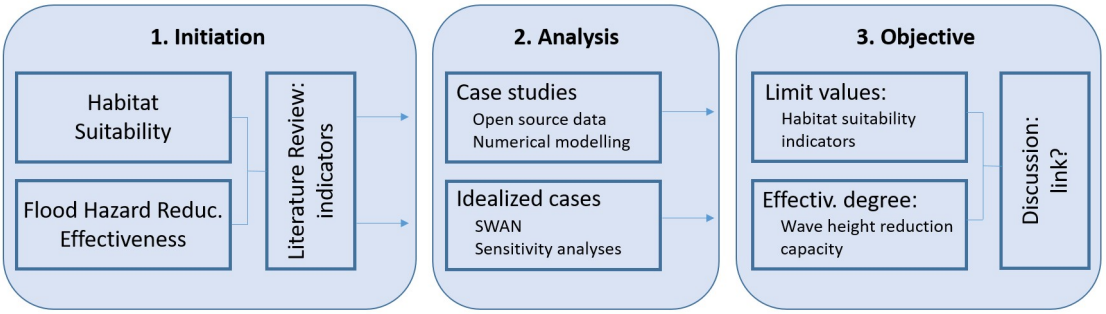

Figure 1.1: Outline of research methodology.

1.4. Report outline

The outline of this thesis will attend each of the research questions stated in section 1.2.

- Chapter 2 discusses the existing literature on salt marsh vegetation capacity as flood hazard mitigation measures; it also presents previously estimated conditions that can serve as habitat suitability and flood hazard reduction effectiveness indicators.
- Chapter 3 treats the habitat suitability indicators and their limit values. The gathered data is assessed and used to establish preliminary applicability limit values for each proposed indicator.
- Chapter 4 discusses the degree of effectiveness of salt marsh habitats under different imposed boundary conditions. A sensitivity analysis is performed on different parameters and general applications are presented.
- Chapter 5 presents the discussion of the results and the methods used throughout the thesis. Moreover, it presents the link between the habitat suitability and flood hazard reduction effectiveness.
- Chapter 6 provides the answers for the research questions addressed along the document.
- Chapter 7 gives recommendations regarding the current document and insight on topics for further assessment.

1.5. 'Building with Nature' philosophy

The overall structure of this thesis follows the first three steps presented as the Building with Nature philosophy, introduced by Ecoshape (2020) (Figure 1.2), where the 1st step in developing such a project is referred as 'Understanding the system'. This first phase of the design cycle is treated by the first research question, regarding the habitat suitability assessment. Once it is known whether a given water system is capable of hosting salt marshes (for this case, the intended 'BwN' solution is predefined), the following design step proposed by Ecoshape (2020) is to 'Evaluate the qualities of alternatives and pre-select an integral solution'. This step is followed by the second research question, where it is assessed whether the introduction of such a habitat serves as an effective coastal protection measure.

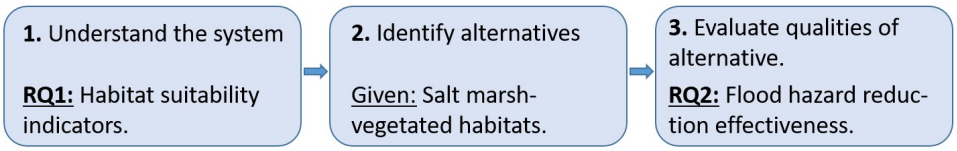

Figure 1.2: Building with Nature design steps, as proposed by Ecoshape (2020), and link with document structure and research questions.

2

Literature review

2.1. Vegetated foreshore system

A vegetated foreshore is a system characterized by a gently sloping sediment body, covered with vegetation, located in front of a dike; moreover, these systems can serve as an effective flood protection measure, since propagating waves experience energy loss due to depth-induced wave breaking, bottom friction and attenuation by vegetation (Vuik et al., 2016a). A stand-alone bare foreshore on its own can already reduce the hydrodynamic loading on the flood defense lying on the hinterland: maximum waves (during storm conditions) can be reduced to up to 55% of the water depth, given the foreshore is wide enough (Jonkman et al., 2018). The addition of vegetation enhances the already-effective wave attenuation capacity of this flood defense system.

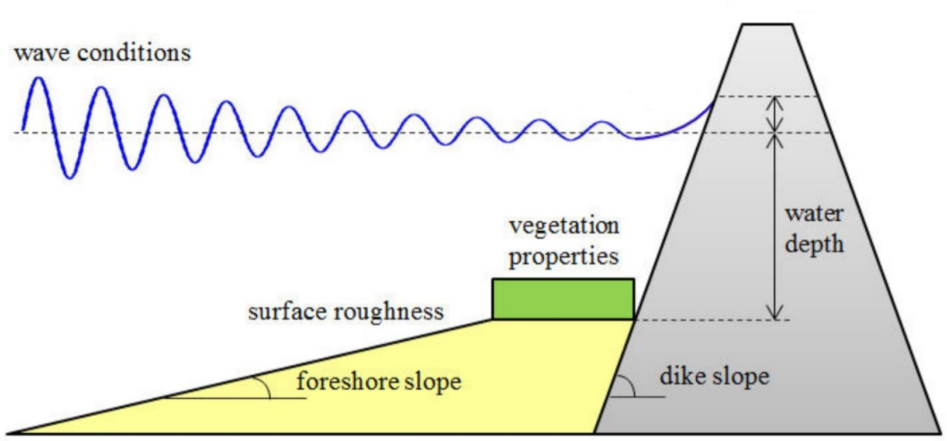

Figure 2.1: Schematic of a typical vegetated foreshore system trailed by a dike. Adapted from Vuik et al. (2016b)

Different types of vegetation can colonize a foreshore, but given that different sections of a foreshore transect become flooded under various scenarios (spring tides, storm surges, etc.), salt-tolerant vegetation such as salt marshes and mangroves are dominant. The presence of either of the aforementioned species is determined by local temperature fluctuations. Given that mangroves can not thrive in locations that experience temperatures below the freezing point (Deltares, 2018), they are found in tropical and subtropical latitudes, while salt marshes colonize foreshores developing in higher and lower latitudes (Figure 2.2).

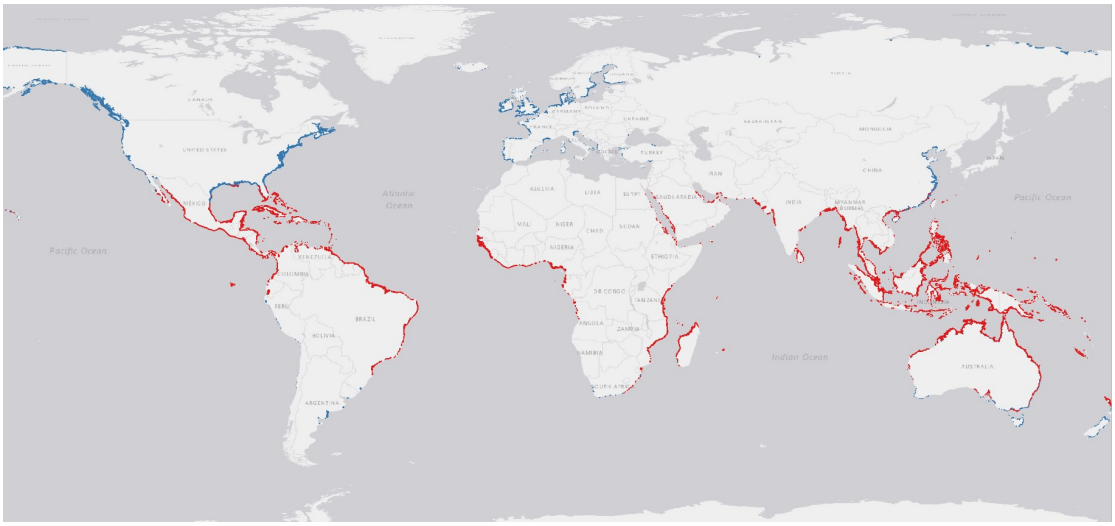

Figure 2.2: Global distribution of mangroves and salt marshes. Sources: Thomas et al. (2018) (mangroves), Mcowen et al. (2017) (salt marshes).

Extensive field and flume research has been done regarding the wave attenuation capacity of waves propagating over both mangrove-vegetated (Massel et al. (1999); Mazda et al. (2006); Quartel et al. (2007); Quang Bao (2011); Horstman et al. (2012); Janssen (2016)) and salt marsh-vegetated sites (Anderson et al. (2011); Yang et al. (2011); Anderson et al. (2014); Songy (2016); Vuik et al. (2016a)). Additionally, this previous research has also provided insight regarding the factors that determine the colonization and survival of both of these ecosystems, and will be treated in the following sections. However, as mentioned in Chapter 1, this thesis will focus on salt marsh vegetation only, leaving a similar study for mangrove habitats for future assessment.

2.2. Salt marshes

Salt marshes are vegetated habitats bordering saline or brackish water bodies under tidal influence (Deltares, 2018). Their capacity to thrive in salt water environments allows them to settle along the banks in coastal or deltaic regions where otherwise fresh water marshes or other vegetation could not survive. This innate characteristic make salt marshes an appealing species to choose as vegetation cover on foreshores located in salt water environments and in temperate climates. Along a foreshore transect, salt marsh habitats follow a specific zonation (Figure 2.3), where pioneering vegetation is found on the most seaward side of the transect, usually fronted by a mud flat, and mature vegetation on the most upper section of the marsh on the landward side. The species that populate these different zones correspond to their respective salinity tolerance, finding mostly sea grasses (e.g., Zostera) and glassworts (e.g., Salicornia) on the pioneer zone, as well as e.g., Spartina in more brackish conditions; whereas the middle and higher marsh zones, given their less frequent flooding exposure, include less salt-tolerant species such as rushes (e.g., Juncus spp.), grasses (e.g., Puccinellia, Sporobolus), and herbs (e.g., Aster, Plantago) (Healy, 2005).

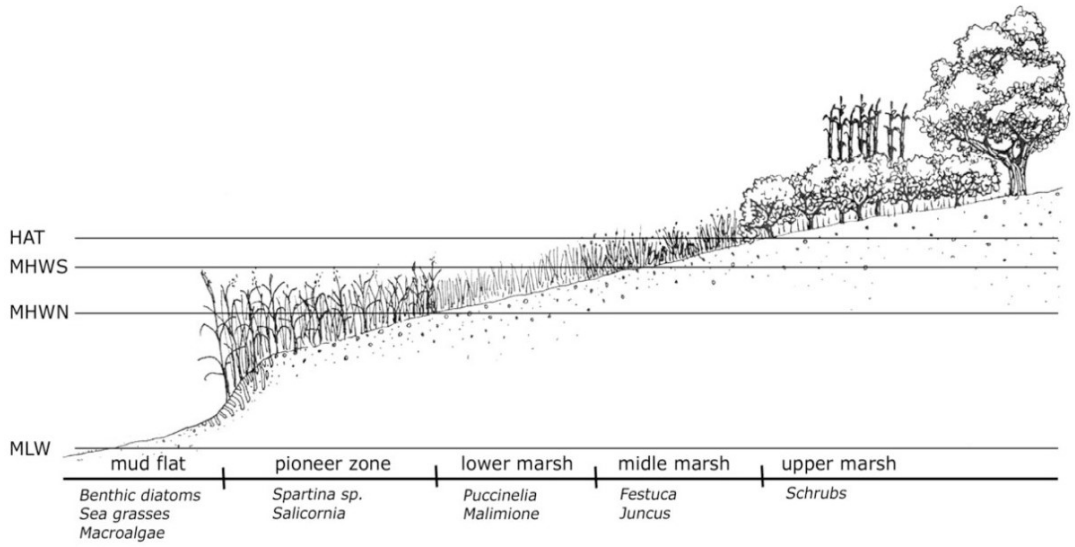

Figure 2.3: Typical transect of salt marsh zonation along a foreshore. Pioneering vegetation found on the seaward side (left) and mature vegetation on the landward side (right) (Vlaams Instituut voor de Zee, 2012).

Given this characteristic zonation, lower sections of a salt marsh experience more recurrent flooding than the upper regions, however the whole transect becomes flooded under certain tidal occurrences. Mean High Water Spring (MHWS) usually determines the upper boundary of the foreshore, while Mean Low Water Spring (MLWS) determines the lower boundary; likewise, Mean High Water Neap (MHWN) tends to set the limit for the salt marsh edge just before the beginning of the mudflat that fronts it (Willemsen et al., 2020). These flooding events occurring at different elevations on the salt marsh, combined with suspended sediment availability and the reduced hydrodynamic forcing caused by the vegetation itself, favors the overall increase of the bed level elevation (Bouma et al. (2007); van Wesenbeeck et al. (2008)). This positive feedback mechanism generates an accretion rate on salt marshes in the order of a centimeter per year, but it is strictly linked to local conditions, such as suspended sediment availability, tidal range and soil stability (Deltares, 2018).

2.2.1. Wave attenuation studies

Many locations around the globe have served as case studies to measure the response of salt marsh habitats to different types of external forcing. This has provided insight regarding intrinsic properties of salt marsh vegetation, and their response to different hydrodynamic conditions, as well as local parameters that favor their survival. Additional to it's wave attenuation capacity, research shows that salt marshes also offer several innate ecosystem services such as erosion control, water purification, carbon sequestration, and can serve as a location for tourism, recreation, education research services (Barbier et al., 2011). These different services, along with the ecosystem's wave attenuation capacity, add to the already increasing appeal of including these ecosystems as means of coastal protection measures.

Nonetheless, when looking at vegetated foreshores as an alternative flood defense measure, it is necessary to study how cost-effective they can be in contrast with traditional flood defenses. Narayan et al. (2016) compared vegetated foreshores to relatable hard structures, such as submerged breakwaters, and found that vegetated foreshores can be more cost-efficient when exposed to wave heights of up to 0.50m and even become more cost effective at greater depths. As presented in Figure 2.2 these habitats have their distinctive presence on different regions around the world, which has been used by researchers and local authorities to introduce this habitat as a coastal protection measure.

Additional to the previously described cost-effectiveness analysis, Narayan et al. (2016) also compiled a list of studies where wave attenuation capacity by salt marsh habitats was measured. Several studies were retrieved as part of this compilation, while making a distinction between already existing natural ecosystems ('Natural Defenses'), and introduced nature-based flood defenses ("Nature-based Defenses'). A summary of the afore-

mentioned salt marsh case studies is presented in Table 2.1. In total, 32 locations can be gathered from the dataset, for both natural and nature-based defenses.

Table 2.1: Previous studies regarding wave height attenuation by salt marsh vegetation. Distinction is made between natural and engineered systems. Adapted from Narayan et al. (2016).

Natural defenses		**Nature-based defenses**	
No. of studies	**Locations**	**No. of studies**	**Locations**
15	USA, UK, China, Netherlands	17	USA, UK, China

All the studies presented in Table 2.1 were aimed at measurement of the wave attenuation capacity of the ecosystem, and yet little is known about their ability to reduce water level increase due to storm surges. It has been previously determined that wetlands have potential to reduce surges, but it is highly dependent on the surrounding coastal landscape and the strength and duration of the storm forcing (Wamsley et al., 2010). For mangrove-vegetated foreshores, Montgomery et al. (2019) found that sufficiently wide and dense forests can reduce storm surge only to some degree; so water level attenuation by vegetated foreshores will not be further discussed in this thesis.

It is important to mention that most of the studies gathered by Narayan et al. (2016) measured wave attenuation under daily conditions; meaning that low waves with relatively low water depths were registered at the study sites. However, due to the increasing interest in adopting salt marsh habitats as an effective flood protection measure, understanding the behavior of these habitats under storm conditions has become a point of focus in recent years. The research done by Vuik et al. (2016a) added larger water depths and wave heights (2.50 m and 0.70m, respectively) to the range of previously registered observations, and concluded that the presence of vegetation leads to additional wave height reduction of 25-50% with respect to dissipation by only wave breaking and bottom friction. More recently, Zhu et al. (2020) determined with documented historical field evidence to which extent do salt marsh vegetation adds safety to engineered structures during severe storms; and concluded that not only salt marsh-vegetated foreshores reduce the likelihood of dyke failure, but also lowers flood impact by limiting breach dimensions (increasing the expected fatality rate from 0.7 to 1.0, instead of from 4.5 to 12.1 for non-vegetated foreshores).

Besides shedding light into the eventual use of vegetated foreshores as an effective flood protection measure, previous research has also added knowledge regarding the conditions that can limit the existence and survival of salt marshes, as well as the extent up to which they remain effective as a flood hazard reduction measure. These limiting conditions can serve as indicators for habitat introduction and, in later stages, as an assessment for flood protection.

2.2.2. Habitat suitability indicators

Habitat suitability limitations refer to local conditions that can favor or enhance the development of salt marsh vegetation in order to colonize a specific site. Existing literature presents information regarding habitat requirements for introduction or survival, along with qualitative estimates of limit values/thresholds. It is important to keep in mind that there are several variables that need to comply with the vegetation requirements in order to consider a site to be completely suitable to host the ecosystem. Deltares (2018) divides this habitat's requirements into biosphere, hydrosphere, lithosphere, and atmosphere (Figure 2.4), which provides the greater picture of the general required conditions. From this Figure, it is clear that different factors are needed for salt marshes to thrive; however, this thesis will focus on the analysis and quantification of hydrodynamic conditions and its derived phenomena, while the local soil composition and source of seeds will be assumed to be present.

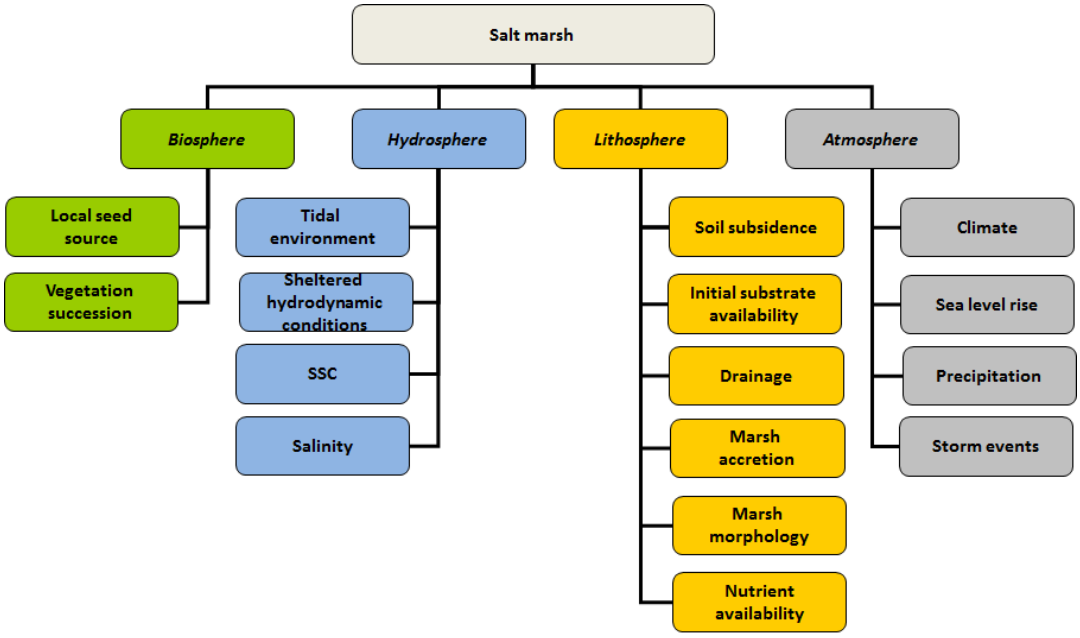

Figure 2.4: Salt marsh habitat requirements, subdivision proposed by Deltares (2018).

Attempts to better understand the required mild/sheltered hydrodynamic conditions have led to the definition of the 'Window of Opportunity' (WoO) term, which has been used to describe moments in time when local conditions (usually hydrodynamic) allow the occurrence of seed settlement (Balke et al. (2011), Balke et al. (2014), Domburg (2018), Hu et al. (2015), Yuan et al. (2020)). WoO for salt marshes have been studied by Hu et al. (2015), who defined two necessary events that need to occur one after the other: the first WoO is characterized by a sufficiently long inundation-free period (disturbance frequency) that allows seeds to settle and root; then, it has to be followed by a second WoO characterized by low hydrodynamic forcing (disturbance magnitude), such that the seedlings (seeds that have just sprouted) are not uprooted at the initial growth stages. Furthermore, Hu et al. (2015) also studied the effects of bathymetry in seedling survival by observing the occurrence of wave-induced and current-induced bed shear stress on both concave and convex foreshores. They found that even though the aforementioned bed shear stress occurring on both bathymetries decrease linearly with increasing elevation, the wave-induced bed shear stress occurring over a convex foreshore was lower than the one occurring on a concave bathymety, with a greater difference found on the pioneer zone.

The WoO concept was further studied in Silinski et al. (2015), who performed flume experiments to measure typical wave forcing on adult salt marsh specimens and seedlings within en estuary. This was analyzed by generating both short and long waves, aimed to mimic locally wind-generated and ship waves, respectively, under two distinctive water depths. Results showed that longer waves (ca. T = 10s) caused severe bending on both mature marshes and seedling stems, while also generating greater scour depths at the base of the stem. These results suggest that a permanent hydrodynamic forcing exerted by longer waves can prevent the occurrence of the required WoO, which hinders the likelihood of seedling establishment. These findings were later favored by the conclusions presented in Silinski et al. (2016a). Further studies aimed to study habitat suitability conditions were presented in Silinski et al. (2016b) and Silinski et al. (2016c), where salt marsh patches were transplanted on different sections along salt marsh sites, in both sheltered (fetch < 2km) and exposed wind conditions. One of the critical differences found between sites was that vegetation planted on the bare mudflat of the sheltered site survived longer than vegetation planted on the exposed bare mudflats. This accentuates the relevance of wave action when explaining the limiting factors for salt marsh survival. Nonetheless, no vegetation patch transplanted on bare mudflats survived at either exposed or sheltered location on a long-term scale, suggesting that local disturbances are the dominant indicators for salt marsh establishment. Moreover, they found that at salt marshes where wave action is limited (sheltered sites), the bed level elevation can possibly serve as a reliable indicator for salt marsh expansion; whereas in sites that are exposed to more aggressive wave loading, the elevation becomes a secondary suitability parameter, since it is overruled by the forcing of the waves themselves.

Considering that the exposure to hydrodynamic forces has a major role in determining the likelihood of a site to host salt marsh vegetation, the exposure to flooding events is also considered a relevant indicator for salt marsh suitability. There are two main proxies that treat this occurrence: inundation duration and inundation frequency. Balke et al. (2016) performed a global analysis of salt marsh extent in locations with different tidal regimes, and looked into the flooding events occurring at the salt marsh edge, which is defined as the spatial limit between the vegetated platform of the salt marsh and the bare mudflat. Results found that even though the salt marsh edge in meso to macrotidal salt marsh sites is located at a higher level when compared to microtidal sites, inundation still occurs twice daily. Additionally, this study shows that the potentially vegetated section of the tidal frame does not increase proportionally with increasing tidal range. This study therefore concluded that inundation frequency, and not inundation duration, defines the global location of the seaward extent of salt marshes. Nonetheless, the inundation duration may be closer linked to the initial seed establishment previously defined in the WoO definition by Balke et al. (2011). Furthermore, Deltares (2018) also suggests inundation frequencies to be the relevant indicator for salt marsh development, while detailing different inundation events per salt marsh zone (Figure 2.3 and Table 2.2).

These previous studies suggest that temporarily variable hydrodynamic conditions are key in the successful establishment and development of vegetated foreshores, and for this reason they will be further assessed in this thesis. Several additional studies related to salt marsh habitat requirements and threshold values have been compiled and presented in Table 2.2, among which we can find limit values for wave-induced orbital velocities for salt marsh stem breakage of different salt marsh species (Vuik et al., 2018a), salinity concentration at different levels of salt marsh elevation (Deltares, 2018), required foreshore slopes for new marshes (van Duin et al., 2012), minimum suspended sediment concentration to keep pace with sea level rise (Kirwan et al., 2010), among others. Even though these limitations often include a threshold based on observations made in field or flume experiments, some habitat limitations are only qualitatively described.

Table 2.2: Summary feasibility indicators found in literature.

Species/zonation	**Habitat suitability**		**Reference**
	Indicator	**Threshold**	
Pioneer zone	Inundation frequency	x2 per day	Deltares (2018)
Low zone		100-400 per year	
Mid/high zone		<100 per year	
-	Hydrodynamic conditions	Sheltered/mild	Deltares (2018)
-	Temperature	Temperate	Deltares (2018)
-	Soil	Silt and clay	Ford et al. (2016)
-	Salinity	18-35 ppt	Deltares (2018)
-	SS Concentration	>20mg/l	Kirwan et al. (2010)
-	Bathymetry	1:50 - 1:500 slope	van Duin et al. (2012)
Spartina	Orbital velocities (winter)	0.50 - 1.20 m/s	Vuik et al. (2018a)
Scirpus		0.30 - 1.00 m/s	Vuik et al. (2018a)
Elymus		Damage >0.42 m/s	Rupprecht et al. (2017)

Considering these previously given qualitative thresholds/limit values for temporarily variable hydrodynamic conditions, such as inundation frequency, wave action and strong currents these are the variables that will be further assessed in the remaining sections of this thesis.

2.2.3. Effectiveness indicators

The previous studies mentioned in Subsection 2.2.1 were targeted at understanding the general wave attenuation capacity of salt marsh habitats, some of them even taking a step forward into studying to which degree they remain an effective measure for flood protection. This previous research introduced several likely indicators for the ecosystem's wave damping capacity, such as increasing relative vegetation height (ratio between vegetation height and water depth - h_v/h) (Augustin et al., 2009; Yang et al., 2011); low water depths and high

salt marsh biomass, as well as the ratio between wave height and water depth (H/h) (Løvås et al., 2000; Vuik et al., 2016a); and higher wave steepness (Anderson et al., 2014; Wu et al., 2015).

From these studies, the water depth above the foreshore stands out as a recurrent factor within the effectiveness indicators. This is due to the fact that the presence of vegetation on the foreshore introduces additional drag forces on the propagating wave, which has been observed to reduce the energy at all frequencies within a spectrum, with higher reduction on the high-frequency end of the spectra (Anderson et al., 2014). This interaction between wave and vegetation was further investigated by Vuik et al. (2016a), where field measurements between November 2014 and January 2015 served to explain the response of salt marsh habitats under storm conditions. The variable recorded hydrodynamics helped to assess the response of vegetation under different H/h ratios. Results showed that, under storm conditions and smaller wave height to water depth ratios, dissipation by vegetation becomes an important energy dissipation mechanism, while depth induced wave breaking is limited; additionally, they showed that for larger wave height to water depth ratios, vegetation prevents intense wave breaking to occur, possibly favoring the stabilization of sediments on the foreshore.

These findings mean that not only wave height to water depth ratio serves as an effectiveness indicator, but also vegetation height (h_v). Yang et al. (2011) found that when water depths above the foreshore were 1.5 - 2.0 times larger than the vegetation height, the wave attenuation rate was reduced in contrast to barely submerged or emerging vegetation. Furthermore, they suggested that when greater water depths (relative to vegetation height) are observed, a lower drag coefficient should be considered when modeling wave growth over a vegetated foreshore. Augustin et al. (2009) further adds to the importance of vegetation height, finding greater rates of wave attenuation for emergent vegetation ($h_v/h > 1.0$) than on barely submerged salt marsh vegetation.

Additionally, in order to further understand the utility of vegetated foreshores as a flood protection measure, van Zelst (2018) attempted to assess their flood hazard reduction capacity on a global scale. This study defined wave damping as the difference between incoming wave height and transmitted wave height (at the end of a transect) on both vegetated and bare foreshores. Results show that salt marsh-vegetated foreshores can reduce wave transmission up to 40% in both sheltered and exposed environments, but it is highly dependent on the modelled vegetation characteristics. Nonetheless, from the global assessment it could be concluded that higher rates of wave attenuation were found for increasing vegetation width (about 10% to 25% of wave attenuation is observed in the first 450m and 900m, respectively). Moreover, this study found the highest wave attenuation rates occurring on waves propagating over milder foreshore slopes, which also falls in line with the findings by Songy (2016).

Even tough the research by van Zelst (2018) assessed global potential for wave attenuation effectiveness, the assessment did not explicitly observe the response with respect to local tidal ranges. Kirwan et al. (2010) already accounted for the different resilient capacity of salt marshes to increasing water levels in areas with different tidal ranges, suggesting that sites with a greater tidal range with high sediment supply could better adapt to rising sea levels, while the contrary occurring in sites with low tidal ranges little sediment supply. Furthermore, Balke et al. (2016) studied the importance of tidal range for the seaward extent of salt marsh habitats. This study gathered historical data from locations experiencing different tidal ranges, and they found that the seaward extent of the pioneering edge of a salt marsh (lowest elevation) grows logarithmically with increasing tidal range. This translates to the fact that the vegetated section below mean high water does not increase for increasing tidal ranges. Given the close relationship between tidal range and salt marsh dynamics, this site-specific characteristic will be further studied as part of this thesis as a likely wave attenuation effectiveness indicator.

Likewise, considering the general importance of water depth in the indicators described in this subsection, both vegetation height to water depth ratio (h_v/h) and wave height to water depth ratio (H/h) will be further assessed in this thesis with the purpose of determining different degrees of effectiveness for both. An overview of the effectiveness indicators found in literature are presented in Table 2.3.

Table 2.3: Summary effectiveness indicators found in literature.

Effectiveness Indicator	Reference
Vegetation width	van Zelst (2018)
Milder foreshore slope	van Zelst (2018)
Biophysical properties	Vuik et al. (2018a)
Relative vegetation height	Yang et al. (2011)
Greater wave steepness	Wu et al. (2015)
Wave height to water depth	Vuik et al. (2016a)

It is important to note that the wave damping capacity of the ecosystem is not only determined by hydrodynamic and topographical conditions, but is also influenced by biophysical properties such as vegetation density (N), canopy height (hv) stem diameter (bv), leaning angle (θ) and flexural strength (σ_{max}) (Vuik et al., 2018a). The ultimate aim of this thesis is to investigate for an arbitrary site whether a vegetated foreshore for coastal protection is (1) suitable and (2) effective at that site. Site characteristics are most important in a screening phase, given a certain ecosystem type. However, it will be the combination of site conditions and ecosystem characteristics that determine the vegetated foreshore's effectiveness.

3

Habitat suitability

The following chapter presents the analysis of the habitat suitability indicators selected in Chapter 2. Each indicator is studied in different sites across two water systems in The Netherlands, where mature salt marsh vegetation is found: the Western Scheldt (WS) and the Wadden Sea (WZ). Similarly, the local conditions are assessed in three additional characteristic sites commonly found in an estuary: i) locations with little/emerging vegetation (referred hereafter as 'Salt marsh patches'); ii) locations on fringing flats without vegetation ('No-marsh locations'); and iii) locations on intertidal shoals ('Tidal flats'). A schematic of the typical estuarine morphology features is presented in Figure 3.1 (de Vet, 2020). These additional characteristic sites serve as means to compare the occurrence of the observed hydrodynamic forcing found in mature salt marsh habitats.

Study period

The salt marsh growth season of the year 2020 (April - July) was chosen as representative for daily conditions in the water systems and will be further referenced in the following sections. The colder months were not included in the analysis since this thesis focuses on conditions that favor the existence of temperate salt marsh vegetation, which growth is hindered by temperature drops and harsher hydrodynamics.

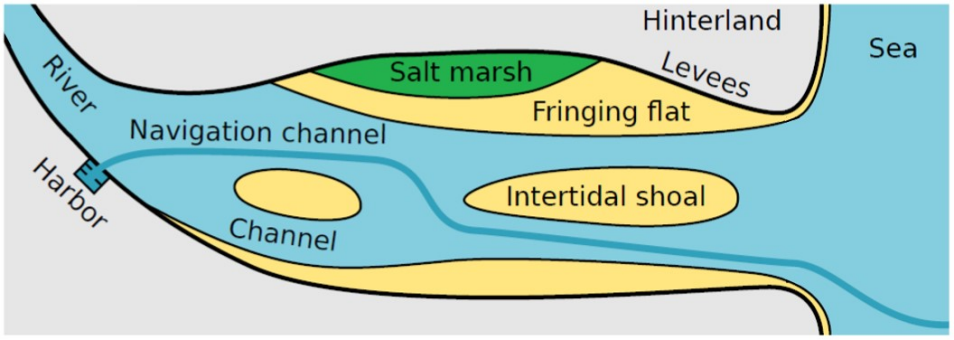

Figure 3.1: Schematic of characteristic estuary morphology, where salt marshes sit on higher elevations. Intertidal flats can be found either on the limits of the estuary (fringing flats) or bordered by tidal channels (intertidal shoals). Adapted from de Vet (2020).

3.1. Case studies

In an attempt to explain the development of salt marshes on a greater spatial scale, this thesis will study the conditions occurring in two separate water systems (Figure 3.2). Even though several differences are found between these systems, such as the tidal regime, sediment composition, general bathymetry, etc; they both host salt marsh habitats in several sites along their interfaces between the hinterland and the sea. Likewise, 'No-marsh sites' and 'Salt marsh patches' can be found in both systems.

Figure 3.2: Geographical location of the referred case studies, where the Wadden Sea and the Western Scheldt are found in the North and Southwest of The Netherlands, respectively.

The Western Scheldt is characterized by a meso and macrotidal regime with some tidal flats and channels along it's stretch (Callaghan et al., 2010). It serves as the entry channel for the port of Antwerp, Belgium, and it is hence submitted to high waterway traffic throughout the year. Many mature salt marsh sites along this estuary have previously served as study locations for research regarding the wave attenuating capacity of vegetation (Vuik et al. (2016a)); Willemsen et al. (2020)) as well as the hydrodynamic forcing acting on them (Callaghan et al. (2010), Silinski et al. (2016c). The existing literature with respect to these mature salt marshes in the estuary serves as a starting point for the current analysis, and it is the reason for the selection of the six (6) vegetated sites. Furthermore, additional observation sites within the Western Scheldt were arbitrarily chosen as follows: three (3) 'No-marsh locations'; four (4) 'Salt marsh patches'; and two (2) 'Tidal flat' locations (Figure 3.3). The reason behind the selection of these types of additional sites was because they may experience a variety of conditions which may differ from the ones experienced at mature marsh sites.

The Dutch Wadden Sea is located on the most northern region of The Netherlands and is located between barrier islands and the mainland (the sea side of the islands face the North Sea and the lea side face the Wadden Sea (Figure 3.2). It is a highly dynamic shallow tidal basin characterized by a micro, semi-diurnal tidal regime, which causes strong current velocities that are in large part responsible for the sediment transport within the water system (de Jonge et al., 1993). Mature salt marshes are typically found on the lea side of the barrier islands and fronting the dikes protecting the mainland. It is important to mention that the presence of salt marshes that front these dikes is favored by the existence of brushwood dams that reduce the hydrodynamic forcing, hence enhancing sediment trapping, soil consolidation and vegetation growth (Vuik et al., 2018b). Within this system, several locations were selected (according the the previously established classification) and consist of the following: six (6) mature salt marsh sites, two (2) 'No-marsh locations', three (3) 'Salt marsh patches', and two (2) 'Tidal flat' locations (Figure 3.4). The rationale behind the selection of these sites follows the one presented for the Western Scheldt.

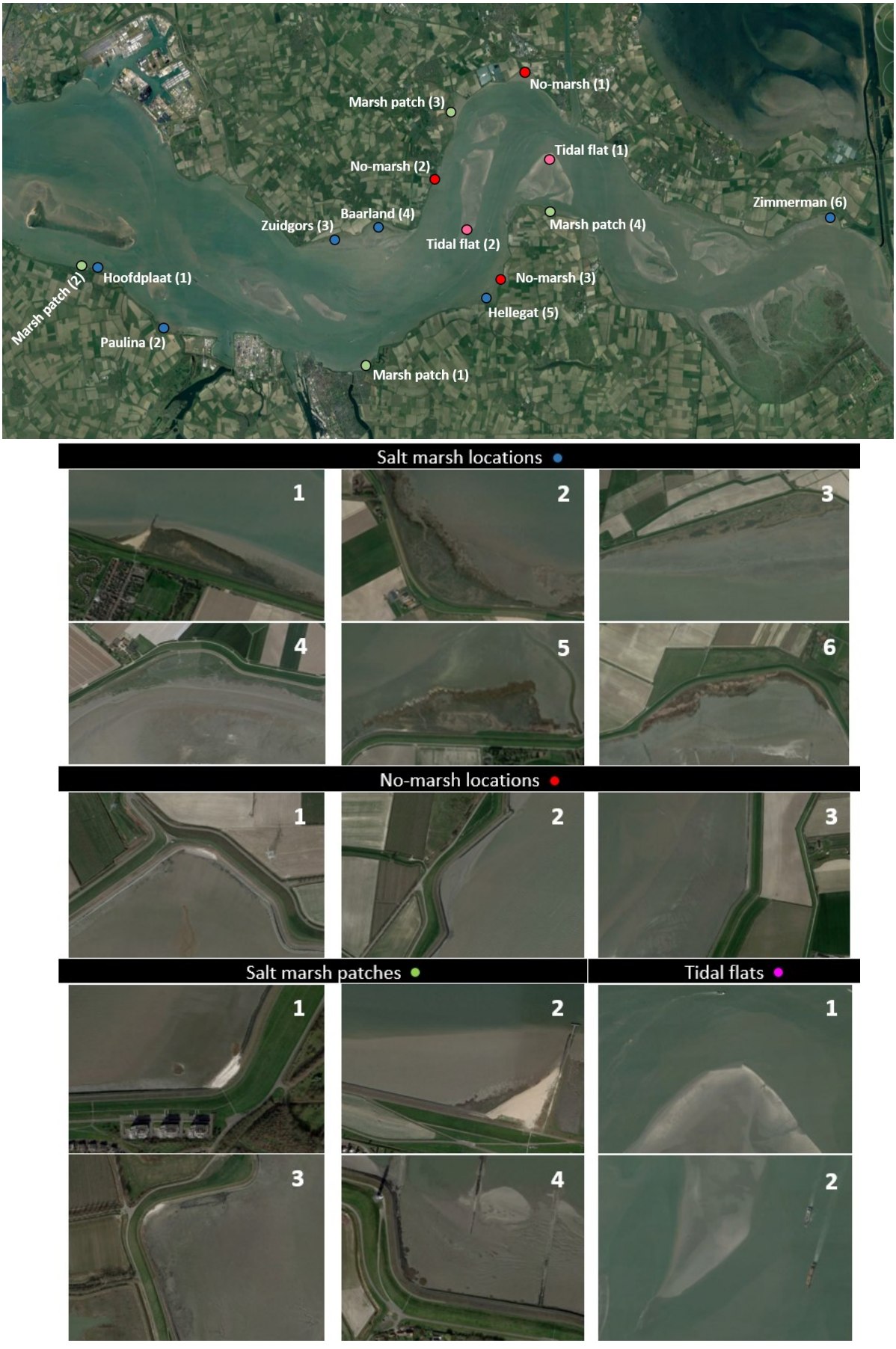

Figure 3.3: Overview of the study locations selected in the Western Scheldt (top) and close-up screenshots (bottom) retrieved from Google Earth. Sites characterized by mature salt marsh vegetation, 'No-marsh' sites, 'Salt marsh patches', and 'Tidal flats' are denoted by blue, red, green, and pink dots, respectively.

Figure 3.4: Overview of the study locations selected in the Wadden Sea (top) and close-up screenshots (bottom) retrieved from Google Earth. Sites characterized by mature salt marsh vegetation, 'No-marsh' sites, 'Salt marsh patches', and 'Tidal flats' are denoted by blue, red, green, and pink dots, respectively.

In total, habitat suitability indicators will be evaluated on twelve (12) salt marsh locations, five (5) non-vegetated fringing flats, seven (7) salt marsh patches/locations with emerging vegetation, and four (4) tidal flats. Table 3.1 presents a summary of the locations treated in this thesis; and Figure 3.5 shows the general layout of the results for the following analysis.

Table 3.1: Summary of selected study sites in each water system.

Water system	Salt marshes	No-marsh locs.	Salt marsh patches	Tidal flats
Western Scheldt	6	3	4	2
Wadden Sea	6	2	3	2

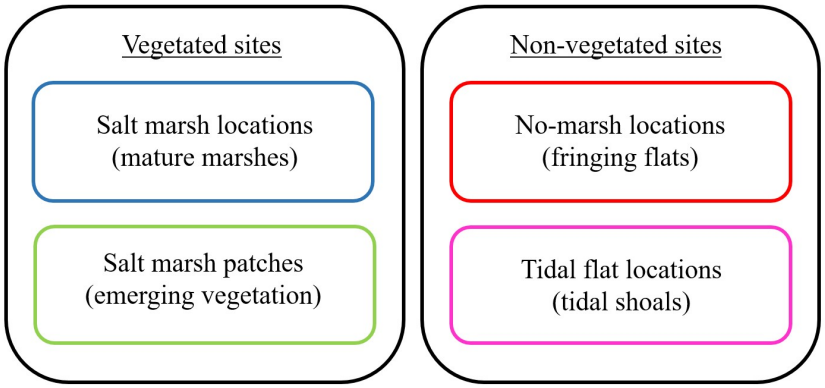

Figure 3.5: Overview of layout used for analysis in following sections. Vegetated locations are divided into mature salt marshes and emerging salt marshes, while non-vegetated locations are divided into no-marsh sites located on fringing flats and tidal flats.

3.2. Inundation-free period

For each of the 'Salt marsh' locations presented in Figure 3.3 and Figure 3.4, the transition between salt marsh vegetation and mud flat (referred hereafter as the 'marsh edge') was studied as the reference location for flooding frequency, based on Google Earth images. This transition was chosen since it suggests the occurrence of limiting conditions for vegetation to exist. The exact assessed location for this analysis corresponds to a point located directly landward from the marsh edge, along a selected transect on each 'Salt marsh location' (Figure 3.6). In 'No marsh locations' and 'Salt marsh patches', due to the absence of vegetation, the highest bed level elevation was selected. In order to compute the occurrence of inundation-free (dry) period, both bathymetric data and water level time series were required. Once this information was retrieved, the inundation free period was computed as the time when the depth was equal or lower than 0, while depth being computed as the difference between water level and bed level.

The elevation data was mainly retrieved from the Actueel Hoogtebestand Nederland database (AHN3), which is a high-resolution altimetry open source platform where the surface area of The Netherlands is readily available. For most locations, this dataset includes the bed level elevation of the intertidal flats and the salt marsh platforms that front the dikes on the sea-ward side. An example of a transect used at a salt marsh site (Hellegatpolder, Western Scheldt) is presented in Figure 3.6. Likewise, this Figure also shows the three points located along the salt marsh edge that were defined and studied at this location. All additional marsh edge locations in mature marsh sites, across both water systems, are presented in Appendix B.

However, AHN3 does not provide the bathymetrical data of the 'Tidal flat' locations previously presented. This missing data was retrieved from the Vaklodingen dataset, which provides the bathymetric data of the Dutch coast, and additional water systems. Bathymetry is available for several years (dating from 1928); however, due to the highly dynamic character of the two systems selected for this thesis, the latest available recordings were chosen. When comparing the Vaklodingen dataset to the AHN3 dataset, a clear distinction is found regarding the spatial resolution, being Vaklodingen much coarser.

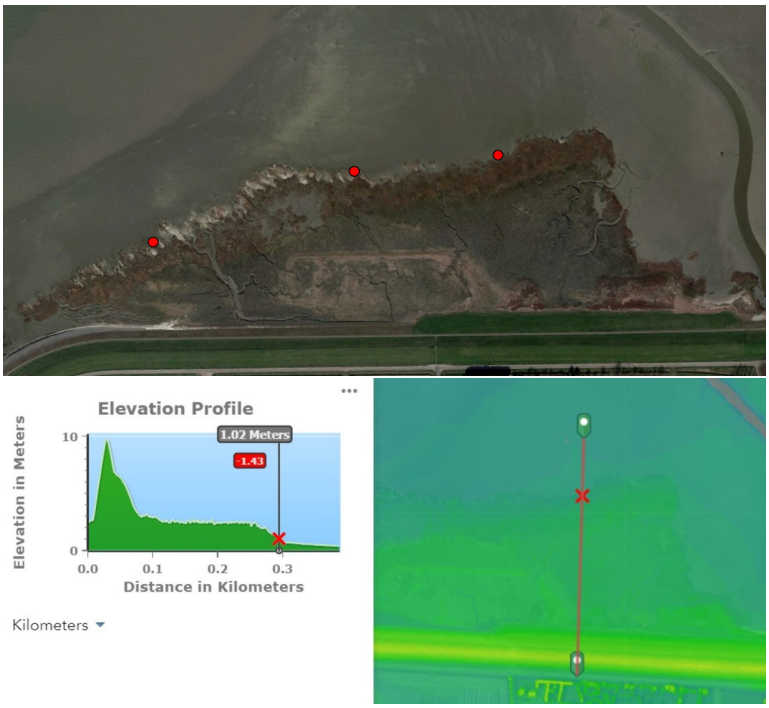

Figure 3.6: Example of the three points selected for the inundation-free period analysis at the salt marsh edge at Hellegatpolder (top panel). The bottom panels depict the transect for one of the points along the aforementioned marsh edge, where the red cross denotes the location where bed level elevation was retrieved from the AHN3 database.

The water level time series were retrieved from the Rijkswaterstaat (RWS) database. which gives with a water level measurement w.r.t. NAP every 10min. Given that both systems are influenced by the tidal behavior of the North Sea, this time step provides a temporal resolution that better describes the occurrence of flooding events. Nonetheless, as Figure 3.7 shows, the RWS stations (green dots) provide data at locations far from the chosen observation locations for this analysis. With the purpose of generating water level time series at the salt marsh edge and additional locations, triangular interpolation was used, where each RWS station serves as node of a triangular plane. With this method, for each RWS reading recorded every 10 minutes, a new time series was generated in the locations situated in the proximity of each plane (Figure 3.7). Each generated time series consists of 22028 readings, corresponding to the length of the provided RWS data.

In order to account for the spatial variability on the mature salt marsh locations, two to three transects were retrieved from the AHN3 dataset, depending on the longitudinal extension of each salt marsh (denoted by numerical subscripts on salt marsh locations in Figure 3.8 and Figure 3.9). Even though some differences were found in the bed elevation between the aforementioned transects, the results of this analysis were not significantly different within the same salt marsh location, as will be presented in the following subsections.

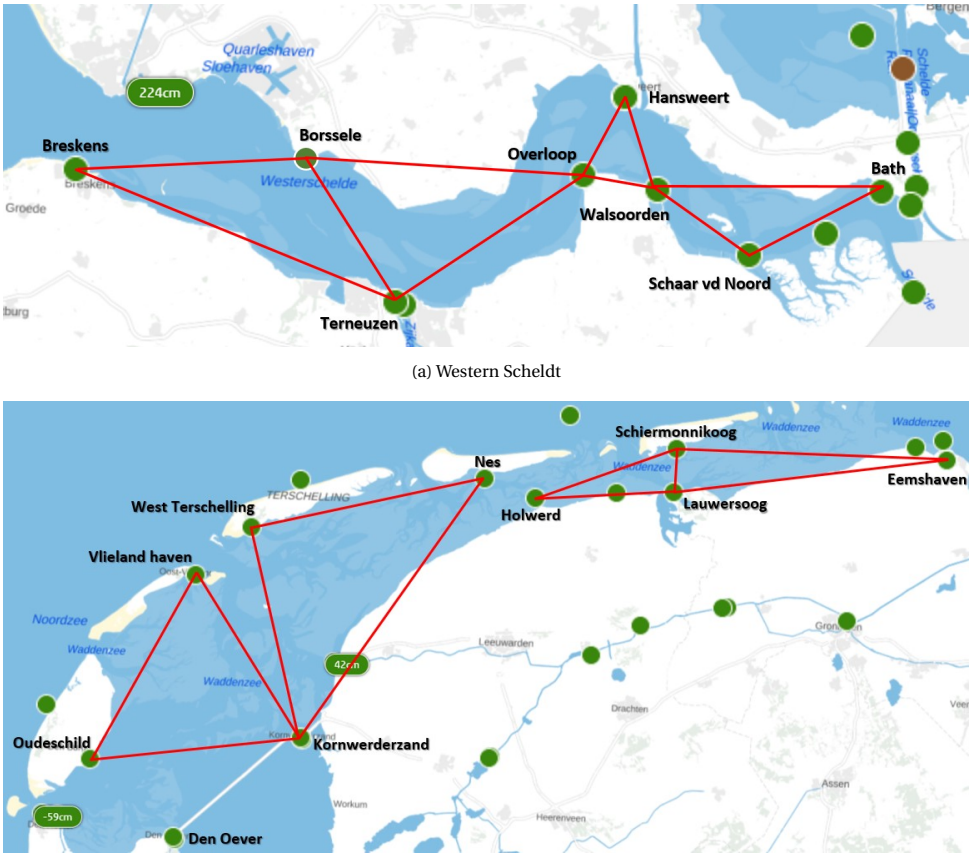

(a) Western Scheldt

(b) Wadden Sea

Figure 3.7: Screenshot of Rijkswaterstaat water level stations in the Western Scheldt (top) and Wadden Zee (bottom), as well as triangular planes used for water level time series generation.

3.2.1. Western Scheldt

Figure 3.8 shows the inundation-free period computed as a fraction of the studied period, at all locations. The vertical red dashed line serves as a distinction between mature salt marsh locations and the additional observation sites. Results show that during the 2020 growth season the salt marsh edges experience variable dry periods, depending on location, and ranging roughly between 70-95% of the time. These findings were compared to the research presented by Willemsen et al. (2020), where a long-term analysis of the salt marshes in the Western Scheldt indicates stable (Zuidgors), retreating (Paulina and Hellegat) or expanding (Hoofdplaat, Baarland and Zimmerman) behavior of the salt marshes.

Transects at Hoofdplaat, Zuidgors, Baarland and Zimmerman result in the highest computed dry periods (above 85% of the time), which is caused by the higher elevations found at these sites. These results coincide with the stable and expanding behavior of the marsh edges previously reported (Willemsen et al., 2020), suggesting that longer dry periods during the growth season favors the lateral expansion of salt marsh habitats. On the other hand, salt marsh edges that are flooded more frequently during the growth season (above 65% of the time), such as Paulina and Hellegat, have shown a retreating behavior in the long term.

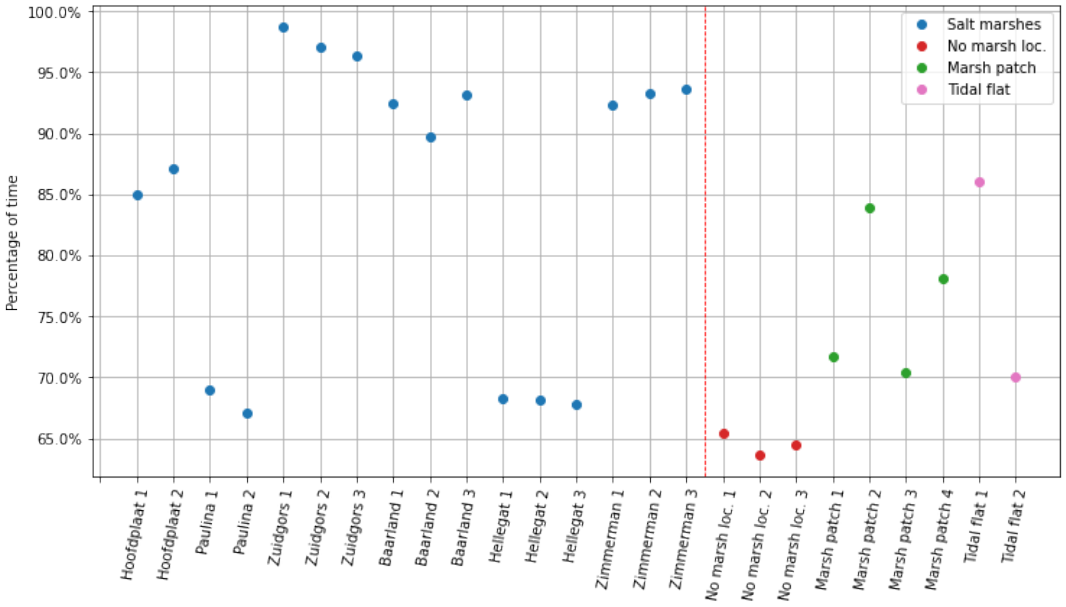

Figure 3.8: Results of inundation-free period analysis in the Western Scheldt. Vertical dashed line (red) separates mature salt marsh locations from additional observation locations.

While looking at the observation points on the right side of the vertical dashed line, Figure 3.8 shows that locations with no salt marsh vegetation experience an inundation-free period of around 65% of the growth season. This inundation frequency approximates the behavior of the salt marshes that show historical retreat, which could be linked as a limiting factor for salt marsh development. Nevertheless, locations which host small salt marsh patches show an inundation-free period that ranges between 70% and 85% of the time. A distinction can be made at 'Salt marsh patch 2', which experiences the highest dry period. This is given by the fact that the bed level elevation at this location is higher in comparison to other salt marsh patches.

The tidal flats show greater differences in inundation frequencies. The first tidal flat location has a higher bed level elevation and hence an inundation-free period slightly above to 85%; however, no salt marsh vegetation is found here. The second tidal flat location has a lower bed level elevation, which results in a dry period of 70%. Even though vegetation is absent on both locations, inundation-free period is variable at both sites. This translates to the possibility that inundation-free period is not a dominant factor in salt marsh habitat suitability, however it is more likely linked to salt marsh edge expansion.

Nonetheless, Figure 3.8 also shows that salt marsh vegetation is apparently feasible at locations that experience inundation-free periods for least 65% of the time during the corresponding growth season. This insight will serve as a first estimate of the a habitat suitability threshold for this indicator.

3.2.2. Wadden Sea

Results gathered from the analysis performed in the Wadden Sea show similar behavior with respect to the previous findings. Figure 3.9 points out that the salt marsh locations experience dry periods for a greater time of the growth season (all above 90% of the time), which coincides with the dry period found in the Western Scheldt expanding or stable salt marshes (Figure 3.8). However, it is unknown whether the presently selected salt marsh locations in the Wadden Sea are either stable, or experiencing expansion or retreat, therefore this assessment cannot be performed in this water system.

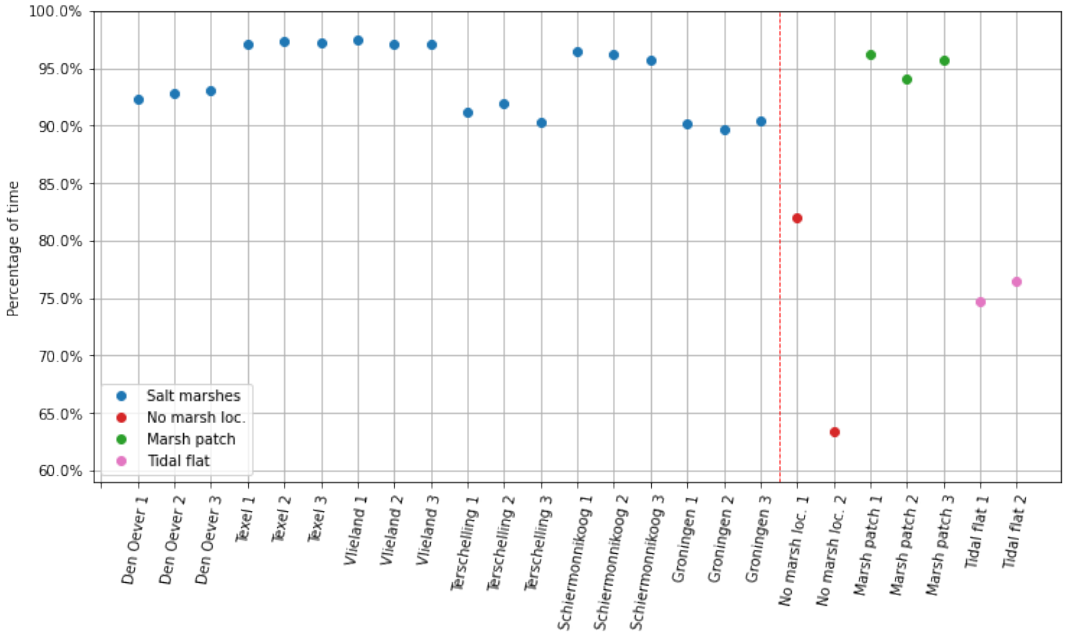

Figure 3.9: Results of inundation-free period analysis in the Wadden Sea. Vertical dashed line (red) separates mature salt marsh locations from additional observation locations.

The behavior found in the additional observation locations show that there is a difference in flood exposure between both selected 'No marsh locations', which is due to the difference in bed level elevation at each site. While 'No marsh location 1' experiences a dry period for more than 80% of the time, 'No marsh location 2' is only dry for a little less than 65% of the time. As mentioned in the previous subsection, these results point at the possibility that inundation-free period on its own is not solely responsible for salt marsh suitability, but given that it is tightly linked to the habitat's experienced hydroperiod, it is a still a relevant proxy for salt marsh survival.

The inundation-free period found at 'Salt marsh patch' locations show that these sites can even experience larger dry periods (around 95% of the time) than some salt marsh locations in the same system. Additionally, even though differences were found between the bed elevation at all three 'Salt marsh patch' locations, Figure 3.9 indicates that they experience similar exposure to dry events. Likewise, both 'Tidal flat' locations experience a flooding-free frequency of around 75% of the time, while they also present differences in bed level elevation.

3.3. Flow velocities

For the following analysis, and considering the absence of readily available open source data describing flow velocities in both systems, two different numerical models were used to describe the required data. The NevLa Delft3D model was used to simulate the flow behavior within the Western Scheldt, while a Delft3D-4 model was used for hydrodynamic simulations on the Wadden Sea. Both models are characterized by a flexible mesh, delimited on the offshore boundary by the North sea, however the spatial resolution varies per location in the domain. For example, the North Sea section of the NevLa model has a resolution of about 400m, while within the Western Scheldt itself the grid size varies between 50 and 100 meters, and down to 10 meters in the Sea Scheldt (Plieger, 2015). A snapshot of the spatial extent of the models is shown in Figure 3.11 and Figure 3.17, along with a zoomed in image of the areas of interest.

The type of imposed forcing on the boundary conditions vary between the models. The Western Scheldt model consists of water level time series characterized by a time step of 10 minutes; and they are located at the offshore limits in the North Sea. Additionally, imposed conditions are discharge locations set at upstream locations and in various navigation channels discharging into the estuary. All these aforementioned parame-

ters characterize daily conditions in the Western Scheldt and will be assessed as a first step in the flow velocity analysis. Boundary conditions in the the Wadden Sea model consist of water levels forced by astronomical components. The tidal behavior is represented by 8 tidal constituents (O1, K1, N2, M2, S2, K2 M4 and MS4) with their respective amplitudes and phases. Even though there are certain discharge locations in the Wadden Sea (Afsluitdijk locks, navigation channels, etc.), they are not included as additional operation points in the model and their effect on morhpo- and hydrodynamics within the system are considered negligible, when compared to the role played by the tidal forcing.

Simulation times for each system is described in the following subsections. Contrary to the inundation-free period analysis, it is not possible within this analysis to accurately observe the salt marsh edges at each location of interest. Therefore, the evaluated flow velocities were the ones occurring in the proximity of every study site. In order to reduce the uncertainty introduced by this approach, several observation points (grid cells) were selected in the proximity of each salt marsh and observation site (Figure 3.10). This was performed in an attempt to represent the most likely occurring flow patterns. Once the flow velocities were gathered at every observation location, post-processing consisted of the following two steps: i) comparing velocity signals between the previously described observation points, and ii) performing an exceedance probability analysis on the signals with the purpose of retrieving characteristic values occurring during a characteristic growth season.

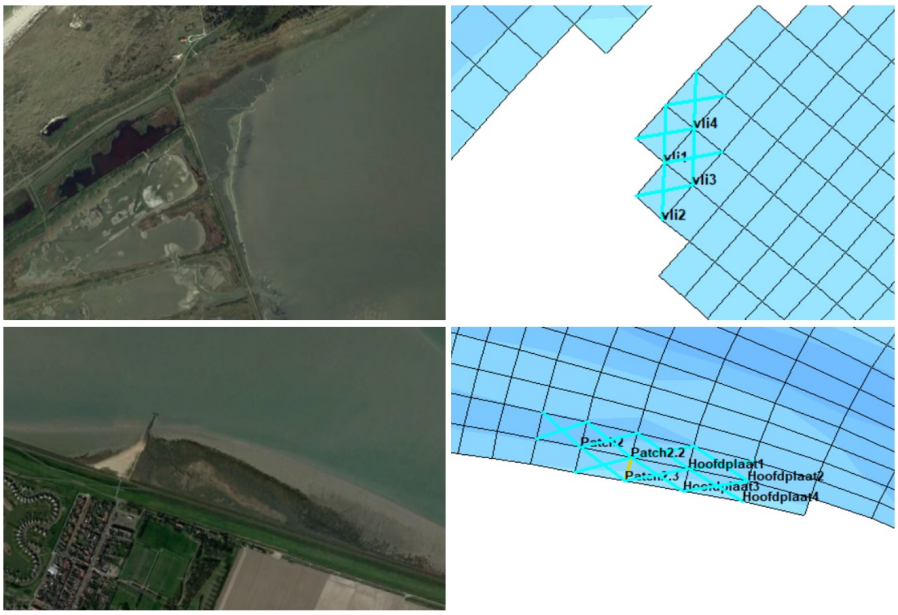

Figure 3.10: Example of selected observation points in locations of interest. Top panels correspond to the salt marsh location 'Vlieland', Wadden Sea. The bottom panels correspond to 'Hoofdplaat' and 'Salt marsh patch 2' in the Western Scheldt.

Even though the selection of several observation points within the numerical models was aimed to reduce the uncertainty in the aforementioned approach, it still remains unclear whether the assessed flow velocities are actually occurring at the desired sites. As an additional check, a comparison between bed level elevations was performed at all sites 3.2. The actual bed level elevation was the same as used in Section 3.2, gathered from the AHN3 database (where the bed level elevation corresponds to a point just landward of the marsh edge, defined by Google Earth imagery). The bed level from the numerical models were gathered from the model outputs.

Table 3.2: Comparison of bed level elevation between the AHN3 database (actual elevation) and the numerical model bathymetry, for the Western Scheldt (left) and Wadden Sea (right).

Western Scheldt			**Wadden Sea**		
Location	**Bed elevation [m]**		**Location**	**Bed elevation [m]**	
	AHN3	**Model**		**AHN3**	**Model**
Hoofdplaat	1.75	-1.98	Den Oever	0.90	0.08
	1.84	-0.75		0.88	-
Paulina	1.02	0.31	Texel	1.13	0.31
	0.95	0.80		1.15	-
Zuidgors	2.67	0.37	Vlieland	1.21	0.50
	2.45	1.26		1.16	0.50
Baarland	2.20	1.96	Terschelling	0.98	1.28
	2.13	0.94		0.95	0.44
Hellegat	1.06	0.23	Schiermonikoog	1.35	1.01
	1.05	0.69		1.37	0.88
Zimmerman	2.54	2.05	Groningen	1.15	1.08
	2.64	1.25		1.17	1.40
No-marsh 1	0.90	0.23	No-marsh 1	0.80	0.77
No-marsh 2	0.70	-4.40	No-marsh 2	0.44	-3.40
No-marsh 3	0.80	0.06			
Marsh patch 1	1.26	-1.92	Marsh patch 1	1.31	0.95
Marsh patch 2	1.71	1.00	Marsh patch 2	1.15	1.12
Marsh patch 3	1.14	0.24	Marsh patch 3	1.48	1.12
Marsh patch 4	1.70	-0.62			
Tidal flat 1	2.08	2.03	Tidal flat 1	0.74	-0.34
Tidal flat 2	1.15	0.67	Tidal flat 2	0.70	-0.22

The previous comparison shows discrepancy between the bathymetry data used in the models and the actual elevation at each site. Nonetheless, Table 3.2 also shows that most of the locations, with a few exceptions, are located above mean sea level (MSL), which can serve as an indication that the flow velocities gathered from the model simulations are the ones occurring on the mudflats that front the salt marshes. Locations that are characterized by deeper bed level elevations, such as 'Hoofdplaat', 'No-marsh loc. 2' in both water systems, 'Salt marsh patches' in the Western Scheldt, and 'Tidal flats' in the Wadden Sea, are also located in the proximity of tidal channels within the water systems. Therefore, the handling of this data is different than in other locations and will be further explained in the following Subsections.

3.3.1. Western Scheldt

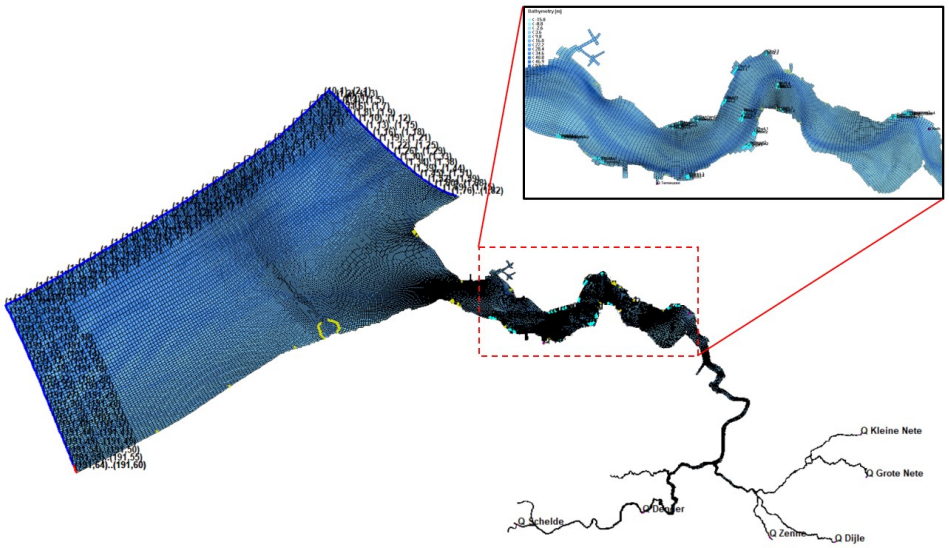

Figure 3.11: Spatial extent of the Delft3D model used for the depth-averaged flow velocity analysis in the Western Scheldt.

Considering that the water level boundary conditions in the NevLa model account for the temporal variability of the tide (neap-spring tidal cycle), the simulation time was chosen to be 2 days during each cycle in order to observe flow velocities during both ebb and flood events. An example of the output flow velocity signal in one of the observation points during the occurrence of both tidal cycles is presented in Figure 3.12. The highest flow velocities were recorded during the spring tidal cycle (similar behavior was observed at all sites). Hence, considering that the focus of this thesis is on limit values for habitat suitability, the spring tidal cycle signals were chosen for further analysis.

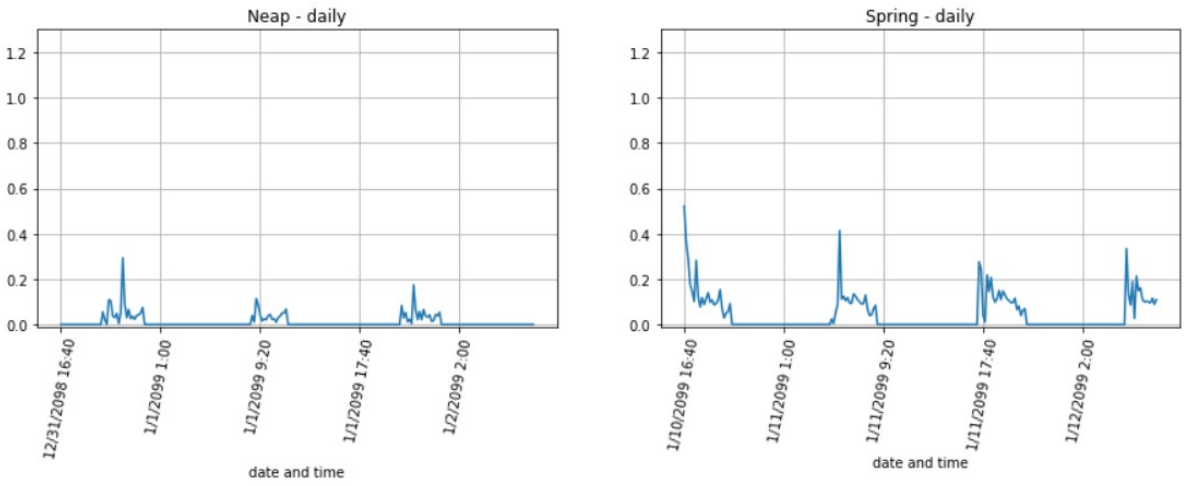

Figure 3.12: Example of the flow velocity signal at one location (Baarland). The left panel shows the signal generated from the neap cycle simulation; the right panel shows the signal generated during spring tide.

From the several observation points placed in the proximity of each site (such as in the examples given in Figure 3.10), the output signal of the two most representative points per salt marsh site were selected to characterize the occurring flow velocities; hence, two exceedance probability curves are given per location. Results are presented in Figure 3.13. It is worth mentioning that, given Hoofdplaat's proximity to a tidal channel (Figure 3.3) and the coarse spatial resolution of the numerical model (Table 3.2), this analysis does not include the flow velocities gathered at this site. This circumstance translated into higher flow velocity magnitudes at

this observation site, when compared to flow velocities found at other salt marsh locations.

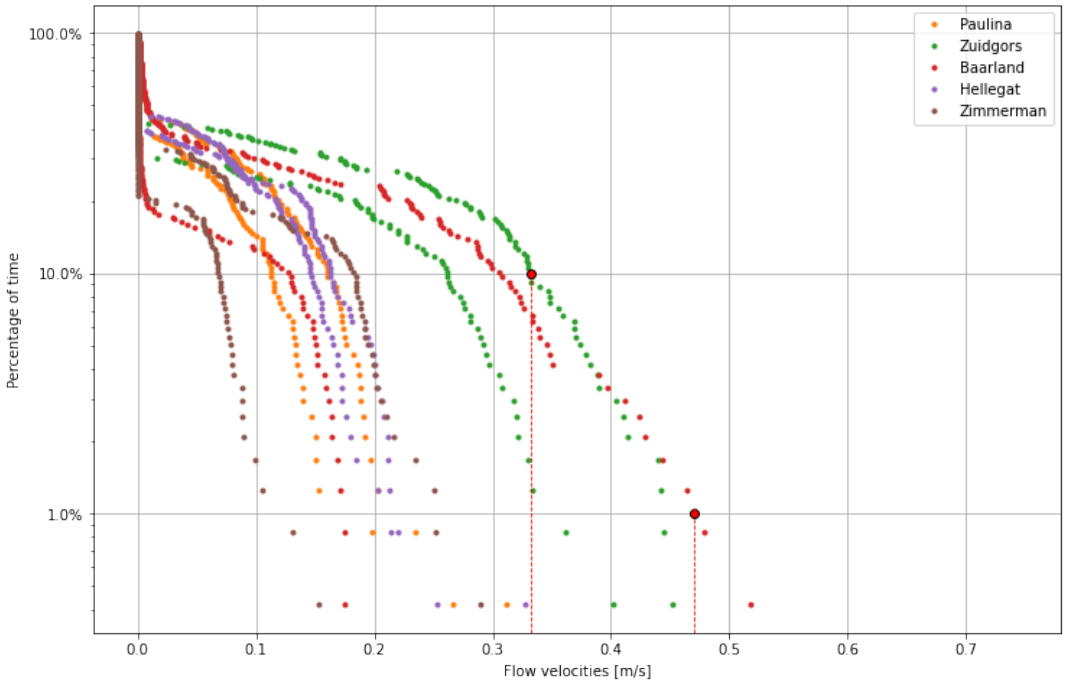

Figure 3.13: Return levels for flow velocities occurring in front of salt marsh vegetation during growth season (daily conditions). Vertical dashed lines (red) denote maximum value observed at characteristic percentages of exceedance. Two signals were used per location, indicated by two curves for every site.

Large variability in flow velocities between different salt marsh locations is presented in Figure 3.13. This can be a result of the previously explained uncertainty introduced by the location of the observation points. However, results also show that flow velocities at all salt marsh locations fall below 0.33 m/s and 0.47 m/s (vertical dashed lines) at 10% and 1% of the time, respectively. These magnitudes can serve as an upper limit value for occurring flow velocities in the proximity of salt marsh habitats. Nevertheless, given the selection of the observation points, it is important to keep in mind that these results can be slightly overestimated, which means that flow velocities occurring exactly at the marsh edge are likely to be lower.

Flow velocities found at the additional observation sites were similarly assessed and later compared to the results retrieved from the mature salt marsh locations (Figure 3.14). Model output in 'No-marsh loc. 1' and 'No-marsh loc. 2' show a a variable behavior, but they nonetheless fall below the upper limits found in mature salt marsh locations. However, 'No-marsh loc. 3' experiences flow velocities that fall well beyond the previously suggested thresholds, which could explain the absence of vegetation in this location. However, given that this site is located in the proximity of a tidal channel (Figure 3.3), a similar issue as the one found in 'Hoofdplaat' is likely to be occurring in this location.

Curves at 'Salt marsh patch' locations, as well as 'Tidal flat 1', show that three 'Salt marsh patch' sites and the previously mentioned tidal shoal fall below the flow velocities limits established in salt marsh locations. However, 'Salt marsh patch 4' and 'Tidal flat 2' exceed the proposed flow velocity thresholds by at least one of the characteristic percentages of occurrence. This is likely due to the fact that 'Tidal flat 2' sits at a lower elevation, experiencing flood events more frequently (also shown in the inundation-free period analysis), and hence encountering higher flow velocities than at higher tidal shoals . For 'Salt marsh patch 4' it could be due to its proximity to tidal channels.

The non-vegetated observation points, whether they are 'Tidal flats' or 'No-marsh locations', that show similar flow velocity magnitudes than vegetated locations can be an indication that additional variables enables the presence of this habitat. Figure 3.14 also shows that sites located in the proximity of deep tidal channels experience the highest flow velocities, which can serve as an additional qualitative indicator for habitat

suitability. Such locations include 'No marsh loc.2', 'Marsh patch 4', and 'Tidal flat 2'.

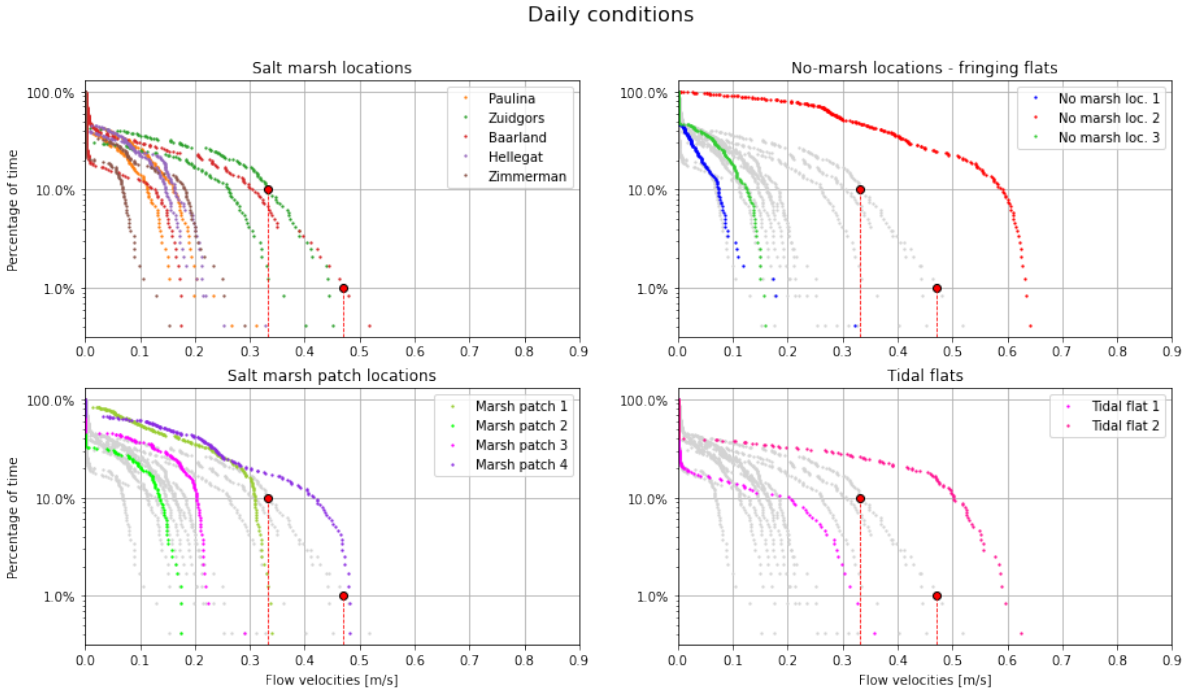

Figure 3.14: Comparison of occurring flow velocities in front of different observed locations (daily conditions).

Storm conditions

The previously presented model outputs represent daily conditions within the Western Scheldt, and serve as a first step in assessing flow velocities occurring within the estuary. As a follow-up step, the boundary conditions were adjusted in order to model storm conditions at every observation site. All water level time series records were increased by 1.0 m to account for storm surge conditions, and the imposed wind speed was increased to 20.0 m/s. The observation points within the model remained the same and the simulation time was set to two days during spring tide, since this tidal cycle gives the highest flow velocities. A comparison between the flow velocity signals during daily and storm conditions at one location is presented in the following figure (comparable with Figure 3.12):

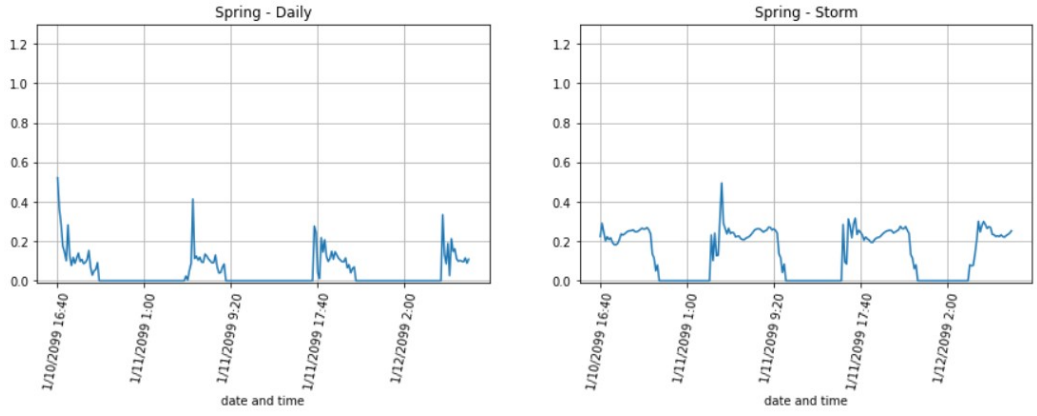

Figure 3.15: Comparison of flow velocity signal at one location during daily (left panel) and storm (right panel) conditions.

The percentage of time that flow velocities were exceeded in all locations is presented in Figure 3.16. Contrary to the assessment during daily conditions, the observation points at Hoodfplaat were included in this evaluation since it was possible to retrieve flow velocity readings on the salt marsh itself. During daily conditions, it was only possible to evaluate flow velocities occurring in the tidal channel in front of it. An observation that

can be drawn from this analysis is that flow velocities occurring in salt marsh locations do not differ largely from the ones found during the daily - spring tide scenario. The magnitudes exceeded 10% and 1% of the time increased from 0.34 m/s to 0.41 m/s, and from 0.52 m/s to 0.62 m/s. This translates to the fact that larger depths have minimal impact on flow velocities occurring at salt marsh locations within the Western Scheldt.

The additional observation sites respond similarly as during daily conditions: flow velocities occurring at 'Salt marsh patch locations' fall below the limits or approaches the upper limit; and 'No marsh loc. 2' surpasses the proposed thresholds. Nonetheless, 'Tidal flat 1' now greatly exceeds the observed flow velocities occurring at mature salt marsh locations, whereas during daily conditions it fell well below these limits (Figure 3.14). This variability under different scenarios shows that this tidal shoal is highly dynamic and experiences high flow velocities during higher water levels. In addition to this, its proximity to the main shipping channel exposes this location to ship-induced waves and currents, which magnitudes can reach up to 0.70 m and 1.0 m/s, respectively (Schroevers et al., 2011).

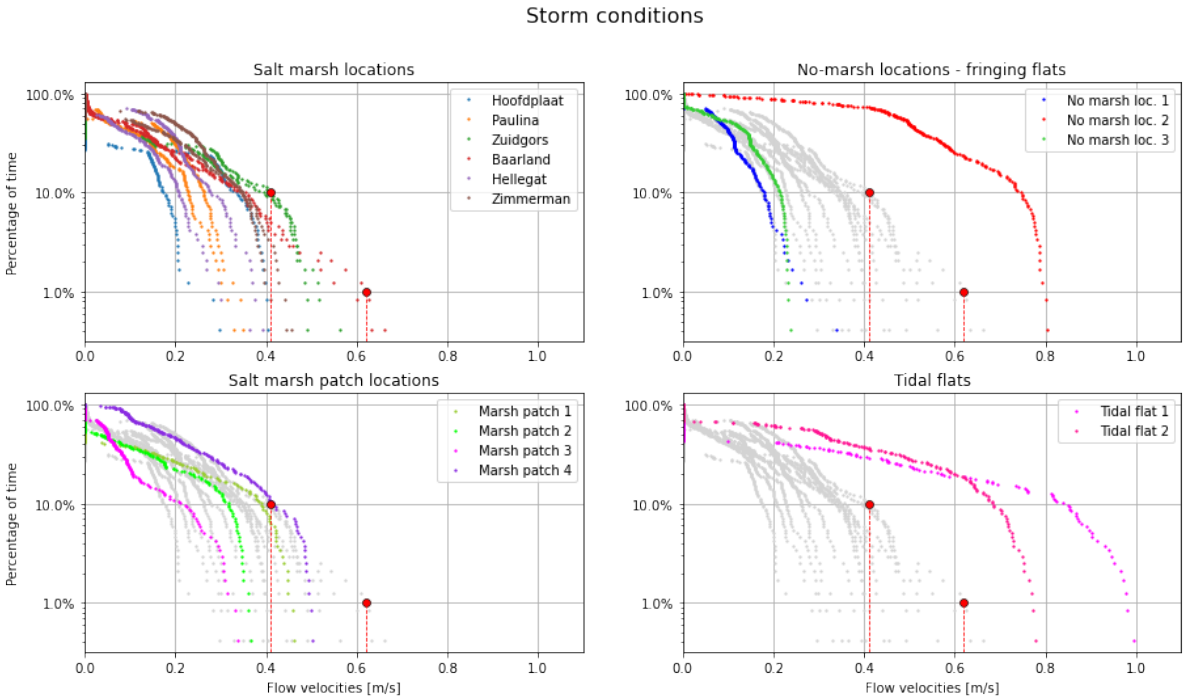

Figure 3.16: Comparison of occurring flow velocities at different observed locations (storm conditions). Vertical dashed lines (red) denote maximum value observed at characteristic percentages of exceedance.

3.3.2. Wadden Sea

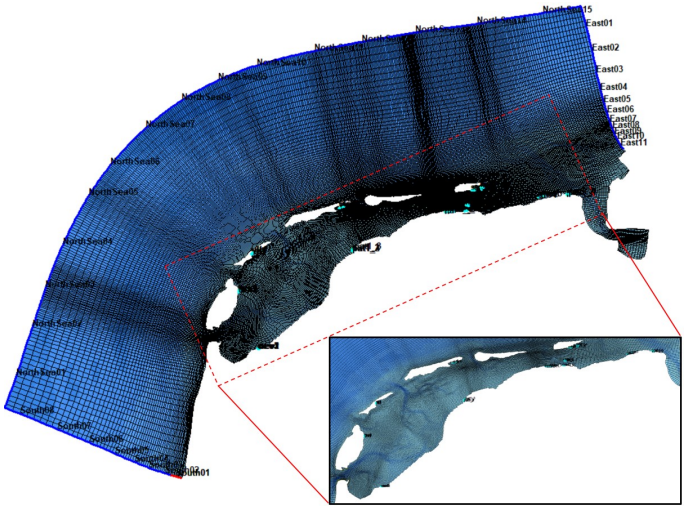

Figure 3.17: Spatial extent of the Delft3D model used for the depth-averaged flow velocity analysis in the Wadden Sea.

Computation time for the Wadden Sea model took far less when compared with the Western Scheldt simulations; hence, modelling of daily hydrodynamic conditions for a month was assumed to be necessary and sufficient. Results of the computations are presented in Figure 3.18. It is relevant to mention that similar limitations as the ones found in the Western Scheldt analysis were found, such as the coarse spatial resolution that makes it difficult to observe the exact location of the salt marsh edges. A quick check was performed with the water depth given as model outputs, in order to determine whether the observation points were comparable with the depths gathered from the inundation-free analysis. Locations that did not comply with this comparison were not included and the results.

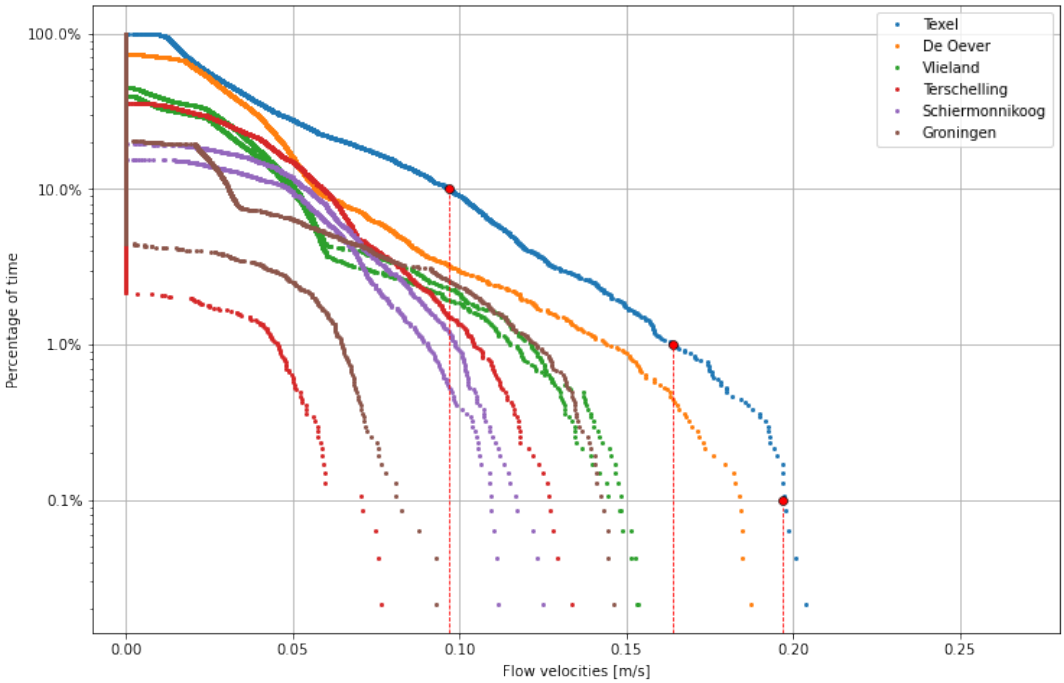

Figure 3.18: Return levels for flow velocities occurring in front of salt marsh sites in the Wadden Sea during growth season (daily conditions). Vertical dashed lines (red) denote maximum value observed at characteristic percentages of exceedance. Two signals were used per location, indicated by two curves for every site.

Results from Figure 3.18 show the flow velocities occurring in the proximity of salt marsh locations. Even though high variability is found in the lower probability levels (0.1 and 1.0%), it seems that at most of the locations the flow velocity occurring 10% of the simulation time approaches $0.10 m/s$. The upper limiting velocities corresponding to the 1.0% and 0.1% approach $0.16 m/s$ and $0.19 m/s$, respectively. When comparing these magnitudes with the results obtained in the Western Scheldt, it is clear that flow velocities magnitudes differ. While the 10% occurring flow velocity in the Western Scheldt approximates $0.33 m/s$, this value is not even exceeded the 0.1% occurring velocity in the Wadden Sea locations. Regardless of this observation, model output was post-processed at all the previously selected observation locations and studied in detail for daily conditions;storm conditions were not simulated in this system. Results are presented in Figure 3.18.

The difference in magnitudes between sites is evident across all observation locations. 'No-marsh loc. 2' was not included in these results due to the difficulty of placing an observation point in the model domain. It's proximity to a tidal channel resulted in a location that presented no dry period (contrary to the findings in the inundation-free period analysis and satellite imagery). 'No-marsh loc. 1' falls within the flow velocities found in vegetated areas and coincides with dry period findings, suggesting that this indicator is not a dominant indicator at this location. Similar behavior can be found in 'Salt marsh patch' locations.

Flow velocities in 'Tidal flat' locations exceed the salt marsh velocities by a factor 3 and 2 at the 10% and 1% return levels; however, this results also suggest that these locations experience flooding 100% and 90% of the time, contradicting results found in the inundation-free period analysis. It is possible that these results are due to the uncertainty introduced by the selection of the observation points within the model, as well as the underlying bathymtery in the model, since high flooding periods were observed in all observation locations (4) placed around the estimated 'Tidal flat' sites.

It is worth mentioning that even though some conclusions can be drawn from the occurrence of flow velocities in the Wadden Sea locations, even the most exceeded magnitudes fall well below the limit values found in the Western Scheldt analysis. Therefore, the flow velocity results found in the Western Scheldt analysis will be used for further reference in this thesis.

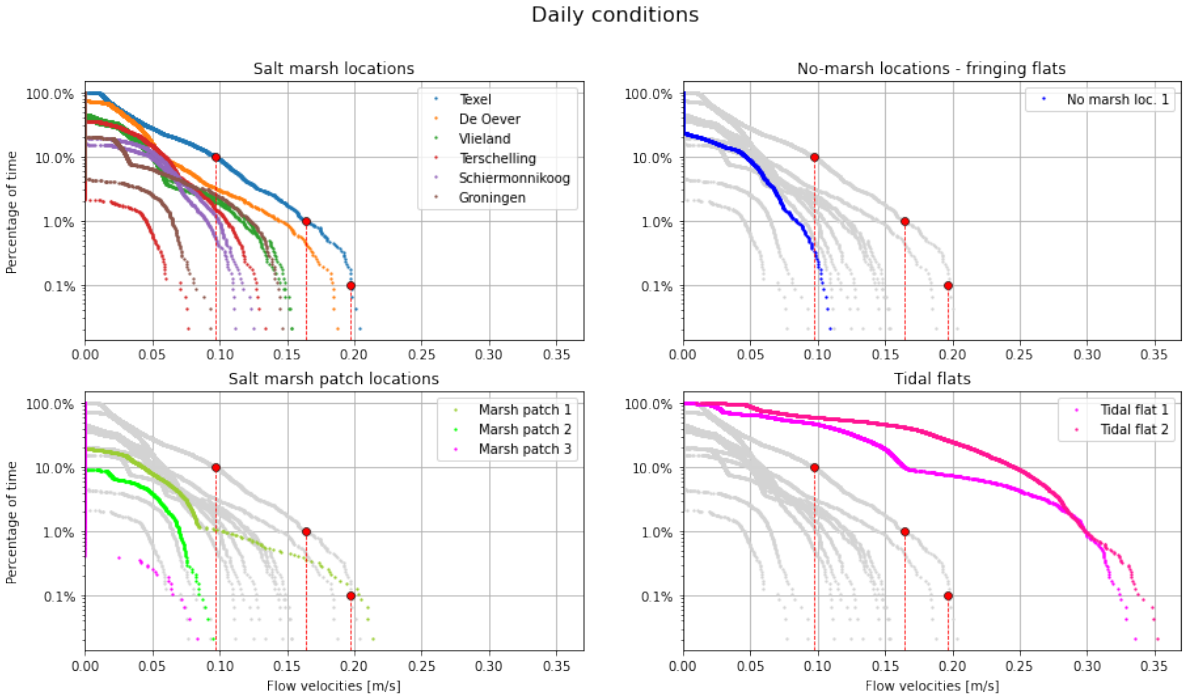

Figure 3.19: Comparison of occurring flow velocities at different observation points in the Wadden Sea model. Vertical dashed lines (red) denote maximum value observed at characteristic percentages of exceedance.

3.4. Wave height

As occurred with the water level data availability, Rijkswaterstaat's database provides wave data at locations that do not coincide with the locations of interest within this thesis; hence, wave heights occurring at all studied sites were modelled by means of a wave growth formulation as adjusted by Young et al. (1996) (Eq. 3.1), which is intended to describe wave growth of locally generated and fetch limited waves propagating in finite water depths. This formula was chosen since the location of interest at every site is on the seaward side of the marsh edge. This means that the incoming waves propagate over the mud flat in front of the salt marsh, which is described by shallow or intermediate water conditions.

$$H_s = \frac{U_{10}^2}{g} \cdot \tilde{H}_\infty \left\{ \tanh\left(0,493\tilde{d}^{0,75}\right) \cdot \tanh\left(\frac{3,13 \cdot 10^{-3} \tilde{F}^{0,57}}{\tanh\left(0,493\tilde{d}^{0,75}\right)} \right) \right\}^{0,87} \tag{3.1}$$

Nonetheless, Equation 3.1 introduces some uncertainty to the analysis given that it estimates H_s with both a constant water depth and wind speed. In reality, both of these variables vary in space (water depths along a transect) and time (water levels and wind magnitude). For the sake of simplicity, the bed level elevation of both water system's bottom was assumed to be uniform for all computations; however the tide-induced water level variations computed from the triangular interpolation step presented in Section 3.2 were used to introduce temporal variability into the water depth variable. For the same purpose, wind speed time series were retrieved from the Rijkswaterstaat database. Each wind speed data point is assumed to exert a permanent force during the propagation of the simulated wave until the mud flat in front of the salt marsh.

Given that the water level time series and wind speeds were retrieved from the same source (RWS), the same time step of 10 minutes was used to model wave propagation within the systems. Regarding wind climate, and considering the spatial extent of each water system (Figure 3.2), records from RWS's station 'Vlissingen' were selected as representative for the Western Scheldt; while stations 'Vlieland' and 'Lauwersoog' were chosen to describe the Wadden Sea. The wind velocity magnitude and wind direction recorded in the aforementioned measurement stations is described in Figure 3.20 for the Western Scheldt, where the dominant wind direction occurring during the months that comprise the current study period (growth season 2020) is also shown.

Fetch was measured for every wind direction that acts on each observation site, as presented by the wind roses on Figure 3.20. Neglected wind directions were the ones that occurred from the landward side of each site, where usually a dike serves as a flood defense (except for 'Tidal flat' locations). Satellite imagery showed that when the tide is low, the fetches on some locations were reduced due to the emergence of a tidal flat. This temporal variability of certain fetches was also included in the wave growth modelling. The nature of the wind climate within the water systems characterize certain locations as 'exposed' or 'sheltered'; for example, the dominant SW wind direction in the Western Scheldt generate more exposed conditions on the northern banks of the estuary, while southern banks remain sheltered from the dominant wind direction. This characteristic was also pointed out by Callaghan et al. (2010).

The bottom bed level elevation was estimated from several transects retrieved from the Vaklodingen database. An example is shown for transects taken in the Western Scheldt locations 'Zuidgors' and 'Hellegat' (Figure 3.21). The characteristic bed level, denoted by the horizontal red line, was approximated as the mean value along the transects. The horizontal blue dashed line denotes the mean high water during spring tidal cycle (MHWS), and was computed from the previously retrieved water level measurements (Section 3.2). Nevertheless, Figure 3.21 serves only as visual guide for the fixed bed bottom used for the model, since the water level vary at each time step.

Figure 3.20: Example of wind data characteristics retrieved from the Rijkswaterstaat database, Vlissingen station. Displayed wind rose shows southwest winds as the dominant wind direction (highest probability of occurrence) during growth season 2020.

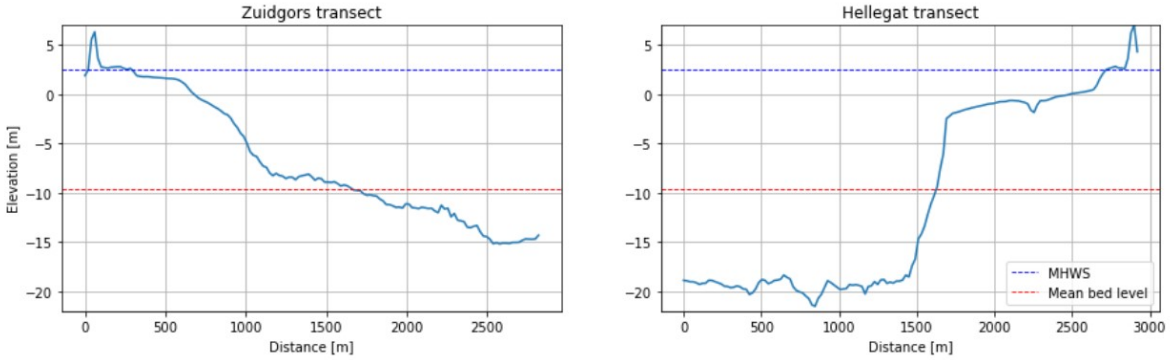

Figure 3.21: Parallel transects of bed elevation in front of salt marsh locations at Zuidgors (left) and Hellegatpolder(right), derived from the Vaklodingen database. Mean bed level for the Western Scheldt estuary characterized by z = - 9.60m (red dashed line).

Additional to the aforementioned considerations, wave growth over the foreshore was limited to 40% of the water depth at the output location corresponding to each time step. Initial results modelled with all previous considerations were validated with wave measurements gathered from previous research done in 'Hellegat' in the Western Scheldt (Vuik et al., 2016a), and in 'Groningen' in the Wadden Sea (Vuik et al., 2018b). Results of the validation step are presented in Appendix A. Finally, Equation 3.1 was used to compute H_s for every occurring wind on each location of interest. The resulting wave heights were processed as done in previous sections to determine the probability of occurrence of each H_s.

3.4.1. Western Scheldt

Figure 3.22 shows that most of the selected salt marsh locations experience similar incoming wave heights, besides 'Hoofdplaat' where wave action is reduced due to the presence of a high-elevation vegetated tidal flat that lies in front of this location (Figure 3.3). This reduces the fetch for wind directions acting on in this site, and hence wave heights are low, relative to other locations. A clear distinction cannot be made between sites located on the northern and southern banks of the estuary, meaning that even though northern banks are more exposed to dominant wind directions, incoming wave height varies only slightly for more frequent events. For less frequent occurring wave heights, southern banks can even experience higher waves. This

can very likely be linked with the findings by Willemsen et al. (2020) regarding expanding or stable foreshores found on the northern banks, while southern banks experience retreat or only a slight increase.

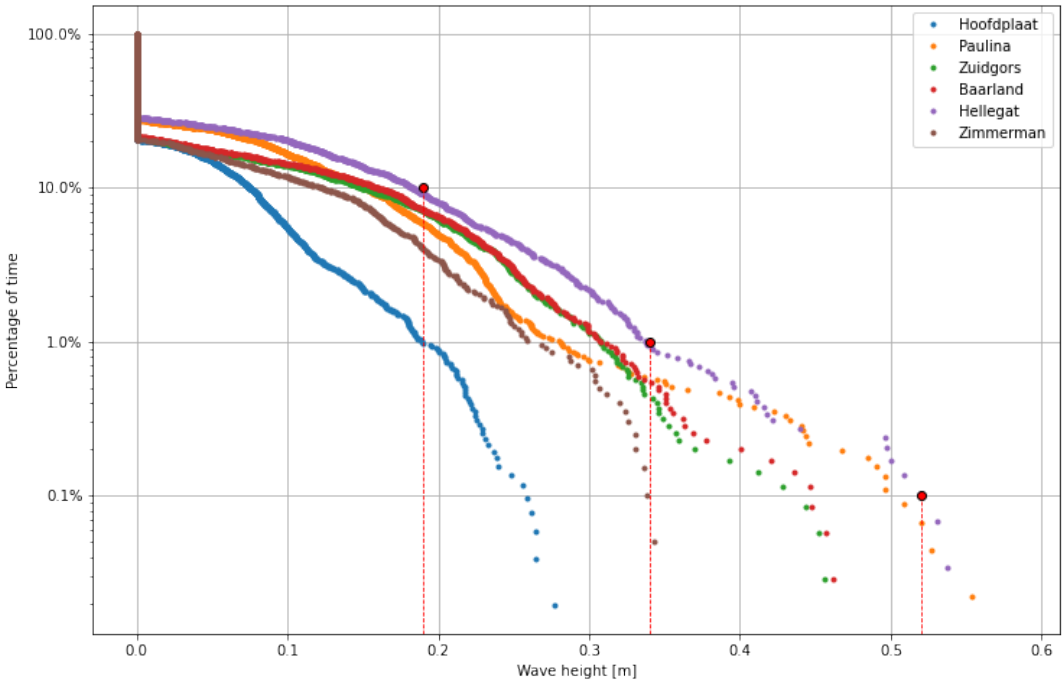

Figure 3.22: Return levels for significant wave height occurring in front of salt marsh vegetation during growth season. Vertical dashed lines (red) denote maximum value observed at characteristic percentages of exceedance.

Figure 3.22 also shows upper limits for wave action in salt marsh habitats during the growth season. A maximum H_s value of 0.19m, 0.34m, and 0.52m are found for 10%, 1%, and 0.1% of the time, respectively (vertical dashed lines). For the lowest probability of occurrence, there is large variability in wave height magnitude. Nevertheless, Figure 3.22 shows that the 0.60m wave height limit is never exceeded during the studied period, which can serve as a maximum wave height threshold value. Following the approach done in Section 3.3, these initial findings were assessed with the resulting waves at the additional sites (Figure 3.23).

When compared to 'No-marsh locations', the wave heights occurring at 'No-marsh loc. 1' and 'No-marsh loc. 3' exceed the previously established limits for salt marsh habitats; while 'No-marsh loc. 2' approaches these limits. Results from several 'Salt marsh patch' locations either resemble or fall below the proposed limit values for salt marsh establishment, however waves at 'Salt marsh patch 1' approach the thresholds at many return levels. This can be the reason behind the presence of small vegetation at this site (Figure 3.3), instead of expanding marshes. Finally, when observing the 'Tidal flat' sites, it is clear that a higher bed level elevation ('Tidal flat 1') prevents the propagation of waves at this location, causing waves to fall below the proposed ranges. Meanwhile, 'Tidal flat 2' experiences wave heights that exceed the proposed salt marsh habitat limits at the 1% and 0.1% occurrence time.

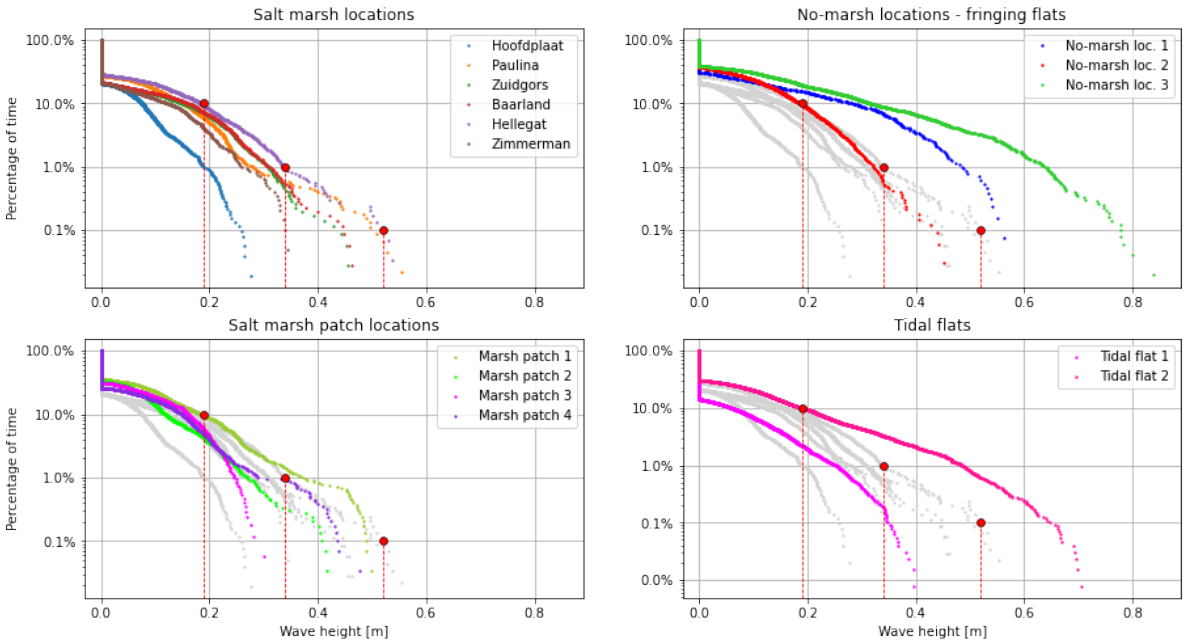

Figure 3.23: Comparison of significant wave height occurrence between different observed locations in the Western Scheldt.

3.4.2. Wadden Sea

Results computed in this water system were of lower magnitude (Figure 3.24) than the ones found in the previous subsection. Considering that this thesis is focused on general forcings that limit the presence of salt marsh ecosystems, the following plots do not show the characteristic values gathered from the salt marsh locations within the same system, but from the higher thresholds retrieved from the Western Scheldt analysis (depicted as vertical red dashed lines). Figure 3.24 shows that all observed salt marsh locations in the Wadden Sea fall below the proposed wave height threshold values, which favors previous results.

A similar supposition can be made from 'Salt marsh patch locations' presented in Figure 3.25, given that wave heights occurring at all characteristic sites fall below the limit values. Additionally, when compared to the occurring wave heights at mature salt marsh locations within the same system (plotted in light-gray, for reference), sites exclusively with pioneering vegetation in the Wadden Sea experience considerable milder wave heights. Nonetheless, Figure 3.25 similarly indicates that wave height threshold values seem to be complied with at non vegetated locations, such as in 'No-marsh loc. 1' and on both 'Tidal flat' sites. These results would suggest that vegetation could be present at these sites, yet none is found.

However, when comparing the occurring hydrodynamic forcing between the observed locations within the water system itself (leaving aside the threshold values gathered from the Western Scheldt), results from Figure 3.25 show that milder conditions are found in vegetated sites, while harsher conditions occur at non-vegetated locations. This observation suggests that wave height incidence alone might not be a limiting factor for salt marsh establishment, but it is however linked to an additional underlying wave-phenomena that hinders the development of pioneer vegetation. Literature suggests that sediment dynamics and sediment composition play a crucial role in salt marsh habitat development and survival, for which reason the wave-induced load exerted on the underlying sediment will be assessed in the following section.

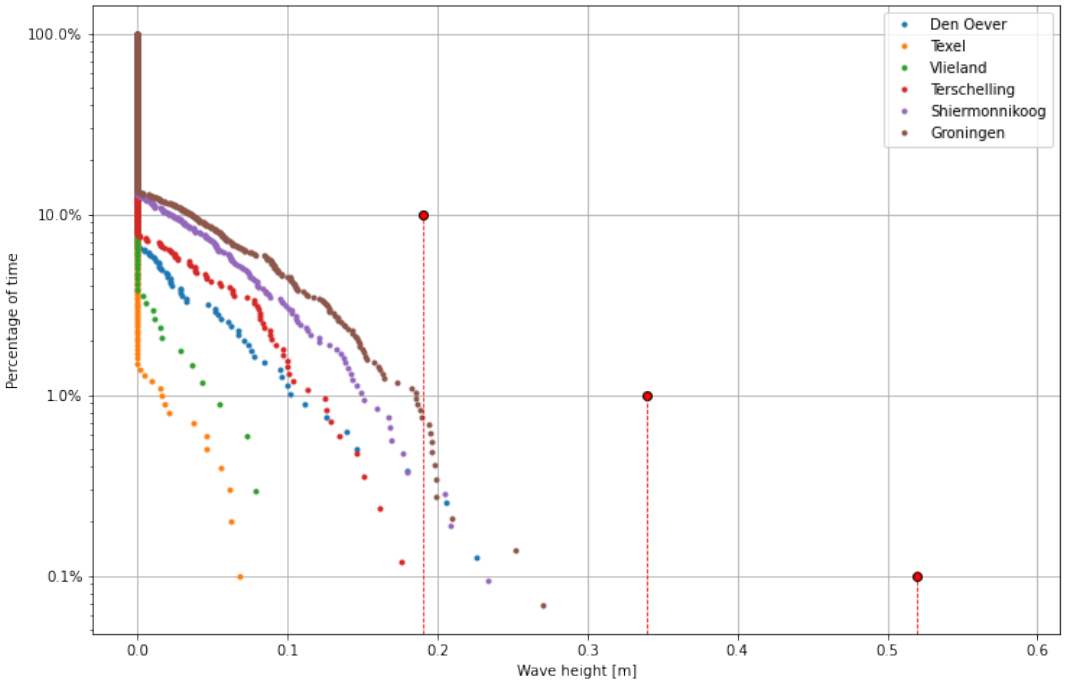

Figure 3.24: Return levels for significant wave height occurring in front of salt marsh vegetation during growth season. Vertical dashed lines (red) denote proposed threshold value for characteristic percentages of exceedance.

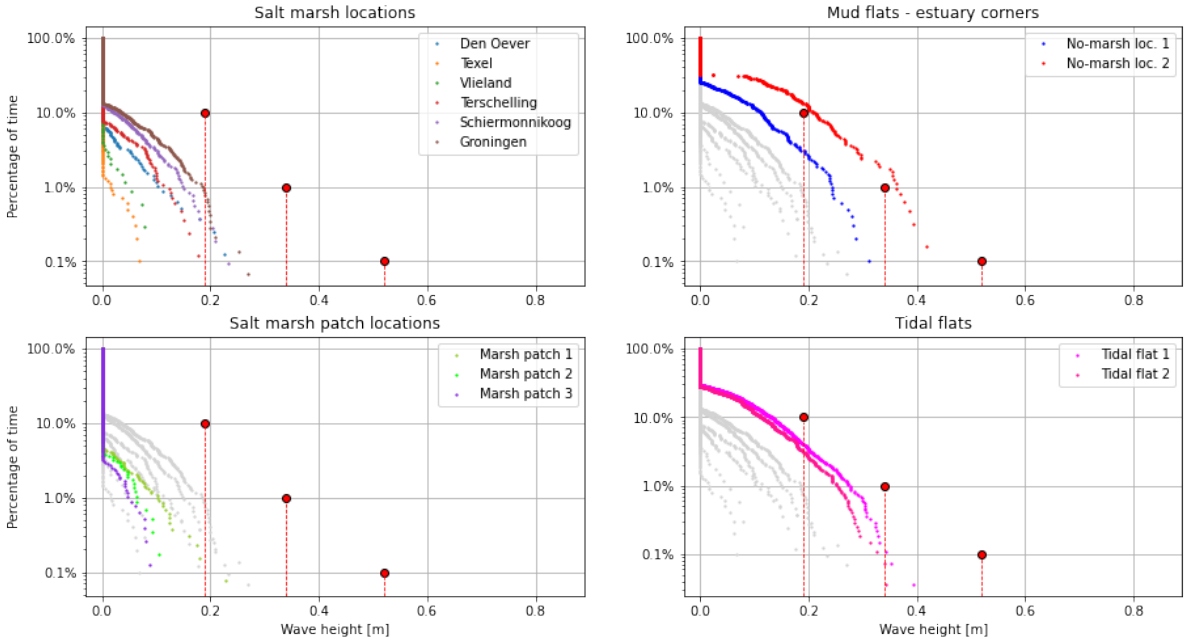

Figure 3.25: Comparison of significant wave height occurrence between different observed locations in the Wadden Sea.

3.5. Dimensionless wave-induced excess bed-shear stress

The previous analysis performed on both water systems focuses purely on the hydrodynamics to which salt marshes are exposed. Even though several initial estimates of threshold values were found, there were locations that were not fully explained by the assessed indicators. For example, comparison of the wave height magnitudes and exposure to flooding periods, the absence of vegetation in Wadden Sea locations 'No-marsh

loc. 1', 'Tidal flat' 1 and 2 could not be explained be either hydrodynamic limit values computed in mature marshes on either of the two evaluated water systems. For this reason, and as pointed out in Chapter 2, other indicators might be preventing the development of vegetation.

It is hypothesized that not only the loading (hydrodynamics) needs to be analysed, but also the resistance of the subsurface (sediment composition) in order to better explain the presence or absence of salt marshes. This hypothesis falls in line with the 'Window of Opportunity' concept introduced in Chapter 2, which suggests that sediment erosion is the main mechanism behind salt marsh seedlings failure, given that the short size of such seedlings in the first days after germination limits the drag forces acting on the seedlings themselves (Hu et al., 2015). Moreover, this additional analysis is brought forward given that soil composition generally varies between the two water systems. As described in previous sections, under daily conditions the Western Scheldt experiences a harsher hydrodynamic forcing than the Wadden Sea. Therefore, both the mud and water content found in the Wadden Sea mudflats are greater than the the ones that characterize the Western Scheldt estuary. Hence, in order to account for sediment response to external forcing, a dimensionless wave-induced excess bed-shear stress factor was computed, described by Equation 3.2.

$$S = \frac{\tau - \tau_{crit}}{\tau_{crit}} \tag{3.2}$$

The critical bed shear stress τ_{crit} is defined as the threshold value for bed shear stress above which particles become entrained (incipient motion), and it is determined by several factors regarding the composition of the soil, such as grain size, mud fraction, and dry bulk density. For this reason, it is necessary to characterize the soil composition in both water systems in order to approximate the soil response to the previously modelled wave climate.

It is important to note that the soil in both water systems is primarily characterized by a sand-mud mixture, which behaves differently for a varying mud content. van Rijn (2020) suggests that when the fine fraction (% fines < $63\mu m$) is less than 30%, the mixture's critical bed-shear stress is dominated by the sand fraction, which is characterized by $\tau_{crit} = 0.2 - 0.4 N/m^2$. Moreover, a distinction is made between different soil dry bulk densities, defining firmly and weakly consolidated sand-mud mixtures with $\rho_{dry} > 800 kg/m^3$ and $\rho_{dry} < 400 kg/m^3$, respectively. On the contrary, when the sand-mud mixture holds a mud content greater than 70%, then the dominant critical bed shear stress is described by the mud fraction, which is in the order of $\tau_{crit} = 0.1 - 0.3 N/m^2$ for a weakly consolidated mixture. van Rijn (2020) proposed Equations 3.3 and 3.4 to describe the aforementioned characteristics when computing the critical bed-shear stress for sand-mud mixtures, which were used for this thesis.

$$\tau_{\text{crit, fine fraction}} = \left(1 + p_{\text{fines}}\right)^{\beta} \tau_{\text{crit, silt}} \tag{3.3}$$

$$\tau_{\text{crit, sand fraction}} = \left(1 + p_{\text{fines}}\right)^{\beta} \tau_{\text{crit, sand}} \tag{3.4}$$

Where,

$$\beta = \left(1 + \frac{\rho_{\text{dry, mixture}}}{\rho_{\text{dry,max}}}\right)^{\alpha} \quad with \quad \alpha = 2 \tag{3.5}$$

For Equations 3.3 and 3.4, van Rijn (2020) proposed the critical bed-shear stresses for fine sand and silt as $\tau_{crit,sand} = 0.2 N/m^2$ and $\tau_{crit,silt} = 0.1 N/m^2$. Moreover, the dry bulk density of the mixture assumed for Equation 3.5 was that of weakly consolidated soils and set equal to $\rho_{dry} = 300 kg/m^3$; while $\rho_{dry,max}$ corresponds to the maximum dry bulk density of a sand-mud mixture and equal to $\rho_{dry,max} = 1600 kg/m^3$ (van Rijn, 2020).

A detailed and individual characterization of the soil composition at all locations would be optimal for this analysis; however, this approach is out of the scope of this thesis and a general characterization of both systems was therefore performed as a first attempt to assess soil response to hydrodynamic loading. The Wadden Sea soil composition was approximated as described by Herman et al. (2016), who found the mud content in the corners of the Ameland - Holwerd shipping channel to be in the order of 75%, while the sand fraction

consisted of roughly 10%. Even though a lower mud content was reported in the middle point of the aforementioned channel (45%), it was not considered to be representative for the current analysis, given that it is affected by higher flow velocities, which is not observed on the mudflats fronting the observation locations described in this thesis (Section 3.3). With this approximation, and given the description presented by van Rijn (2020), the critical bed shear stress used to characterize the locations in the Wadden Sea system was approximated as $\tau_{crit} = 0.25 N/m^2$.

The Western Scheldt was approximated as a sandier environment ($p_{fines} < 0.30$), given the previously described harsher daily hydrodynamic conditions occurring in this estuary. Even though a site-specific soil characterization was not performed, a general description of the soil composition in the Western Scheldt was performed by McLaren (1994) and adapted by Dam et al. (2013), where a distinction can be observed between muddier and sandier locations along the system (Figure 3.26). Dam et al. (2013) presents a maximum mud content of up to 60% at the muddier locations in this estuary, hence the mud fraction is considered to be dominant for these sites, as defined by van Rijn (2020). Both vegetated and non-vegetated sites such as 'No-marsh loc. 1', 'No-marsh loc. 2', 'Marsh patch2', and 'Marsh patch 3' fall in this description. At the sandier locations, the mud content ranges roughly between 20% and 40% (Dam et al., 2013), therefore an average value of $p_{fines} = 30\%$ was assumed for the sake of simplicity. Application of Equations 3.3 and 3.4 returns critical bed-shear stress values of $\tau_{crit} = 0.24 N/m^2$ and $\tau_{crit} = 0.45 N/m^2$ for muddier and sandier locations in the estuary, respectively.

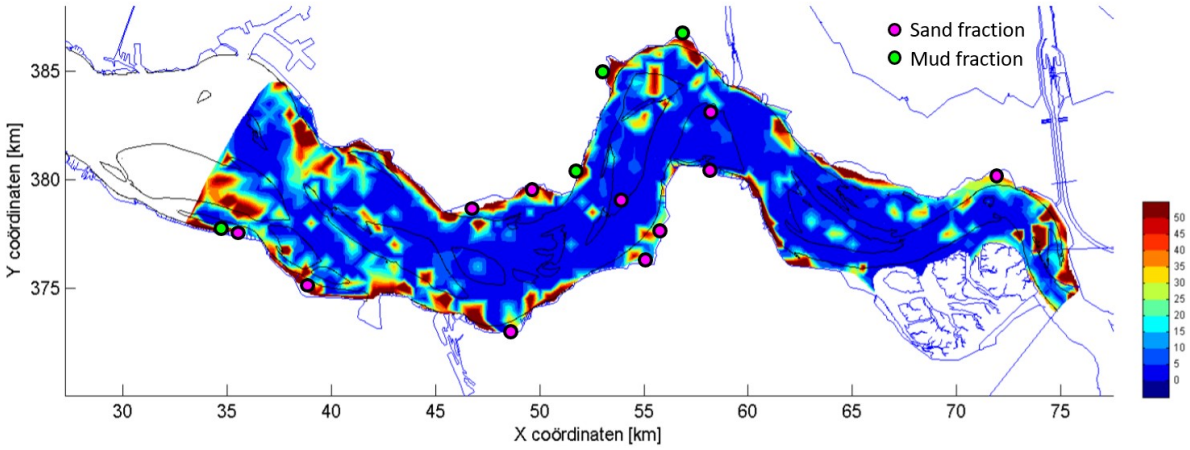

Figure 3.26: Bed composition of the Western Scheldt, as proposed by McLaren (1994), and adapted by Dam et al. (2013). Magenta dots denote locations assumed to have a dominant sand fraction, while the green dots denote more muddier site. The color bar on the right side of the Figure describes the mud content of the soil (percentage of fines < 63μm).

The previous results for characteristic critical bed-shear stresses for each system is presented in Table 3.3.

Table 3.3: Summary of sand-mud soil mixture characterization for both water systems, based on literature presented by van Rijn (2020).

Water system	Dominant fraction	Mud content (< 63μm)	τ_{crit} [N/m^2]
Western Scheldt (1)	Sand frac.	0.30	0.45
Western Scheldt (2)	Mud frac.	0.60	0.24
Wadden Sea	Mud frac.	0.75	0.25

The actual maximum wave-induced bed-shear stress is derived from linear wave theory, and responds to Equation 3.6:

$$\tilde{\tau}_w = 0.5 \rho f_w \tilde{u_0}^2 \tag{3.6}$$

The friction factor f_w was computed for a rough turbulent hydraulic regime (Soulsby, 1997), described by Equation 3.7, where the relative roughness r is computed as a function of the peak orbital excursion amplitude and the Nikuradse bed roughness coefficient ($r = \frac{\xi}{k_s}$):

$$f_w = 0.237 r^{-0.52} \tag{3.7}$$

The Nikuradse bed roughness k_s is usually given as a function of the grain size. For finer sediment, the bed roughness coefficient describes the height of the bed ripples. A relationship between the Manning number, the Nikuradse coefficient, and the water depth was used to characterize k_s in the Western Scheldt and the Wadde Sea, and is presented in Table 3.4.

Table 3.4: Description of bed roughness coefficients (Nikuradse coefficient) used in each of the water systems.

Water system	**Surface type**	**Manning n**	**Nikuradse k_s [m]**
Western Scheldt	Estuarine water	0.025	0.002
Wadden Sea	Muddy bottom	0.012	0.001

To compute the amplitude of the velocity near the bottom, the wave period is required additionally to the wave heights computed in previous subsections. In order to account for the aforementioned wave heights, a relationship between the two wave properties was used. Measurements of wave height and wave period occurring at the salt marsh location of Hellegat in the Western Scheldt (Vuik et al., 2016a) provided the relation between the two parameters (Figure 3.27), which was used to generate an approximation of the wave period for all computed wave heights. Wave length was derived from the dispersion relationship with the approximation by Fenton, which gives an exact solution in deep and shallow water conditions, and an error of 0.05% in other situations (Holthuijsen, 2010).

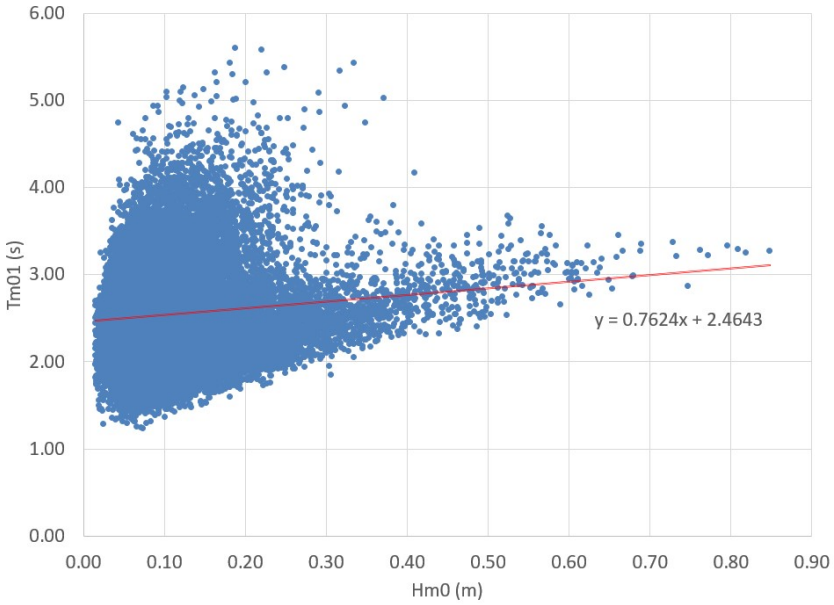

Figure 3.27: Relationship between wave height (H) and wave period (T) retrieved from measurement conducted in the Western Scheldt (Vuik et al., 2016a).

Following the post-processing approach performed in previous sections, the dimensionless excess wave-induced bed-shear stress factor was computed at all study locations and the exceedance curves were plotted with respect to the phenomena modelled at mature salt marshes. A difference worth mentioning is that given the overall milder conditions found in the Wadden Sea, the values used as the reference threshold (vertical red dashed lines in Figures 3.28 and 3.28) are the limiting values computed in the Western Scheldt marshes.

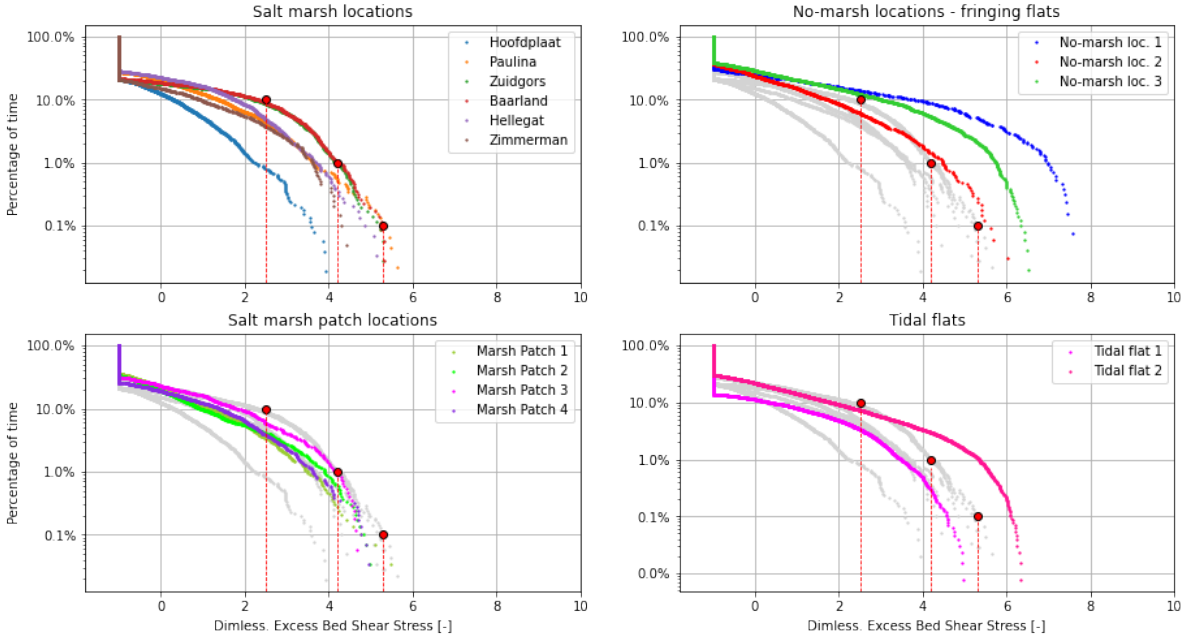

Figure 3.28: Excess wave-induced bed-shear stress computed in the Western Scheldt.

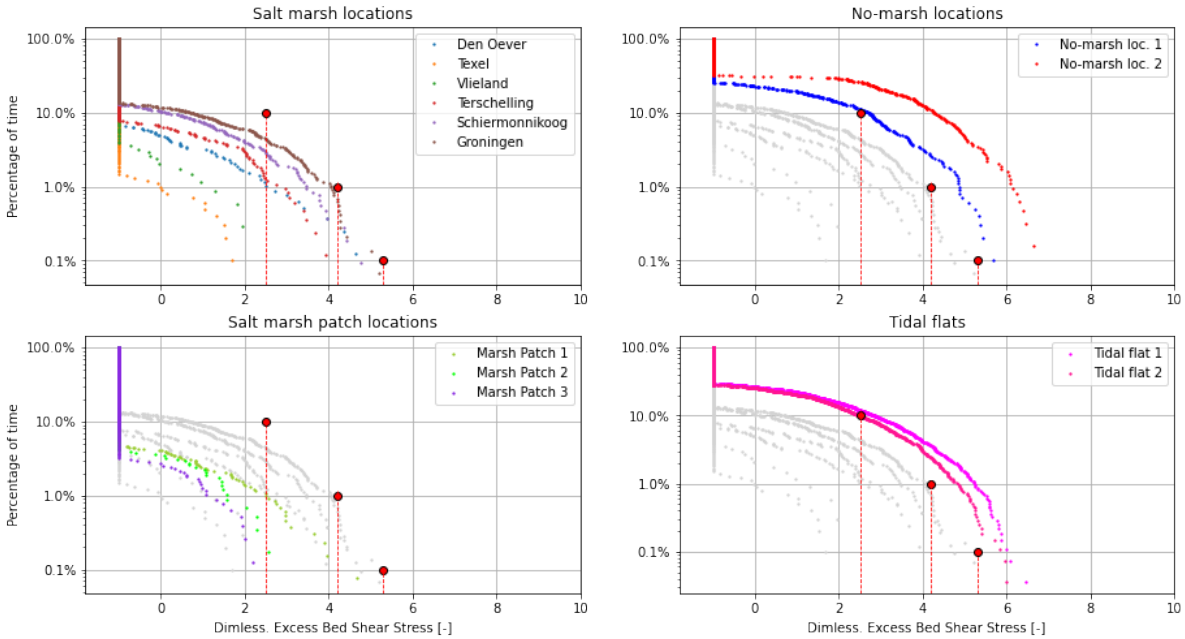

Figure 3.29: Excess wave-induced bed-shear stress computed in the Wadden Sea.

The inclusion of sediment properties in the current analysis provides an additional insight in the factors that play a role in the natural establishment of salt marshes. Results show that at vegetated sites in both water systems, whether they are 'Salt marshes' or 'Salt marsh patches', the computed dimensionless wave-induced excess bed-shear stress factor complies with or falls below the occurring phenomena modelled in mature salt marsh locations. Moreover, the aforementioned Figures show that the upper thresholds found in mature salt marshes in the Wadden Sea now approach the limiting values modelled in the more dynamic Western Scheldt estuary. This occurs in contrast to the wave height analysis, where the magnitudes largely differed between systems at different probabilities of occurrence (Section 3.4, Figure 3.25).

Furthermore, this additional step serves to explain the absence of vegetation in 'No-marsh loc. 1' in the Wadden Sea. At this site, all three previously analyzed indicators complied with the proposed threshold values proposed by study on vegetated sites. However, the bottom right panel in Figure 3.29 shows that the wave forcing modelled on this site are high enough to entrain sediments, which in turn can impede the settling of seeds or establishment of seedlings. The occurrence of this phenomena at this site can also serve as an explanation for vegetation absence at additional non-vegetated sites, such as in 'Tidal flat' locations.

3.6. Discussion

This Chapter presented the analysis performed on salt marsh habitat suitability indicators, which was done in an attempt to quantify threshold values that help explain the presence/absence of this habitat. The assessment was performed by the generation of exceedance curves from data generated through numerical modelling of hydrodynamics and sediment dynamics occurring during the months of April/2020 and July/2020 (salt marsh growth season) at 28 several locations in the Western Scheldt and the Wadden Sea. Habitat suitability indicators were inundation-free period, flow velocity, wave height, and dimensionless wave-induced bed-shear stress factor.

An overview of the results is presented in Figure 3.30, where different hues denote the compliance (or not) of each indicator at every observation location. Green, red, and yellow represent compliance, non-compliance and proximity to the proposed limit value, respectively. The yellow hue (proximity to the limit value) was defined as an arbitrary range per indicator in the following manner: inundation-free period ±3.0 % points; flow velocities, wave heights, and dimensionless excess bed-shear stress ±15%. These ranges were given in order to account for the underlying uncertainty in the determination of these threshold values, as previously explained.

System	Location	Inundation-free period [%]	Flow velocities [m/s]		Wave height [m]			Dimensionless wave-induced BSS [-]		
			Pct. of time		Pct. of time			Pct. of time		
			10%	1%	10%	1%	0.1%	10%	1%	0.1%
Salt marsh limits		> 67.0	< 0.33	< 0.47	< 0.19	< 0.34	< 0.52	< 2.5	< 4.2	< 5.3
Wester Scheldt	No-marsh 1	65.4	0.07	0.17	0.28	0.49	0.56	4.0	7.5	7.8
	No-marsh 2	63.6	0.58	0.63	0.18	0.32	0.44	1.8	4.7	5.8
	No-marsh 3	64.5	0.12	0.15	0.32	0.63	0.78	3.0	5.7	6.4
	Marsh patch 1	71.6	0.31	0.34	0.19	0.37	0.49	1.1	3.5	4.7
	Marsh patch 2	83.9	0.14	0.18	0.12	0.27	0.41	0.5	2.9	3.6
	Marsh patch 3	70.4	0.20	0.22	0.16	0.25	0.29	1.9	4.4	4.9
	Marsh patch 4	78.1	0.42	0.48	0.15	0.30	0.44	1.4	3.6	4.8
	Tidal flat 1*	86.0	0.84	0.97	0.06	0.25	0.35	0.3	3.5	4.6
	Tidal flat 2*	70.0	0.68	0.76	0.20	0.49	0.65	1.7	5.3	6.1
Wadden Sea	No-marsh 1	82.0	0.05	0.08	0.11	0.24	0.31	2.7	4.9	5.7
	No-marsh 2	63.4	0.00	0.00	0.21	0.36	0.42	4.3	6.1	6.7
	Marsh patch 1	96.2	0.04	0.10	0.00	0.10	0.17	0.0	2.5	4.3
	Marsh patch 2	94.0	0.00	0.07	0.00	0.07	0.11	0.0	1.6	2.6
	Marsh patch 3	95.7	0.00	0.06	0.00	0.05	0.08	0.0	1.1	2.2
	Tidal flat 1	74.7	0.16	0.30	0.13	0.28	0.35	2.8	5.2	6.0
	Tidal flat 2	76.4	0.25	0.30	0.11	0.25	0.34	2.5	4.8	5.9

Figure 3.30: Summary of results gathered from habitat suitability indicators observed at locations in the Western Scheldt and Wadden Sea. Harsher conditions modelled in the Western Scheldt sites serve as general salt marsh threshold values. Colors denote agreement (green), proximity (yellow), or disagreement (red) with proposed habitat suitability indicators. * Flow velocities in the Western Scheldt 'Tidal flat' locations correspond to magnitudes gathered from a storm simulation. Salt marsh limits under storm conditions were: 10%=0.41 m/s and 1%=0.62 m/s.

The proposed threshold values for salt marsh habitat suitability are presented in the Figure above (**Salt marsh**

limits). These results suggest that, as found in literature, the presence of this habitat is enabled by the combination of various factors; additionally, it suggests that when comparing two different water systems, it does not suffice to assess the loading on a site of interest (hydrodynamics), but also the resistance (sediment). A relevant proxy for this purpose was considered to be the wave-induced excess bed-shear stress factor, with characteristic values of 2.5, 4.2, and 5.3 exceeded 10%, 1%, and 0.1% of the time. Figure 3.30 shows that in Wadden Sea non-vegetated locations the dimensionless excess BSS better explains the absence of this habitat, considering that purely hydrodynamics predicted vegetation presence.

It is important, however, to keep in mind that even though the previously assessed indicators shed light onto the mechanisms that favor the presence of this habitat, it is the combination of several factors that allow the establishment of salt marshes at a given location. Such is the case of 'Tidal flat' locations in the Western Scheldt, which vegetation presence was ruled out by storm conditions, rather than by daily conditions. Results presented in Figure 3.30 show the proposed threshold values for relevant indicators found in literature, however additional parameters such as water temperature, salinity, and suspended sediment concentration play a major role in salt marshes habitat suitability.

4

Effectiveness: wave height reduction

The following chapter presents the analysis of the (salt marsh) wave height attenuation effectiveness indicators selected in Chapter 2. The assessment was done by means of a sensitivity analysis performed on different wave attenuation formulae found in literature, where several parameters were modified so as to represent different conditions that are likely found in nature, such as deep/shallow water conditions, and different tidal regimes. This analysis aims to provide a first step in the development of an assessment tool for salt marsh habitat introduction as an effective flood defense measure, and it was performed in two sections: i) an initial study of the sole effect of vegetation regarding wave height reduction, and ii) an additional assessment focused on the vegetated foreshore system as a whole, accounting for the added value of the system's change in bathymetry. As a final step, the findings of this Chapter were used to make a qualitative assessment of the water systems treated in Chapter 3.

4.1. Vegetation

The degree of wave height reduction by vegetation was studied in this thesis through two different measurements of effectiveness found in literature: the rate of wave attenuation (per meter length) proposed by Mazda et al. (2006) (Eq. 4.1) and the wave attenuation factor β from the empirical model for waves propagating over vegetated fields, proposed by Mendez et al. (2004) (Eq. 4.2). Given that these Equations are expressed as a function of vegetation properties, wave characteristics, and water depth, they were both used to assess the relative vegetation height (vegetation height/ water depth - h_v/h) of a salt marsh field, which was proposed as an effectiveness indicator in Chapter 2.

$$r = \frac{\Delta H}{H_0} \cdot \frac{1}{\Delta x} \tag{4.1}$$

$$\tilde{\beta} = \frac{B_o H_{rms,o}}{2} = \frac{1}{3\sqrt{\pi}} \tilde{C}_D b_v N H_{rms,o} k \cdot \frac{\sinh^3 k\alpha h + 3\sinh k\alpha h}{(\sinh 2kh + 2kh)\sinh kh} \tag{4.2}$$

Equation 4.1 shows that the wave height reduction factor r is computed in terms of a length scale, in this case the length of the domain Δx; hence, it is not a dimensionless parameter (as with β). Therefore, and in order to compare the results of this analysis to the water systems presented in Chapter 3, the domain length chosen was $\Delta x = 200m$. This selection was done for the sake of simplicity, as well as the fact that most of the observed salt marsh locations range from under 100m up to 300m, depending on the location from which a transect is measured.

4.1.1. Relative vegetation height

In order to account for likely scenarios to which a salt marsh habitat might be exposed to, deep ($kh \sim 3.0$), intermediate($0.3 < kh < 3.0$), and shallow water ($kh \sim 0.3$) conditions were imposed on a 1D model characterized by a spatial extent of $\Delta x = 100m$, fixed bed and water level (hence a constant depth), and a fixed incoming significant wave height H_s, while assigning for a varying peak period T_p, in order to account for the different conditions mentioned above. Moreover, vegetation height h_v was also varied so as to observe the wave height reduction response to ten (10) different h_v/h ratios, ranging roughly between $h_v/h = 0.0 - 0.7$. A summary of the adopted characteristic vegetation and wave parameters is presented in the following Table 4.1, and a schematic of the 1D model is presented in Figure 4.1. It is worth mentioning that this analysis was performed on conditions that approached the limit states for deep and shallow water conditions, hence the values of $kh = 3.13$ and $kh = 0.33$, respectively.

Table 4.1: Summary parameters for sensitivity analysis.

Condition	H_s [m]	T_p [s]	h [m]	kh	h_v/h
Deep water	0.50	3.00	7.00	3.13	0.0 - 0.70
Intermediate water	0.50	3.00	3.50	1.56	0.0 - 0.70
Shallow water	0.40	6.00	1.00	0.33	0.0 - 0.70

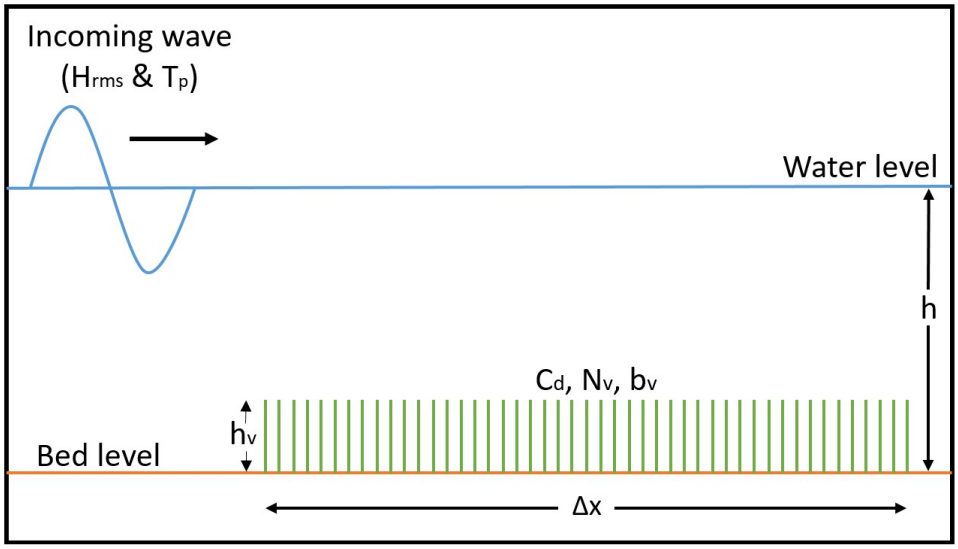

Figure 4.1: Schematic of 1D model used to asses the degree of effectiveness of the relative vegetation height (h_v/h).

Results of the sensitivity analysis are presented in Figure 4.2, for deep, intermediate and shallow water conditions in the top, middle and bottom panels, respectively. The analysis shows that at the imposed deep water limit state condition ($kh = 3.13$), the vegetation is not effective anymore for h_v/h ratios lower than 0.3, meaning that under this condition the vegetation has to extend to at least 30% of the water column in order to play a role on energy dissipation on the wave propagating above it. At values of $0.3 < h_v/h < 0.4$, the effect of vegetation with respect to both β and r (in absolute terms) grows exponentially for increasing h_v/h ratios. A similar trend was found for ratios of up to $h_v/h = 1.0$.

In other words, in deep water conditions the vegetation height needs to occupy at least 30 - 40% of the water column in order to exert drag forces on the incoming wave; else, there is no energy dissipation by vegetation in deep water conditions.

The middle and bottom panels of Figure 4.2 show the transition from deep water conditions to the determined shallow water limit state ($kh = 0.33$). From the two panels it is possible to observe the response change of β and r with increasing h_v/h ratios. Whereas β changes from an exponential into a linear growth, the response of r evolves from exponential into a logarithmic growth, showing an increase of 10% for ratios

$h_v/h > 0.35$.

The response of β suggests that in shallow water conditions the effect of vegetation simply scales linearly with increasing h_v/h, reaching a maximum wave height reduction for emerging vegetation ($h_v/h > 1.0$). The logarithmic response of the r factor is given due to the fact that r is expressed as a function of the length of the domain (Equation 4.1), and for this particular case characterized by a $\Delta x = 200m$, the wave energy dissipation by vegetation increases by 10% for ratios $h_v/h > 0.35$. For the same shallow water condition and a shorter Δx, the response of r resembles the linear increase found for the β factor. It is important to mention, however, that in shallow water conditions the dissipation caused by bottom friction and possibly wave breaking also play a role in wave energy dissipation, and hence in wave height reduction rates. Nonetheless, these dissipation mechanisms were not assessed in the analysis of this effectiveness indicator.

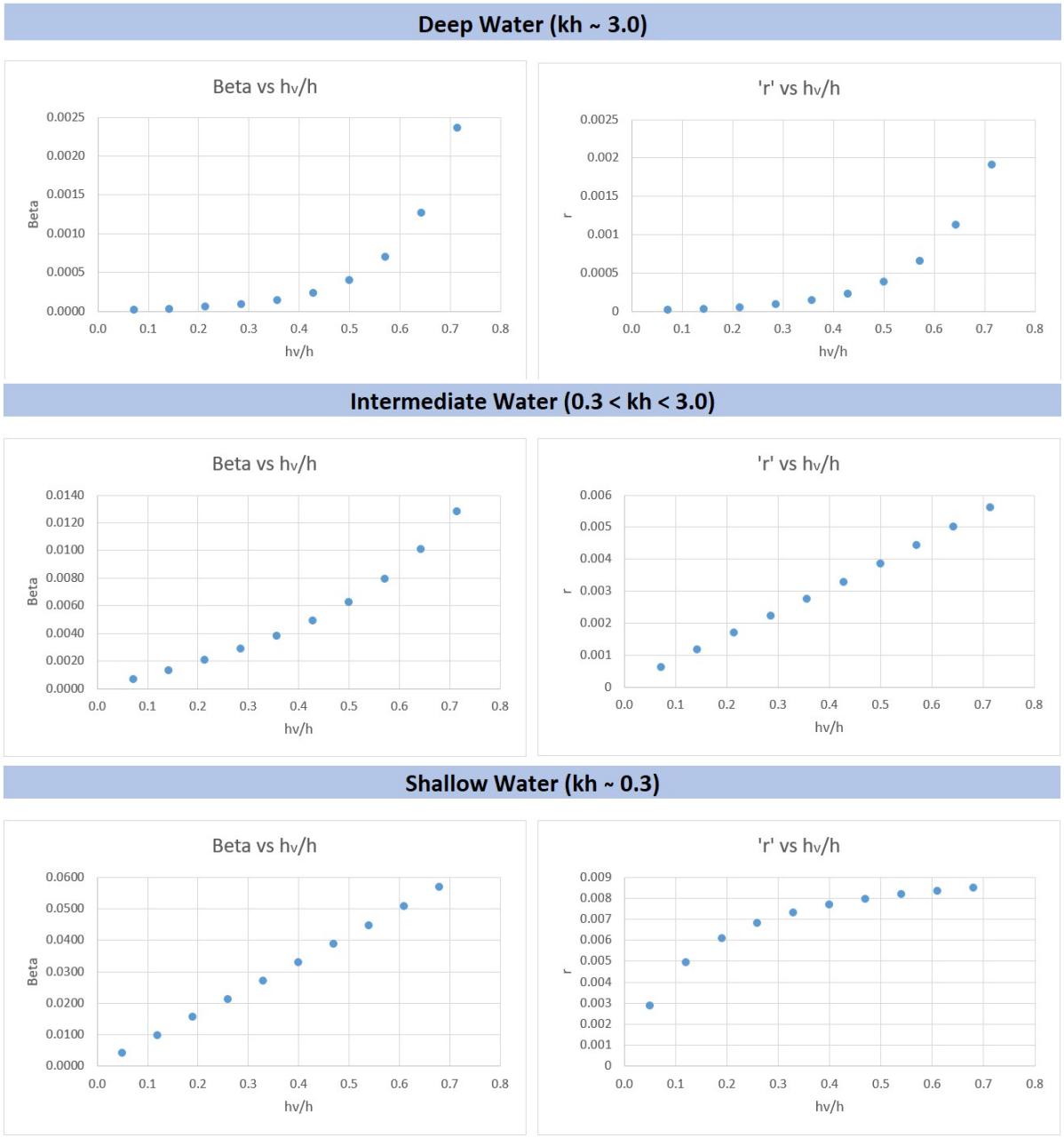

Figure 4.2: Results depicting the response of β and r wave attenuation factors with respect to relative vegetation height (h_v/h); evaluated at deep and shallow water limit state conditions (kh 3.0 and kh 0.3, respectively) and in intermediate water conditions ($0.3 < kh < 3.0$).

4.2. Foreshore system

In order to assess the effect of a vegetated foreshore system, it is proposed to proceed in a two-step approach (Figure 4.3). An initial condition is evaluated with a flat surface at MSL, which represents the mud flat that lies in front of the foreshore. The first step is evaluated by adding the foreshore at an elevation which is given by the local tidal regime; and the second step is to re-evaluate the foreshore with the same hydrodynamic boundary conditions while adding a vegetation cover with constant biophysical properties (h_v, C_d, N_v, b_v). For this purpose, the spectral wave model SWAN (Simulating WAves Nearshore; Booij et al. (1999)) was used, which includes the wave energy attenuation by vegetation model proposed by Mendez et al. (2004), a concept that was also used in the previous Section.

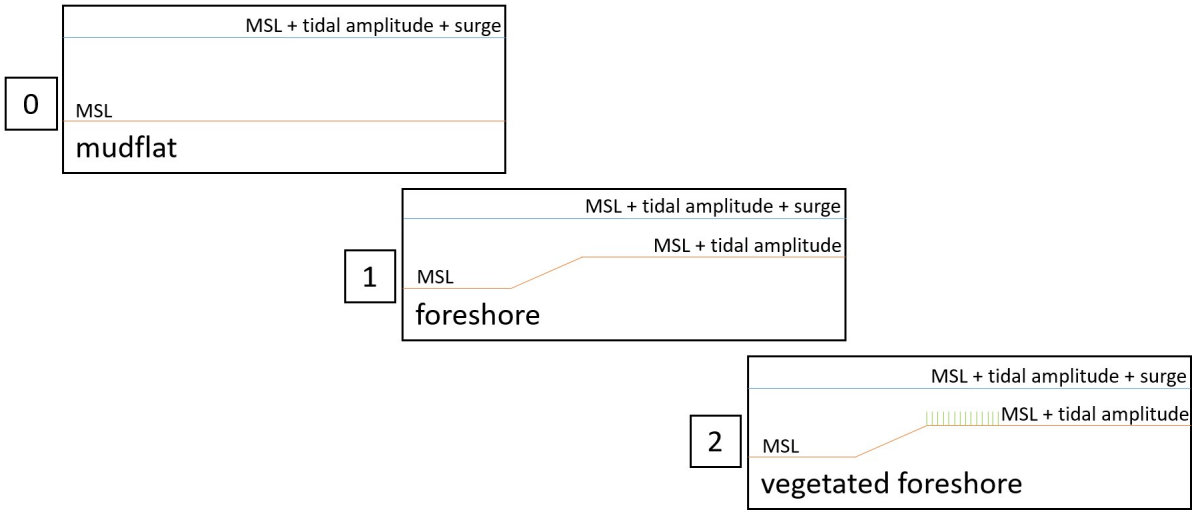

Figure 4.3: Schematization of two-step approach followed to assess effectiveness of foreshore+vegetation system. Wave energy dissipation ratios r were computed at every scenario with the aim of comparing dissipation of the foreshore system in terms of the dissipation in the mudflat scenario (step 0).

To account for different elevations at which a foreshore can naturally develop, the three tidal regimes which can characterize a coastal area were considered (micro-, meso- and macrotidal). Moreover, these tidal regimes were evaluated with imposed hydrodynamic boundary conditions that are intended to simulate three different possible scenarios of exposure, as well as 5 different design storm surge levels. These different combinations are proposed in such a way so that it is possible to evaluate the degree of effectiveness of vegetated foreshores in terms of different tidal regimes, as well as the effect of varying wave height to water depth ratios (H/h). A summary of the exposure types used for the following assessment as well as the imposed hydrodynamic conditions are presented in Table 4.2.

Table 4.2: Summary of parameters used for combinations run for foreshore system analysis.

Condition	H_s [m]	T_p [s]	Tidal regime	Tidal amplitude [m]	Surge levels [m]
Exposed, local waves	1.00	4.00	Micro, Meso, Macro	0.50, 1.50, 2.50	0.50, 1.25, 2.00, 2.75, 3.25
Exposed, swell waves	1.00	12.00			
Sheltered, local waves	0.50	4.00			

4.2.1. Tidal regime

Results of the analysis performed on different tidal regimes are presented in Figures 4.4 - 4.6, and they show that vegetated foreshore systems can be 2.0 – 4.0 times more effective regarding wave attenuation than the mudflat scenario (step 0, Figure 4.3). Moreover, these systems can be 2.0 – 5.0 times more effective in macro tidal regimes than in micro tidal regimes, due to the accretion of the foreshore at the tidal amplitude level. In macro tidal regimes, the bed level difference between salt marsh platform and mud flat (change in water

depth) dissipated the most energy, suggesting that vegetated foreshores can be a far more effective measure under this tidal regime.

Additionally, it is possible to gather information from the proposed coastal scenarios that can be found in nature. Results show that longer waves (swell) are dissipated the least by a vegetated foreshore; and steeper waves are dissipated the most. Moreover, across all scenarios the rate of wave attenuation with respect to the bare mudflat scenario (absence of vegetated foreshore) increases linearly with increasing surge, given that water depth was defined as the surge level added on the tidal amplitude assessed. In other words greater depths (tidal amplitude + surge) imply less wave height attenuation in the bare mudflat scenario and greater attenuation by the change in bathymetry introduced by the foreshore.

Scenarios

Exposed coast, locally generated wind waves

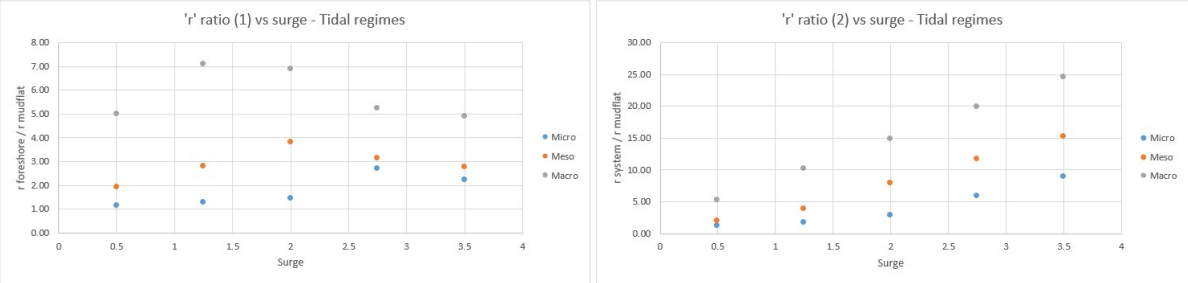

Figure 4.4: Rate of wave attenuation ratio between 'bare foreshore vs bare mudflat' (left panel) and 'vegetated foreshore vs bare mudflat' (right panel). Scenario: exposed coast, locally generated wind waves.

Exposed coast, swell waves

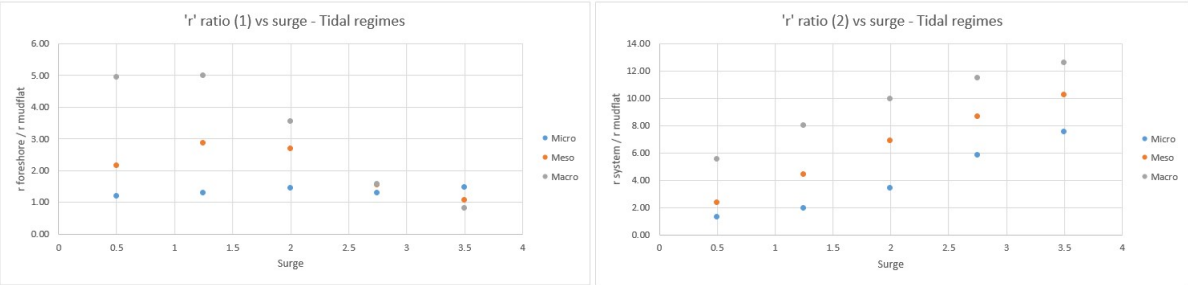

Figure 4.5: Rate of wave attenuation ratio between 'bare foreshore vs bare mudflat' (left panel) and 'vegetated foreshore vs bare mudflat' (right panel). Scenario: exposed coast, swell waves.

Sheltered coast, locally generated wind waves

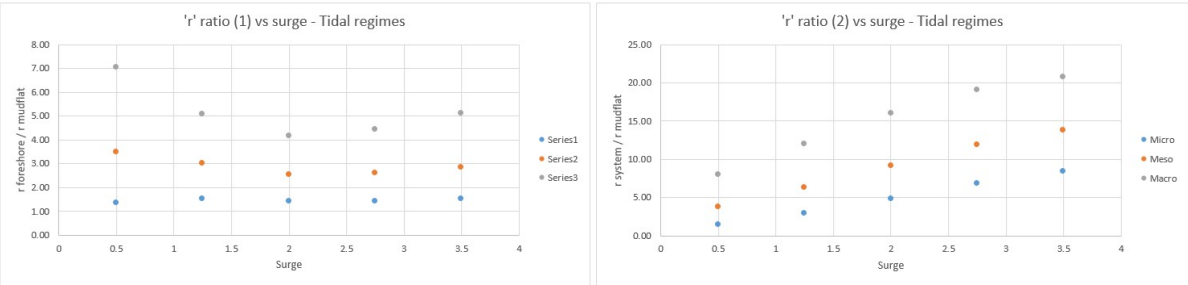

Figure 4.6: Rate of wave attenuation ratio between 'bare foreshore vs bare mudflat' (left panel) and 'vegetated foreshore vs bare mudflat' (right panel). Scenario: sheltered coast, locally generated wind waves.

4.2.2. H/h

When looking at lower water depths (lower surge levels), the change in bathymetry dissipates the most wave energy possibly due to wave breaking. The wave later propagates in shallow water conditions, where wave attenuation by vegetation responds linearly w.r.t hv/d ratio (4.1.1). Figure 4.7 shows that the highest wave energy dissipation relative to dissipation over the mudflat scenario is achieved for lower H/h ratios, across all tidal regimes. This step of the analysis, however, is highly case dependent and may vary for different imposed conditions. Further assessment of this step in the analysis is discussed in the following section.

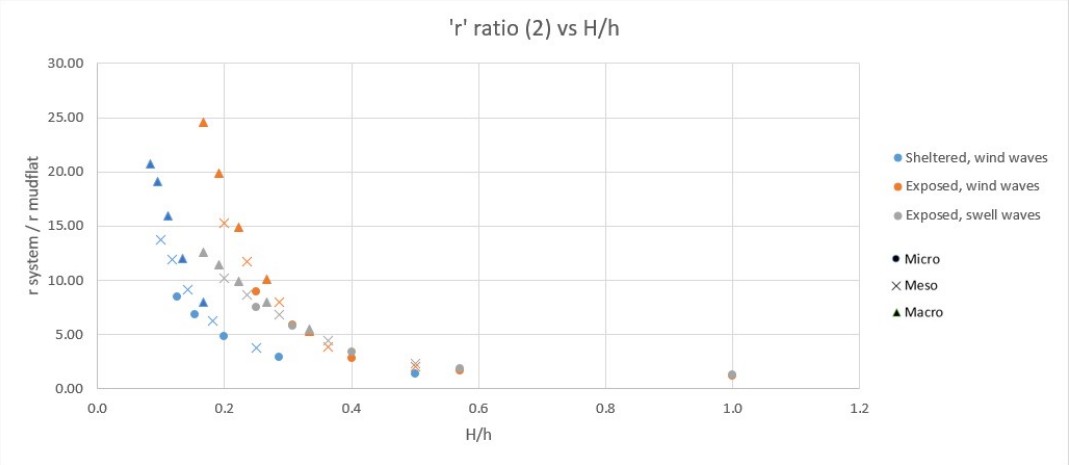

Figure 4.7: Results of wave height to water depth ratio analysis in different tidal regimes.

4.3. Discussion

This Chapter presented the analysis of the degree of effectiveness of several indicators presented in Chapter 2, while defining effectiveness as the wave height reduction capacity of a salt marsh-vegetated site. The analysis focused on indicators such as relative vegetation height (h_v/h), wave height to water depth ratio (H/h), and the tidal regime characterizing a specific site. The analysis of h_v/h was done through a sensitivity analysis carried out on a 1D model with uniform bathymetry, and performed on different formulae describing wave propagation over vegetation fields (Mendez et al., 2004; Mazda et al., 2006). Separately, another 1D model was set up in the wave spectral model SWAN (Booij et al., 1999) to asses the tidal regime and H/h ratio. This model was run under several combinations of imposed boundary conditions, which were selected in order to approximate conditions found in nature.

Results for the first analysis regarding h_v/h indicate different rates of wave height attenuation for deep, intermediate, and shallow water conditions (in terms of kh). It is suggested that under shallow water conditions, the rate of wave height attenuation of a vegetated foreshore with respect to a bare mudflat increases linearly for increasing h_v/h ratios, in terms of β. Waves propagating under these conditions are long enough to 'feel the bottom' and hence be attenuated by the vegetation lying underneath, finding greater wave attenuation rates for increasing vegetation height. In terms of r, a similar linear growth is found at the beginning of the spatial domain, however given that this parameter is expressed as a function of Δx (Equation 4.1), these results suggest a logarithmic growth which increases only by 10% for ratios $h_v/h > 0.40$. Given that this growth in terms of r is case-specific, it cannot be generalized for additional cases.

For the same indicator, the transition from shallow to deep water condition suggests a change in the growth trend from linear into exponential, both in terms of β and r. For both variables, the trend seems to remain constant at 0 for values of $h_v/h < 0.3$, after which the curve follows the exponential growth previously described. Therefore it can be hypothesized that under deep water conditions, vegetation does not interact with the propagating wave for vegetation heights that cover less than 40% of the water column. It is important to keep in mind that this analysis is largely expressed in terms of kh, and is hence case-specific and dependent on the value assigned to this parameter. Nonetheless, the imposed boundaries of $H_s = 0.50m$, $h = 3.50m$,

and $T_p = 2.00s$ can be found in nature (Vuik et al. (2018a) reported values of $H_{m0} = 0.35m$, $h = 3.07m$, and $T_{m01} = 2.70s$ at a given time on the marsh edge of Hellegat during a measuring campaign).

Results of H/h were presented in Figure 4.7, and whereas several observations can be withdrawn, there is no generalization that can be applied for additional cases. This is due to the assumptions made in this assessment, such as the definition of effectiveness as the rate of wave attenuation of the system as a function of the same parameter computed for the absence of such a foreshore (only mudflat scenario, located at MSL). Under these assumptions, the higher wave attenuation for lower H/h ratios can be explained due to the fact that the incoming wave propagates from the offshore boundary on the mudflat and towards the vegetated foreshore. For greater water depths (tidal amplitude + surge), initially the wave is only slightly disturbed on the mudflat section of the domain, however upon reaching the vegetated foreshore, the change in depth dissipates energy by various mechanisms defined for the simulation (bed friction, wave breaking, and triads). This occurrence largely decreases the wave height at the end of the domain, with respect to a simulation with the same boundary conditions (water depth) without the foreshore.

Nonetheless, this second analysis also served to assess the effect of different tidal regimes and possible scenarios that can be found in coastal areas, and in an attempt to generalize the findings of this Chapter, they were synthesised and presented in the Figure 4.8. However arbitrary the previously described assumptions regarding the rate of wave attenuation computation, they are valid for the tidal regime analysis given the natural development of the foreshore at the tidal amplitude level and the typical location of the mudflat at MSL. Figure 4.8 suggests that vegetated foreshores located in macro tidal coastal areas can result in a more effective coastal protection measure, regarding wave height attenuation, when compared sites characterized by meso- or micro tidal regimes.

Furthermore, regarding the different exposure conditions, a clear distinction can be made between the characterized locally wind generated and swell waves at larger water depths, encountering greater rates of wave attenuation for the former. Longer waves, in general, were not dissipated as much as the dissipation rates found for local wind waves at either exposed or sheltered conditions. Even though there is a slight difference between these two scenarios, Figure 4.8 does not show a significant variability between them.

Table 4.3: Relation between water levels and tidal regime depicted in Figure 4.8.

Tidal regime	Modelled water levels
Micro	1.00 - 4.00
Meso	2.00 - 5.00
Macro	3.00 - 6.00

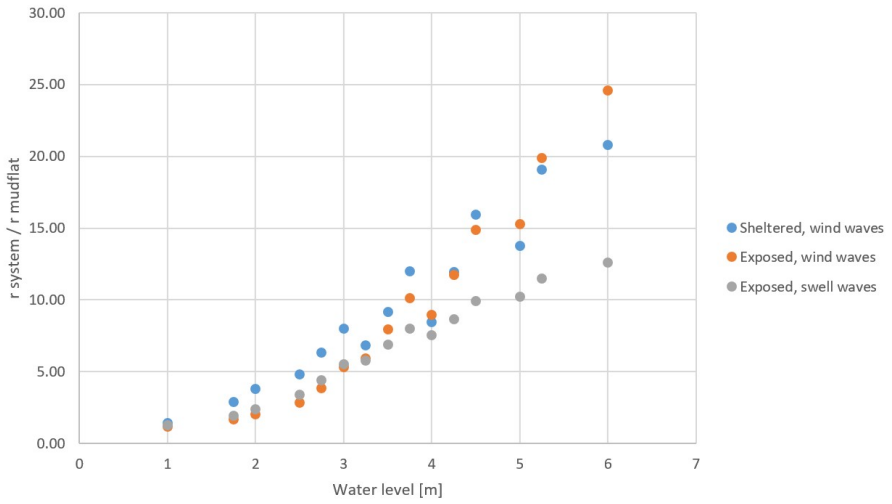

Figure 4.8: $r_{system}/r_{mudflat}$ ratio across all evaluated scenarios. Water levels plotted on the x axis correspond to the imposed tidal regimes + surge level (micro = 1.0m - 4.0m; meso = 2.0m - 5.0m; macro = 3.0m - 6.0m).

4.4. Application on water systems

The sensitivity analysis performed in this Chapter was executed parallel to the habitat suitability study presented in Chapter 3. As explained in the previous section, many of the findings on the analysis are case-dependent, and are therefore not generally applicable as a standard guideline for flood safety. Nonetheless, some of the simulations executed were aimed at representing the actually occurring hydrodynamics on both the Western Scheldt and the Wadden Sea water systems, which include evaluations regarding different tidal regimes, storm surge heights, and type of wave forcing (local wind waves, swell waves, etc.). The conclusions of these variables can serve to hypothesize the degree to which salt marshes act as an effective wave reduction measure in both water systems, and will be presented in this section.

Results describing the role of tidal regimes (Figures 4.4 - 4.6 Figure 4.8) point at the likelihood of experiencing higher wave height attenuation rates in macro tidal regimes than in micro or meso tidal regimes. This translates to the the possibility that salt marshes located in the Western Scheldt (macro tidal) are more effective for wave attenuation than salt marshes that develop in the Wadden Sea (micro-meso tidal). The vegetated platform on the Western Scheldt sites accrete at higher elevations with respect to MSL, due to sediment deposition on higher levels occurring during MHWS. This means that the change in bathymetry between the mudflat fronting the vegetated foreshore and the vegetated foreshore has a great effect in wave energy dissipation. In micro tidal regimes, such as the Wadden Sea, the bed level elevation does not change significantly between mudflat and foreshore; and hence can be inferred that the vegetated foreshore has hardly any effect on the waves.

Moreover, the assessment regarding the different types of loading scenarios (local wind, swell) also allows for a comparison between the water systems. Salt marsh locations in the Wadden Sea may be exposed to both locally generated wind (short) waves, as well as swell (long) waves penetrating from the tidal inlets between the Wadden Islands (salt marsh sites located on the lea-side of such islands are only exposed to locally generated wind waves); whereas Western Scheldt salt marshes are only exposed to locally wind generated waves. This occurrence further reinforces the assumption that more wave energy dissipation should be expected by vegetated foreshores in a water system such as the Western Scheldt, given that results presented in this Chapter suggest that longer waves are dissipated the least by such a system.

Regarding the role of vegetation itself (h_v/h) with respect to wave energy dissipation, previous considerations of deep water conditions ($kh \sim 3.0$) do not apply on the salt marshes on either of the studied water systems, given that waves propagating over the mudflats and the foreshore itself are typically characterized by a period of $T_p = 3.0s$, and maximum water depths of about $h = 3.0m$ at the lowest point of the platform, the marsh edge (depending on wind + tide occurrence; hence, usually even lower water depths). This means that, considering that intermediate and shallow water conditions are expected, high relative vegetation height ratios should be aimed for maximum wave energy dissipation in terms of β (Figure 4.2. Similarly, in terms of wave energy dissipation per unit length (r), the same Figure suggests that in salt marshes that extend over 200m (such as the ones found in both the Western Scheldt and Wadden Sea) higher attenuation is achieved for higher relative vegetation heights.

5

Discussion

This thesis consisted of two main sections: i) the assessment of occurring local conditions that favor the existence of salt marsh habitats (Chapter 3); and ii) the degree of effectiveness of these systems as a flood protection measure (Chapter 4). The current chapter will evaluate the previous results while accounting for the different methods used to compute them (including the uncertainty they introduce), as well as their relationship with the existing literature presented in Chapter 2. Furthermore, herein a connection between the two sections of the thesis will be presented as a first step in the development of assessment tool for introduction of this system as a flood defense system at a given site.

5.1. Habitat suitability

5.1.1. Water levels

Determination of the water levels at every location of interest was performed by means of triangular interpolation between RWS stations located in the proximity of such sites, as explained in Chapter 3. The input data at each measuring station consisted of a water level elevation reading every 10 minutes, throughout the selected study period, which allows the inclusion of tide and surge in the analysis. Given that the output of the water level generation is not only used for the inundation-free period analysis, but also for the wave growth assessment and, consequently, the dimensionless wave-induced excess bed shear stress computation, the inclusion of surge in this initial step is a characteristic that adds robustness to the results that stem from it, considering the tidal behavior of both the Western Scheldt and the Wadden Sea.

The triangular interpolation may become an inaccurate method for sites located at greater distances from the measurement stations, and in water systems with complex geometry and bathymetry; however, for daily conditions with small spatial water level variations, it is assumed to be sufficiently accurate. Such is the case for the locations within the Western Scheldt estuary. On the contrary, the tidal basins that characterize the much larger Wadden Sea may have an effect on the water levels generated from the triangular interpolation computations. From Figure 3.7 it is possible to see that the triangular planes generated from the available RWS stations in this water system are actually crossing watersheds between such tidal basins. In order to check the performance of this approach in the Wadden Sea, water level time series were retrieved from the 'Vlieland' and 'Terschelling' observation points in the Delft3D model previously used to compute flow velocities. These sites were selected given that water level elevation in these locations was generated from RWS stations located in 3 different tidal basins within the water system (Figure 3.7).

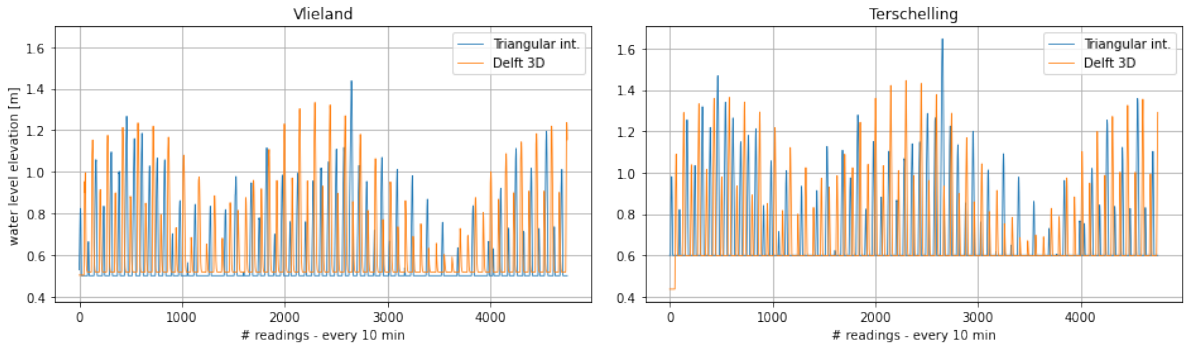

Figure 5.1: Water level time series comparison between Delft 3D model and triangular interpolation results generated in mature salt marsh locations 'Vlieland' (left panel) and 'Terschelling' (right panel) in the Wadden Sea. Time span corresponds to 1 month of simulated signals.

As explained in Chapter 3, the Delft 3D model describing the Wadden Sea is forced by tidal constituents which describe a spring-neap tidal cycle that characterizes the North Sea. This pattern is well described by the orange signals in Figure 5.1, corresponding to the Delft 3D model out for water level elevation over the simulation period of a month. On the other hand, the triangular interpolation assessment was conducted over a period of 4 months (growth season); hence, for comparison purposes, the month where the spring-neap tidal signal was more clearly distinguishable was selected for this evaluation. This water level time series corresponds to the blue signals in Figure 5.1.

Both water level signals capture the spring-neap tidal cycle which characterizes the Wadden Sea system. Moreover, both modelling results agree with the estimation of slightly higher water levels at the 'Terschelling' site, when compared to the 'Vlieland' location, adding some robustness to the triangular interpolation assessment used throughout this thesis. Nonetheless, Figure 5.1 also suggests some discrepancy between the two signals, such as a slight underestimation of the water levels by the triangular interpolation approach during the second modelled spring tide (for this arbitrarily selected month). In general terms, the triangular interpolation analysis conducted to generate water level time series at locations of interest seems to agree with the Delft 3D model output.

5.1.2. Marsh edge bed level

Similar as the water level analysis, the determination of the bed level elevation at the marsh edge plays a major role in the assessment of additional indicators treated in Chapter 3 e.g. the wave growth computation is limited by 40% of this water depth. The data gathered from AHN3 was considered to be representative for the bed elevation in the marsh edge, which is assessed throughout this thesis. Even though several transects were used in order to account for the spatial extent and variability of a salt marsh edge (Appendix B), the vertical accuracy of the data may introduce some uncertainty into the modelling. Moreover, the selected three (or two) points along the salt marsh edges does not cover all the variability of this interface between the bare mudflat and the vegetated foreshore.

A validation of the exact elevation of each site was beyond the scope of this thesis; however, in order to assess the sensitivity of the model to changes in bed level elevation, the retrieved data was further analyzed within the inundation-free period analysis for changes in elevation of +0.05m. This analysis showed that this vertical variability resulted in maximum changes of 1.5 - 2.0 percentage points with respect to the dry period computation (% of time when depth < 0), whereas most of the observed transects varied less than one percentage point e.g. average Zimmerman marsh edge inundation-free period increased from 93.06% to 93.84% for a bed level increase of 0.05m.

Thus, even though a constant and spatially uniform bed level was assumed at the marsh edge during the 4-month period computation, the sensitivity analysis suggests that slight changes in bathymetry do not largely affect the water depth computation. Therefore, the bed level elevation retrieved from the AHN3 database is considered to be representative of the actual elevation at the marsh edge.

5.1.3. Inundation frequency vs. inundation duration

In Chapter 2 both indicators of inundation occurrence were cited as part of relevant characteristic of salt marsh sites. This thesis however focused on inundation (-free) duration during a characteristic growth season, rather than inundation frequency, given that the focus was on initial salt marsh establishment at a given location. This requires, by the WoO (Window of Opportunity) definition, sufficiently long dry periods for seeds to settle, followed by disturbance-free periods for seedlings to establish. The importance of inundation duration was further mentioned by Silinski et al. (2016c), who stated that the elevation on the foreshore, which directly determines the inundation period, could serve as a proxy for salt marsh clonal expansion in sheltered sites. Even though the concepts of 'sheltered' and 'exposed' sites as defined by Silinski et al. (2016c) were not used in this thesis (fetch of 2km vs 8km, respectively), the insight regarding the inundation duration relevance was considered. On the other hand, inundation frequency has been rather linked to prediction of the salt marsh edge location, rather than an indication for habitat suitability itself. An example of this link was presented by Balke et al. (2016) after observation of at least two inundation events per day on salt marsh edges in water systems with different tidal regimes, including macro tidal.

Thus, the inundation frequency may be more relevant to predict the location of the marsh edge, while inundation duration may serve better as an indicator for salt marsh habitat suitability, e.g. flood events can occur twice per day at several different bed levels along a transect at a semidiurnal site; whereas the duration of the flood would be lower at higher elevations. Results from this thesis further suggests the relevance of inundation-free period as a habitat suitability indicator, given the similarities found between vegetated sites versus non-vegetated locations across two different water systems. Even though solely inundation duration cannot determine the suitability of a site to host salt marsh vegetation, it is nonetheless the mean by which additional hydrodynamic forcing can be exerted at an arbitrary location, and hence a relevant proxy for salt marsh introduction. This thesis did not explicitly compare both indicators (frequency and duration), and is therefore recommended to do so in future studies.

5.1.4. Determination of flow velocities

As presented in Table 3.2, the bed level elevation registered at the observation sites selected within the Delft3D models show some differences with respect to the actual bed level as described by the AHN3 database. This difference translates into different water depths and hence occurring depth-averaged flow velocities. Given the fact that the bathymetry of both water systems is characterized by tidal channels, an observation point that should fall in the proximity of (or right on) such a channel might register higher flow velocities that the ones occurring on the higher-located salt marsh edge. This spatial resolution that characterize the Delft3D models used for this assessment might not fully represent the actual occurring flow velocities at the locations of interest.

However, the same Table also shows that even though the salt marsh edge bed elevation is not accurately described, most of the locations represent flow velocities occurring on the intertidal flats (bed level elevation > 0) and not on the tidal channels. Thus even though the approach used to determine the flow velocities might be slightly inaccurate to determine the occurring flow velocities exactly at the marsh edge, it is safe to assume that at most locations the analyzed results correspond to velocities occurring at the proximity of such marsh edge. Furthermore, topographical features found on the water systems are included in the models, which further adds to a proper description of the flow pattern at the locations of interest. Thus even though this thesis focuses on limiting phenomena occurring at the marsh edge, the results from this section should be treated as a description of the flow pattern on the mudflats fronting each location.

5.1.5. Wave heights

The modelling of wave heights fell in agreement with the data measured by Vuik et al. (2016a) and Vuik et al. (2018a) (Appendix A). Modelling consisted of wave growth formulation proposed by Young et al. (1996), and was limited at the marsh edge by 40% of the water depth, which was computed in sections that preceded this step. Additionally, the dry period was well represented for a large period of the assessed time, however the data also shows that the method used might slightly overestimate the actual occurring inundation-free

period. This comparison additionally suggests that assumptions made on variables such as water level and bed level elevation were likewise in accordance.

This approach can be contrasted by research done by Callaghan et al. (2010), who studied the lateral behavior (expanding/retreating) of salt marshes in the Western Scheldt during the period 1987-2008. For this research, a SWAN 2D wave model was forced by temporarily variable wind and water level data. Conclusions suggested that a wind speed and fetch length approach could not explain the lateral behavior of the marsh edge at the assessed locations, given the description of milder conditions at sites where shrinking was observed; hence, suggested that spatial modelling is necessary to explain this phenomenon. Nonetheless, a main difference that can be pointed out with respect to the current analysis is the assessed temporal scale, which is characterized by 5 months during a growth season, typically described by milder conditions than the ones found during the winter period. Given that the validation step performed in this thesis (Appendix A) fairly well corroborates the modelled data, it suggests that the wave modelling approach used for this thesis, along with all the water and bed level elevation assumptions, is applicable for short temporal scales.

5.1.6. Sediment dynamics

The inclusion of sediment dynamics was the final step in Chapter 3 of this thesis, and was performed in order to expand the assessment from exclusively hydrodynamics, which was the original focus of this thesis. This additional step was performed given that the literature presented in Chapter 2 mentions soil composition as part of the different factors that play a role in salt marsh establishment. The spatial scale of this analysis (observation of 28 sites at two different water systems) made it difficult to precisely assign sediment properties at each of the sites, reason for which general assumptions were made regarding the critical bed-shear stress characterizing the soil of each system, which were explained in Chapter 3.

This general soil characterization, however, might not be representative at all locations in the water systems and therefore a certain degree of uncertainty may be introduced by this approach. Even though a critical bed-shear stress of a sand-mud mixture was given for both systems, the dominant fraction may vary between locations within a system itself. In an attempt to reduce this uncertainty, a small distinction was made within several Western Scheldt locations, given the estuary soil characterization reported by McLaren (1994) and presented by Dam et al. (2013). At locations where mud content was evidently higher, a dominant mud fraction was assigned for the analysis, while the remaining locations were characterized by a dominant sand fraction. This distinction between sites was not performed for the Wadden Sea locations, which were generally assumed to be characterized by a sand-mud mixture with a dominant mud fraction.

Moreover, ideally the flow velocities should also be evaluated for their impact on soil dynamics as current-induced bed-shear stress, given that it can play an important role as pointed out by Zhu et al. (2016), who found though field measurements performed on the Yangtze delta that current-induced bed shear stress was 2.3 times larger than the measured wave-induced bed shear stress.A thorough research into this variable could not be included as part of this thesis because of time limitations; however, the general soil characterization of the systems was considered to be relevant as a final step in the habitat suitability assessment, given that it may offer the explanation as to the establishment of vegetation on certain sites. Given the likely importance of this parameter as a general feasibility indicator, it is highly suggested to further evaluate it in more detail.

5.1.7. Topography

During the elaboration of this thesis, several topographic features were observed at the assessed vegetated locations, mostly characterized by groynes located in the proximity of such sites. Figure 5.2 shows several examples of this existing infrastructure. It is clear from the previously performed analysis that vegetated sites are generally located at higher elevations than additional observed sites, hence experiencing less flooding events which in turn reduces the exposure of these locations to harsher hydrodynamics (and morphodynamics).

Figure 5.2: Aerial Google Earth imagery at locations Hoofdplaat and Zimmermanpolder in the Western Scheldt (top panels); and at Texel and Groningen in the Wadden Sea (bottom panels).

These structures have a certain effect on the local occurring hydrodynamics, which generates milder conditions in the surrounding landscape by providing a sheltered geometry. Consequently, these milder conditions erode (re-suspend) less sediment, therefore suggesting bed level increase at such sites. At Hoofdplaat, for example (top left, Figure 5.2) the salt marsh developed on the wake of the groyne, a location which is typically characterized by milder flow velocities with respect to the ones found in the absence of such structure. However, on the other side of the Hoofdplaat salt marsh, a vegetation patch is found ('Salt Marsh patch 2') that is still partially sheltered by a groyne located at some 500m downstream (to the West, not visible in Figure 5.2). This characteristic topography suggests that the results gathered from this analysis may be influenced by such existing infrastructure, and should be taken into account as the likely causes for the milder conditions found in most vegetated sites.

5.2. Effectiveness

5.2.1. Definition of effectiveness

Throughout the effectiveness assessment presented in Chapter 4, the term 'effectiveness' was defined as the vegetated foreshore's capacity to dissipate incoming wave energy with respect to attenuation of the same wave by a mudflat located at MSL. Additionally, attenuation was defined as the wave height reduction achieved after propagation over a given vegetated transect. This definition was selected since the aim of this thesis was to evaluate salt marsh habitats as an effective flood protection measure.

Even though the analysis of vegetation response in terms of β and r could be made for different conditions, the results of the vegetated foreshore system assessment may be highly dependent on this definition. The study of H/h, for example, falls into this category and was already discussed in the final section of Chapter 4, where the dependence of the results on this initial definition may have an influence on the presented outcomes. It is therefore advised to consider these definitions when interpreting the conclusions therein introduced.

5.2.2. Generalization

Similar as the assessment performed in Chapter 3, the effectiveness analysis was aimed at determining a general degree of effectiveness of several wave height reduction indicators gathered from literature. Even though results presented in Chapter 4 shed light upon this range of applicability of salt marshes with respect to wave height reduction, it is important to keep in mind that much of the behavior observed from the formulae is case-dependent and varies with changing boundary conditions. The results that fall into this description were discussed in Chapter 4.

This characteristic poses a challenge when it comes to generalization or standardization of results. Such conclusions include findings for relative vegetation height under deep water conditions. This results are highly dependent on kh, and therefore suggest that under deep water conditions (which are hardly reached in coastal areas) the vegetation canopy should cover large part of the water column in order to exert drag forces on the propagating wave. Considering high water levels (tide + surge), tall vegetation may be very well attainable during summer conditions; however, during the winter period (where harsher conditions are generally observed) the biomass of the salt marsh reduces considerably (Vuik et al., 2018a) due to the natural seasonality of vegetation and stem breakage during winter storms, making it difficult to achieve the limit for h_v/h ratios.

Nonetheless, it is hypothesized that results gathered from the tidal regime analysis could be generalized for further study and application. Such results show that a higher rate of wave attenuation was found for macro tidal systems, given the several assumptions regarding the location of the foreshore platform with respect to the tidal amplitude and the considered surge levels (Chapter 4). Additionally, a positive feedback is generated due to the sandier bed composition found in such macro tidal environments (higher flow velocities erode the finer sediments). Coarser sediment can withstand harsher wave climate, favoring the establishment of seedlings which in turn trap additional sediment and accrete at higher elevations than in micro tidal regimes. These conclusions are less case-dependent which consequently suggest their general applicability, as will be presented in the following section.

5.3. Applicability

The purpose of is thesis was to determine threshold values for habitat suitability indicators, as well as looking into the degree of effectiveness regarding flood hazard reduction indicators for salt marsh habitats. This was performed in order to conclusively propose a first step in the elaboration of an assessment tool for decision makers, which would serve to determine whether it is physically feasible to introduce salt marshes onto an arbitrary location as an effective measure against flooding hazard. For this final step, and with the purpose of addressing the 3rd research question, it was attempted to combine results of Chapter 3 and 4 into a single set of conclusions, however it was not possible to conceptualize such an assessment tool given the several parameters that play a role within such a habitat.

Nonetheless, the separate set of conclusions may serve for at an initial screening phase for the introduction of this habitat as an effective coastal protection measure, and are presented in Figure 5.3. This quick scan might start with the measurement of bed level elevations in order to perform an assessment of the inundation-free period experienced at such site (which is suggested to be larger than ~ 70% of the time during growth season). Likewise, information of wave action, flow velocities, and sediment composition should be gathered with the goal of determining the occurring excess bed-shear stresses at the site, advising that sediment re-suspension should occur less than 20% of the time (and maximum values at 10%, 1%, and 0.1% of the time as suggested in Chapter 3).

Finally, with respect to habitat suitability, additional variables necessary for salt marsh survival such as salinity, temperature, and others (Chapter 2) should be kept in mind. As for the degree of effectiveness at a screening phase, the determination of the tidal regime which characterizes the coastal area may already be a relevant proxy, assuming a higher tidal range results in higher rates of wave attenuation with respect to the mudflat that naturally fronts a foreshore. Furthermore, design surge heights and whether such a location is loaded by swell or wind waves can aid in a first-level estimation of the effectiveness of this coastal protection measure.

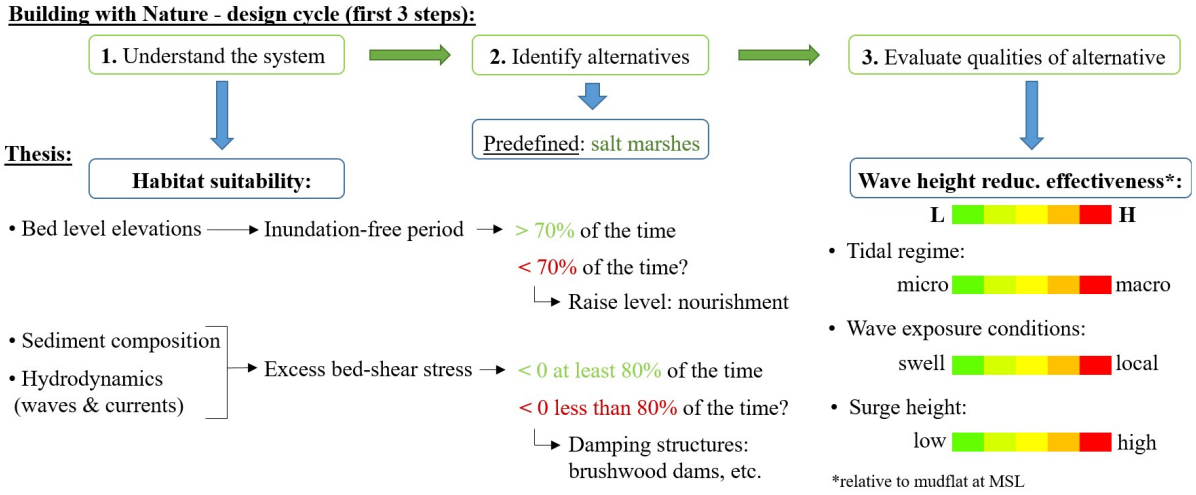

Figure 5.3: Set of conclusions gathered from the previous analysis regarding habitat suitability and wave height reduction effectiveness of salt marsh habitats.

6

Conclusions

This thesis was performed with the aim to better understand the naturally occurring mechanisms that favor the existence of salt marsh habitats at a specific location. This was done in an attempt to assess whether it is possible to introduce such an ecosystem as an effective flood defense measure at a given site. The habitat suitability assessment was performed by observing hydrodynamics occurring during a characteristic growth season at several locations in coastal water systems in The Netherlands; while the effectiveness study was carried out by performing sensitivity analyses on formulae describing a vegetated field's wave attenuation capacity, which results were later used to reflect on the degree of wave height reduction effectiveness of salt marshes on the same water systems used for the habitat suitability analysis.

Based on site-specific conditions, can general threshold values be given to salt marsh habitat suitability indicators?
Results suggest that within a water system with similar sediment composition, inundation-free period and daily-occurring hydrodynamics, such as flow velocities and wave height, can explain the presence/absence of vegetation in some locations; whereas at other sites, flow velocities during storm conditions seem to be the determining factor for salt marsh absence. Nonetheless, it is not possible to standardize these limiting values when evaluating salt marsh habitats in different water systems. In this thesis, the Western Scheldt and the Wadden Sea presented a different hydrodynamic forcing during daily conditions (the latter by milder conditions than the former). However, as mentioned in literature, the introduction of additional parameters into the feasibility assessment, such as sediment composition, plays an important role.

Sediment characterization of both estuaries returned results that indicate a similar behavior between both systems with respect to the dimensionless wave-induced excess bed-shear stress factor. According to results gathered for a characteristic growth season (April-July 2020), the values of 2.5, 4.2, and 5.3 were not exceeded at 10%, 1%, and 0.1% of the assessed time at the observed vegetated locations, whereas the same values were exceeded at non-vegetated sites. When such factor in characterized by negative values, it means that the forcing is not high enough to re-suspend the sediment, whereas positive values translate into re-suspension (erosion) of bed particles. Results indicate the occurrence of sediment re-suspension during approximately 20% of the assessed time in the most energetic vegetated sites (Western Scheldt), and as little as 1% in the least energetic locations (Wadden Sea). This indicator, which combines wave forcing with bed resistance, seems to be a feasibility indicator which best explains the likelihood of salt marsh establishment in most observed sites. Additionally, current-induced bed-shear stress should also be added to this assessment, given the proximity of some locations to tidal channels that are typically characterized by higher flow velocities during both daily and storm conditions.

To which degree are different characteristics of salt marsh-foreshore systems effective regarding their flood hazard reduction capacity?
Several of the results gathered from this modelling study remained case-dependent and can therefore not be standardized into this set of conclusions. However, considerations for tidal regime, surge height, and type of wave forcing were used to determine the degree of effectiveness of salt marshes in the studied water systems, while measuring effectiveness in terms relative to the absence of the system at all (such a case was modelled

by a mudflat located at MSL). Evaluation of the different tidal regimes suggests that salt marshes that develop in macro tidal coastal areas can dissipate more wave energy than habitats located in micro or meso tidal areas. Such is thought to be the case for salt marshes found in the Western Scheldt, in contrast to salt marshes located in the micro-to-meso tidal Wadden Sea. The vegetated foreshores on the Western Scheldt sites accrete at higher elevations with respect to MSL, due to sediment deposition on higher levels occurring during MHWS.

Additionally, results regarding the effectiveness of this habitat while loaded by swell waves ($H_s = 1.0m$; $T_p = 12.0s$), sheltered locally wind-generated waves ($H_s = 0.5m$; $T_p = 4.0s$), and exposed wind-generated waves ($H_s = 1.0m$; $T_p = 4.0s$) further suggest that greater wave height attenuation - relative to the mudflat scenario - may be found in the Western Scheldt salt marshes than in the Wadden Sea, given that local wind waves returned the highest attenuation rates and swell waves the least. This is due to the fact that swell waves are longer and higher, and are hence likely dissipated by other mechanisms (such as wave breaking and bottom friction); whereas the foreshore has a greater effect in attenuation shorter propagating waves. This observation suggests that introduction of this system as a flood protection measure may be more effective in sheltered than in exposed coastal areas.

Can the previously assessed indicators and limit values serve as an assessment tool for salt marsh habitat introduction as a flood hazard reduction measure?
Even though the elaboration of an assessment tool was not achieved as part of these set of conclusions, several results suggest that a generalization can be made for certain parameters, while others remain case-dependent. Considering that the conceptualization of such a tool was aimed to provide a quick assessment regarding the introduction of salt marshes into an arbitrary site, in terms of habitat suitability and effectiveness, the conclusions presented in the previous research questions considered the indicators that are suggested to be generally applicable.

Regarding habitat suitability, dimensionless excess bed-shear stress is suggested by results to be applicable on both studied water systems, given the inclusion of hydrodynamic loading and bed resistance in the same parameter. As for the effectiveness results, the higher rates of wave height attenuation found on macro tidal regimes (given the assumption that foreshores accrete at higher levels with respect to the mudflats fronting them) indicate this characteristic of coastal areas to be a general effectiveness indicator. Considering these two simplified results, it would be suggested as a quick assessment for salt marsh introduction as a flood defense measure (at an arbitrary site) to collect data describing the wave and current velocity occurrence, along with information describing the critical bed-shear stress of the local sediment. Likewise, determination of the tidal regime describing such a site, along with the design surge height, may serve as a first estimate regarding the ecosystem's wave height attenuation capacity.

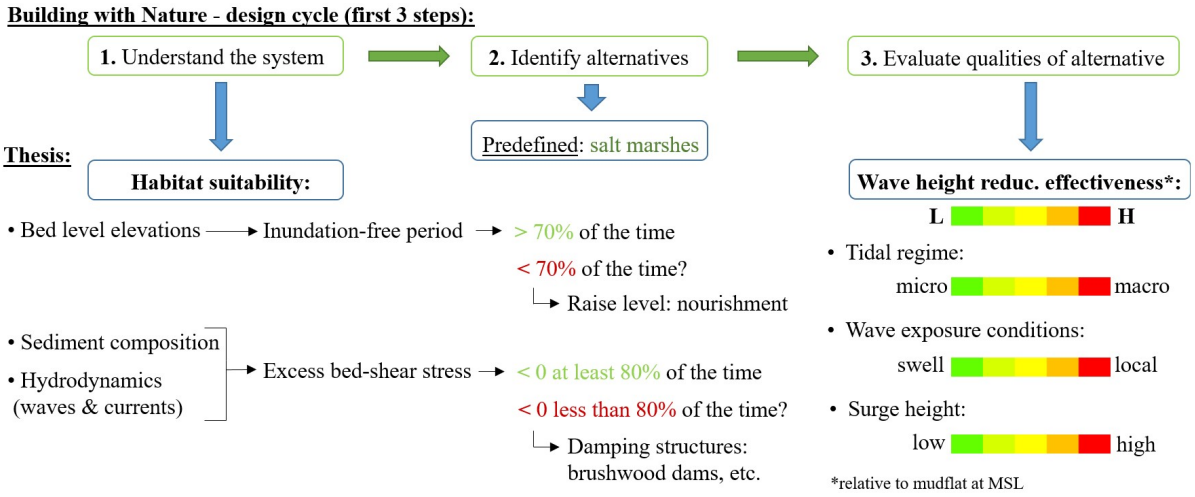

Figure 6.1: Set of conclusions gathered from the previous analysis.

7

Recommendations

This Chapter presents a set of recommendations based on the practical applications brought forth throughout this thesis. Furthermore, it proposes ideas for future or ongoing research regarding the introduction of salt marsh habitats as a nature-based solution for coastal protection.

- When comparing the occurring phenomena between water systems that are fundamentally different (tidal regime, sediment composition, bathymetry, wind occurrence, etc.), analysis of the hydrodynamic loading alone does not suffice when attempting to describe the presence/absence of a vegetative species which depends on soil stability for establishment. Response of this bed resistance to external loading by waves and currents is therefore necessary.
- If introduction of a salt marsh-vegetated foreshore is being considered as a coastal protection measure at an arbitrary site, the main considerations that have to be taken into account are the following: bed level elevations on the site of interest in order to define inundation-free periods; sediment composition and hydrodynamics to determine the resistance of the salt marsh to external loading; and exposure conditions, tidal regime, and design surge height to estimate the degree of effectiveness of the vegetated foreshore.
- The inclusion of a larger temporal scale would help standardize the findings presented in the habitat suitability analysis. This thesis observed and modelled occurring conditions during the period spanning over the months of April-July of the year 2020. This temporal scale was chosen to be representative of daily conditions during a growth season at both water systems. However an expansion of the observed period, possibly into the growth season of several years, might add valuable information onto the already found data.
- An accurate description of the sediment composition at the observation sites can better help model the excess bed-shear stress occurring at each location. Given that this habitat suitability indicator served as a final piece in the comparison between the two water systems, the sediment composition that was generalized for both water systems should be characterized in more detail.
- Observe and record flow velocities occurring at the marsh edges (and additional observation locations) as well as on the mudflats fronting the sites during a characteristic growth season, in order validate the data retrieved from the numerical models. Additionally, evaluate such velocities in terms of excess current-induced bed-shear stress, so as to consider the response of the soil to both currents and waves. As reported by Zhu et al. (2016), current induced bed-shear stress on an intertidal flat can at times exceed the wave-induced bed-shear stress, suggesting the relevance of this parameter regarding salt marsh establishment.
- Approach wave modelling with a spectral wave model such as SWAN. Even though the validation step presented in Appendix A suggests the modelled data agrees with measurements, this approach still neglects sink and source terms such as bottom friction, white capping, wave-wave interactions (triads and quadruplets), etc. Additionally, mechanisms such as wave refraction and shoaling are also accounted for in SWAN, which are relevant for wave propagation in the nearshore Holthuijsen (2010).

- Perform a comparative assessment of wave height attenuation rates between several sites characterized by different tidal regimes, in order to evaluate the hypothesis presented in this thesis regarding the higher rates of wave attenuation found through modelling of idealized conditions. This would either reinforce or discard such hypothesis, considered to be a generally applicable conclusion from the overall effectiveness assessment.
- For a further, more ecological assessment, make a distinction between limiting values for different salt marsh species, given the differences reported in literature, such as flexural strength (Vuik et al., 2018a) and salinity (Deltares, 2018). Perhaps at a seedling stage, some species might be able to withstand a larger external forcing, inundation time, etc.

Bibliography

Anderson, M.E. and Smith, J.M. (2014). "Wave attenuation by flexible, idealized salt marsh vegetation". In: *Coastal Engineering* 83, pp. 82–92.

Anderson, M.E., Smith, J.M., and McKay, S.K. (2011). "Wave dissipation by vegetation". In:

Augustin, L., Irish, J., Balsmeier, G., and Kaihatu, J. (Jan. 2009). "Laboratory measurements of wave attenuation and wave setup by vegetation". In: pp. 324–330. DOI: 10.1142/9789814277426_0027.

Balke, T., Bouma, T., Horstman, E. M., Webb, E.L., Erftemeijer, P. L. A., and Herman, P. L. J. (2011). "Windows of opportunity: thresholds to mangrove seedling establishment on tidal flats." In: *Marine Ecology Progress Series*.

Balke, T., Herman, P. M. J., and Bouma, T. J. (2014). "Critical transitions in disturbance-driven ecosystems: identifying Windows of Opportunity for recovery". In: *Journal of Ecology* 102(3), pp. 700–708. DOI: 10.1111/1365-2745.12241.

Balke, T., Stock, M., Jensen, K., Bouma, T. J., and Kleyer, M. (2016). "A global analysis of the seaward salt marsh extent: The importance of tidal range". In: *Water Resources Research* 52(5). DOI: 10.1002/2015WR018318.

Barbier, E., Hacker, S., and Kennedy, C. (Jan. 2011). "The value of estuarine and coastal ecosystem services". In: *Ecological ldots* 81, pp. 169–193.

Booij, N., Ris, R., and Holthuijsen, Leo (Jan. 1999). "A third-generation wave model for coastal regions, Part I, Model description and validation". In: *J. Geophys. Res.* 104, pp. 7649–7656.

Bouma, T. J., van Duren, L. A., Temmernam, S., Claverie, T., Blanco-Garcia, A., Ysebaert, T., and Herman, P. M. J. (2007). "Spatial flow and sedimentation patterns within patches of epibenthic structures: Combining field, flume and modelling experiments". In: *Continental Shelf Research* 27(8). Natural Coastal Mechanisms - Flume and Field Experiments on Links between Biology, Sediments and Flow, pp. 1020–1045. ISSN: 0278-4343. DOI: https://doi.org/10.1016/j.csr.2005.12.019. URL: http://www.sciencedirect.com/science/article/pii/S0278434306004055.

Callaghan, D., Bouma, T., Klaassen, P., Wal, D., Stive, M., and Herman, P. (Jan. 2010). "Hydrodynamic forcing on salt marsh development: distinguishing the relative importance of waves vs. tidal flow". In: *Estuarine Coastal and Shelf Science - ESTUAR COAST SHELF SCI*, pp. 73–88.

Dam, G. and Cleveringa, J. (2013). *De Rol van het Slib in de Sedimentbalans van de Westerschelde - Eindrapport*. Tech. rep. 1630. Rotterdam, The Netherlands: Svasek Hydraulics.

de Jonge, V.N., Essink, K., and Boddeke, R. (1993). "The Dutch Wadden Sea: a changed ecosystem". In: *Hydrobiologia* 265(1-3), pp. 45–71.

de Vet, P.L.M. (2020). "Intertidal Flats in Engineered Estuaries: On the Hydrodynamics, Morphodynamics, and Implications for Ecology and System Management". PhD thesis. TU Delft. DOI: 10.4233/uuid:2b392951-3781-4aed-b093-547c70cc581d.

Deltares (2018). *Building with Nature Guidelines*. URL: https://publicwiki.deltares.nl/display/BTG/Habitat+requirements+for+salt+marshes.

Dodo, T. and Warren, M. (1985). "Flood damage mitigation: a review of structural and nonstructural measures and alternative decision frameworks". In: *Water Resources Research* 21, pp. 411–424. DOI: 10.1029/WR021i004p00411.

Domburg, Tim van (2018). "Identifying Windows of Opportunity for Mangrove Establishment on a Mud Coast: A case study for the BioManCo project in Demak, Indonesia". In:

Ecoshape (2020). *Building with Nature Philosophy*. URL: https://www.ecoshape.org/en/the-building-with-nature-philosophy/five-basic-steps-for-generating-building-with-nature-designs/.

Ford, H., Garbutt, A., Ladd, C., Malarkey, J., and Skov, M.W. (2016). "Soil stabilization linked to plant diversity and environmental context in coastal wetlands". In: *Journal of Vegetation Science* 27(2), pp. 259–268. DOI: 10.1111/jvs.12367.

Healy, T.R. (2005). "Salt Marsh". In: *Encyclopedia of Coastal Science*. Springer Netherlands: Dordrecht, pp. 819–820. ISBN: 978-1-4020-3880-8. DOI: 10.1007/1-4020-3880-1_264. URL: https://doi.org/10.1007/1-4020-3880-1_264.

Herman, P.M.J., Villars, N., Winterwerp, H., van Kessel, T., Wang, Z., Briere, C., van Rijn, L., and Cleveringa, J. (2016). *Analyse Vaargeul Holwerd-Ameland - Eindrapport*. Tech. rep. 123078-05. Delft, The Netherlands: Deltares.

Holthuijsen, L.H. (2010). *Waves in Oceanic and Coastal Waters*. Cambridge University Press. ISBN: 9781139462525. URL: https://books.google.nl/books?id=7tFUL2blHdoC.

Horstman, E., Dohmen-Janssen, M., Narra, P., Van den Berg, N.J., Siemerink, M., Balke, T., Bouma, T., and Hulscher, S. (July 2012). "Wave attenuation in mangrove forests; field data obtained in trang, Thailand". In: vol. 1. DOI: 10.9753/icce.v33.waves.40.

Hu, Z., Van Belzen, J., Van Der Wal, D., Balke, T., Wang, Z. B., Marcel, S., and Bouma, T. J. (2015). "Windows of opportunity for salt marsh vegetation establishment on bare tidal flats: The importance of temporal and spatial variability in hydrodynamic forcing". In: *Journal of geophysical research : Biogeosciences* 120(7), pp. 1450–1469. ISSN: 2169-8953. DOI: 10.1002/2014JG002870.

Janssen, M. P. J. (2016). "Flood hazard reduction by mangroves." MA thesis. TU Delft.

Jonkman, S.N., Jorissen, R.E., Schweckendiek, T., and Bos, J.P. van den (2018). *Flood Defenses: Lecture notes*. 3rd Edition. TU Delft.

Kirwan, M. L., Guntenspergen, G. R., D'Alpaos, A., Morris, J. T., Mudd, S. M., and Temmerman, S. (2010). "Limits on the adaptability of coastal marshes to rising sea level". In: *Geophysical Research Letters* 37(23). DOI: 10.1029/2010GL045489.

Løvås, S. M. and Tørum, A. (Jan. 2000). "Effect of submerged vegetation upon wave damping and run-up on beaches: A case study on Laminaria Hyperborea". In: *Coastal Engineering 2000 - Proceedings of the 27th International Conference on Coastal Engineering, ICCE 2000* 276, pp. 851–864.

Luijendijk, A., Hagenaars, G., Ranasinghe, R., Baart, F., Donchyts, G., and Aarninkhof, S. (2018). "State of the World's Beaches". In: *Sci Rep* 8(6641). DOI: 10.1038/s41598-018-24630-6.

Massel, S R, Furukawa, K, and Brinkman, R M (Apr. 1999). "Surface wave propagation in mangrove forests". In: *Fluid Dynamics Research* 24(4), pp. 219–249. DOI: 10.1016/s0169-5983(98)00024-0. URL: https://doi.org/10.1016%2Fs0169-5983%2898%2900024-0.

Mazda, Y., Magi, M., Ikeda, Y., Kurokawa, T., and Asano, T. (Aug. 2006). "Wave reduction in a Mangrove forest dominated by Sonneratia sp". In: *Wetlands Ecology and Management* 14, pp. 365–378. DOI: 10.1007/s11273-005-5388-0.

McLaren, P. (1994). *Patterns of Sediment Transport in the Western Portion of the Westernschelde*. Tech. rep. Cambridge, United Kingdom: GeoSea Consulting.

Mcowen, C., Weatherdon, L., Bochove, J. W., Sullivan, E., Blyth, S., Zöckler, C., Stanwell-Smith, D., Kingston, N., Martin, C., Spalding, M., and Fletcher, S. (Mar. 2017). "A global map of saltmarshes". In: *Biodiversity Data Journal* 5, e11764. DOI: 10.3897/BDJ.5.e11764.

Mendez, F. and Losada, I.J. (Apr. 2004). "An empirical model to estimate the propagation of random breaking and nonbreaking waves over vegetation fields". In: *Coastal Engineering* 51, pp. 103–118. DOI: 10.1016/j.coasaleng.2003.11.003.

Montgomery, J. M., Bryan, K. R., Mullarney, J. C., and Horstman, E. M. (2019). "Attenuation of Storm Surges by Coastal Mangroves". In: *Geophysical Research Letters* 46(5), pp. 2680–2689. DOI: 10.1029/2018GL081636.

Narayan, S., Beck, M. W., Reguero, B. G., Losada, I. J., van Wesenbeeck, B., Pontee, N., Sanchirico, J. N., Ingram, J. C., Lange, G. M., and Burks-Copes, K. A. (2016). "The Effectiveness, Costs and Coastal Protection Benefits of Natural and Nature-Based Defences." In: *PLoS ONE* 11. DOI: 10.1371/journal.pone.0154735.

Plieger, R. (2015). *Roosterschematisatie Zuidwestelijke Delta (Deel 2)*. Deltares.

Quang Bao, Tran (2011). "Effect of mangrove forest structures on wave attenuation in coastal Vietnam". In: *Oceanologia* 53(3), pp. 807–818. ISSN: 0078-3234. DOI: https://doi.org/10.5697/oc.53-3.807. URL: http://www.sciencedirect.com/science/article/pii/S0078323411500259.

Quartel, S., Kroon, A., Augustinus, P.G.E.F., Van Santen, P., and Tri, N.H. (2007). "Wave attenuation in coastal mangroves in the Red River Delta, Vietnam". In: *Journal of Asian Earth Sciences* 29(4). Morphodynamics of the Red River Delta, Vietnam, pp. 576–584. ISSN: 1367-9120. DOI: https://doi.org/10.1016/j.jseaes.2006.05.008. URL: http://www.sciencedirect.com/science/article/pii/S1367912006001672.

Rupprecht, F., Möller, I., Paul, M., Kudella, M., Spencer, T., van Wesenbeeck, B.K., Wolters, G., Jensen, K., Bouma, T.J., Miranda-Lange, M., and Schimmels, S. (2017). "Vegetation-wave interactions in salt marshes under storm surge conditions". In: *Ecological Engineering* 100, pp. 301–315. DOI: https://doi.org/10.1016/j.ecoleng.2016.12.030.

Schroevers, M., Huisman, B., van der Wal, M., and Terwindt, J. (Mar. 2011). "Measuring ship induced waves and currents on a tidal flat in the Western Scheldt estuary". In: DOI: 10.1109/CWTM.2011.5759539.

Silinski, A., Heuner, M., Troch, P., Puijalon, S., Bouma, T., Schoelynck, J., Schröder, U., Fuchs, E., Meire, P., and Temmerman, S. (2016a). "Effects of contrasting wave conditions on scour and drag on pioneer tidal marsh plants". In: *Geomorphology* 255.

Silinski, A., van Belzen, J., Fransen, E., Bouma, T., Troch, P., Meire, P., and Temmerman, S. (2016b). "Quantifying critical conditions for seaward expansion of tidal marshes: A transplantation experiment". In: *Estuarine, Coastal and Shelf Science* 169, pp. 227–237. ISSN: 0272-7714. DOI: 10.1016/j.ecss.2015.12.012. URL: www.sciencedirect.com/science/article/pii/S0272771415301694.

Silinski, A., Fransen, E., Bouma, T., Meire, P., and Temmerman, S. (2016c). "Unravelling the controls of lateral expansion and elevation change of pioneer tidal marshes". In: *Geomorphology* 274, pp. 106–115. ISSN: 0169-555X. DOI: 10.1016/j.geomorph.2016.09.006. URL: www.sciencedirect.com/science/article/pii/S0169555X16308200.

Silinski, A., Heuner, M., Schoelynck, J., Puijalon, S., Schröder, U., Fuchs, E., Troch, P., Bouma, T., Meire, P., and Temmerman, S. (2015). "Effects of Wind Waves versus Ship Waves on Tidal Marsh Plants: A Flume Study on Different Life Stages of Scirpus maritimus". In: *PLOS ONE* 10. DOI: 10.1371/journal.pone.0118687.

Songy, G. (2016). "Wave attenuation by global coastal salt marsh habitats." MA thesis. TU Delft.

Soulsby, Richard (1997). *Dynamics of marine sands: A manual for practical applications*. T. Telford London.

Thomas, N., Bunting, P., Lucas, R., Hardy, A., Rosenqvist, A., and Fatoyinbo, L. (Sept. 2018). "Mapping Mangrove Extent and Change: A Globally Applicable Approach". In: *Remote Sensing* 10. DOI: 10.3390/rs10091466.

UNDRR (2016). *Report of the open-ended intergovernmental expert working group on indicators and terminology relating to disaster risk reduction*. United Nations Office for Disaster Risk Reduction.

van der Nat, A., Vellinga, P., and van Slobbe, E. (2016). "Ranking coastal flood protection designs from engineered to nature-based". In: *Ecological Engineering* 87, pp. 80–90. DOI: 10.1016/j.ecoleng.2015.11.007.

van Duin, W. E. and Dijkema, K. S. (2012). "Randvoorwaarden voor kwelderontwikkeling in de Waddenzee en aanzet voor een kwelderkansenkaart." In: *Wageningen University Research*.

van Rijn, L. (2020). "Literature review of critical bed-shear stresses for mud-sand mixtures". In: URL: http://www.leovanrijn-sediment.com..

van Wesenbeeck, B., van De Koppel, J., Herman, P., and Bouma, T. (2008). "Does scale-dependent feedback explain spatial complexity in salt-marsh ecosystems?" In: *Oikos* 117(1), pp. 152–159. DOI: 10.1111/j.2007.0030-1299.16245.x.

van Zelst, V. T. M. (2018). "Global flood hazard reduction by foreshore vegetation." MA thesis. TU Delft.

Vlaams Instituut voor de Zee (2012). *Salt marsh zonation*. [Online; accessed July, 2020]. URL: http://www.vliz.be/wiki/Bestand:Figure_salt-marsh_zonation.JPG.

Vuik, V., Jonkman, S.N., Borsje, B.W., and Suzuki, T. (2016a). "Nature-based flood protection: The efficiency of vegetated foreshores for reducing wave loads on coastal dikes". In: pp. 42–56. DOI: 10.1016/j.coastaleng.2016.06.001.

Vuik, V., Jonkman, S.N., and van Vuren, S. van (2016b). "Nature-based flood protection: using vegetated foreshores for reducing coastal risk". In: *E3S Web of Conferences* 7, p. 13014. DOI: 10.1051/e3sconf/20160713014.

Vuik, V., Suh Heo, H.Y., Zhu, Z., Borsje, B.W., and Jonkman, S.N. (2018a). "Stem breakage of salt marsh vegetation under wave forcing: A field and model study". In: *Estuarine, coastal and shelf science* 200, pp. 41–58. DOI: 10.1016/j.ecss.2017.09.028.

Vuik, V., van Vuren, S., Borsje, B.W., van Wesenbeek, B.K., and Jonkman, S.N. (2018b). "Assessing safety of Nature-based Flood Defenses: dealing with extremes and uncertainties". In: *Coastal Engineering* 139, pp. 47–64. DOI: 10.1016/j.coastaleng.2018.05.002.

Wamsley, T., Cialone, M. A., Smith, J. M., Atkinson, J. H., and Rosati, J. D. (2010). "The potential of wetlands in reducing storm surge". In: *Ocean Engineering* 37(1). A Forensic Analysis of Hurricane Katrina's Impact: Methods and Findings, pp. 59–68. ISSN: 0029-8018. DOI: https://doi.org/10.1016/j.oceaneng.2009.07.018.

Willemsen, P., Borsje, B., Vuik, V., Bouma, T., and Hulscher, S. (2020). "Field-based decadal wave attenuating capacity of combined tidal flats and salt marshes". In: *Coastal Engineering* 156, p. 103628. DOI: https://doi.org/10.1016/j.coastaleng.2019.103628.

Woodruff, J., Irish, J., and Camargo, S. (2013). "Coastal flooding by tropical cyclones and sea-level rise". In: *Nature* 504, pp. 44–52. DOI: 10.1038/nature12855.

Wu, W. and Cox, D. (Aug. 2015). "Effects of wave steepness and relative water depth on wave attenuation by emergent vegetation". In: *Estuarine Coastal and Shelf Science* 164, pp. 443–450. DOI: 10.1016/j.ecss.2015.08.009.

Yang, S., Shi, B., Bouma, T., Ysebaert, T., and Luo, X. X. (Jan. 2011). "Wave Attenuation at a Salt Marsh Margin: A Case Study of an Exposed Coast on the Yangtze Estuary". In: *Estuaries and Coasts* 35, pp. 169–182. DOI: 10.1007/s12237-011-9424-4.

Young, I. and Verhagen, H.J. (Dec. 1996). "The growth of fetch limited waves in water of finite depth. Part 1: Total energy and peak frequency". In: *Coastal Engineering* 27, pp. 47–78. DOI: 10.1016/S0378-3839(96)00006-3.

Yuan, L., Chen, Y., Wang, H., Cao, H., Zhao, Z., Tang, C., and Zhang, L. (2020). "Windows of opportunity for salt marsh establishment: the importance for salt marsh restoration in the Yangtze Estuary". In: *Ecosphere* 11(7). DOI: 10.1002/ecs2.3180.

Zhu, Q., van Prooijen, B.C., Wang, Z.B., Ma, Y.X., and Yang, S.L. (2016). "Bed shear stress estimation on an open intertidal flat using in situ measurements". In: *Estuarine, Coastal and Shelf Science* 182, pp. 190–201. ISSN: 0272-7714. DOI: https://doi.org/10.1016/j.ecss.2016.08.028. URL: http://www.sciencedirect.com/science/article/pii/S0272771416302839.

Zhu, Z., Vuik, V., Visser, P.J., Soens, T., van Wesenbeeck, B., van de Koppel, J., Jonkman, S.J., Temmerman, S., and Bouma, T. (2020). "Historic storms and the hidden value of coastal wetlands for nature-based flood defence". In: *Nature Sustainability*. DOI: 10.1038/s41893-020-0556-z.

A

Validation: wave growth formulas

Modelling of waves propagating towards the observation sites was performed by means of the wave growth formula proposed by Young et al. (1996), presented in Equation A.1. This approximation of wave height growth was selected due to the fact that this equation was determined by measurements performed in Lake George, a water body characterized by fetch limited and finite depth conditions (Young et al., 1996). These characteristics were considered to approach the conditions found in the Western Scheldt (mostly fetch limited, partly depth limited on the mudfalts) and the Wadden Sea (mostly depth limited).

$$H_s = \frac{U_{10}^2}{g} \cdot \tilde{H}_\infty \left\{ \tanh\left(0,493\tilde{d}^{0,75}\right) \cdot \tanh\left(\frac{3,13 \cdot 10^{-3} \tilde{F}^{0,57}}{\tanh\left(0,493\tilde{d}^{0,75}\right)} \right) \right\}^{0,87} \tag{A.1}$$

Nonetheless, the modelled wave occurrence was validated with actual measurements gathered from previous research done along transects in Hellegat in the Western Scheldt (Vuik et al., 2016a), and in Groningen in the Wadden Sea (Vuik et al., 2018a). Considering that the measured data dates from the years 2015 and 2017 (Hellegat and Groningen, respectively), water level and wind data from the same period was retrieved in order to assess the validity of the complete wave height modelling steps described in Chapter 3. Finally, the data measured at the marsh edges was compared to the modelled data, and the results are presented in Figures A.1 and A.2.

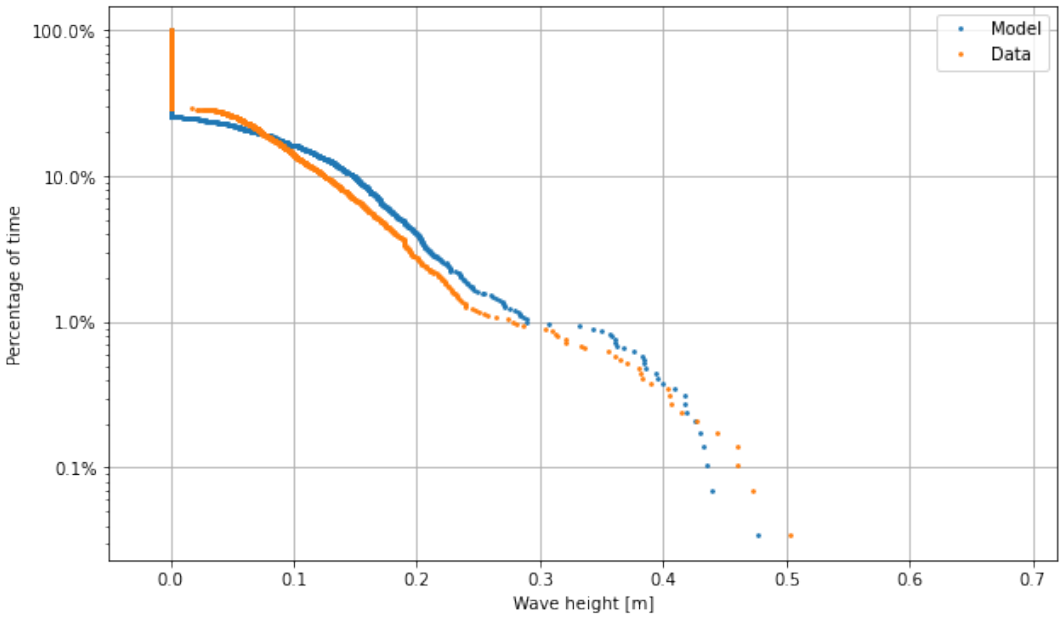

Figure A.1: Validation of modelled wave heights by means of wave growth formula. Actual data was retrieved from previous measurements on the marsh edge along a transect on the Hellegat salt marsh (WS) during the months April-July 2015.

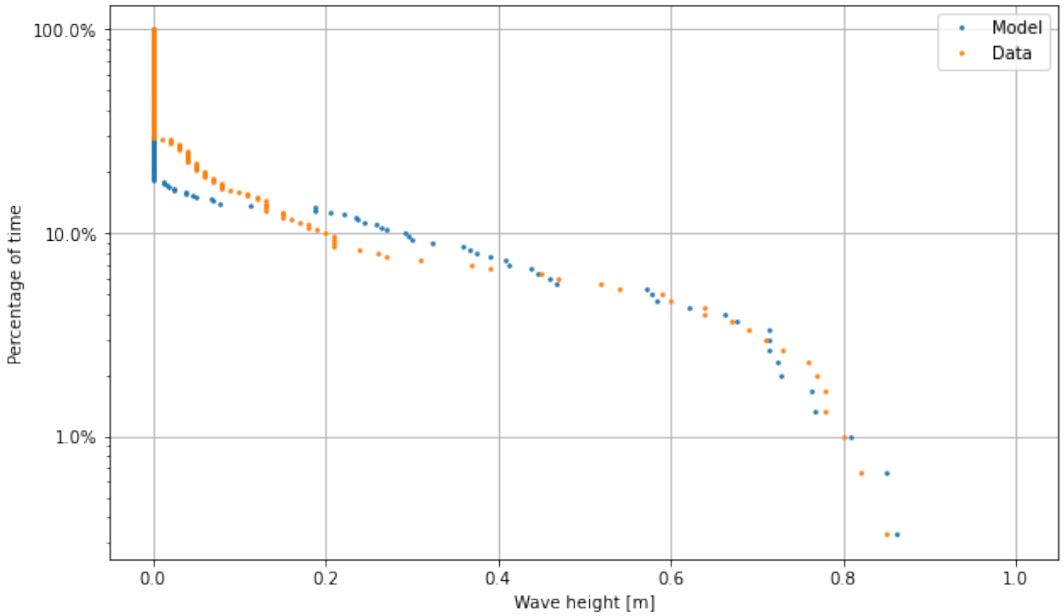

Figure A.2: Validation of modelled wave heights by means of wave growth formula. Actual data was retrieved from previous measurements on the marsh edge along a transect on the Groningen salt marsh (WZ) during the month of January,2017.

The Figures above show that the modelled wave heights approach the measured data. This check can be performed visually or analytically. The latter assessment was performed by means of the Root Mean Squared Error (RMSE) statistical tool, which provides an absolute measure of fit between observed and modelled data. RMSE values of $0.01m$ and $0.03m$ were computed from the analysis performed in Hellegat and Groningen, respectively. It is worth noting that these low RMSE values are due to the agreement between modelled and measured data with respect to the dry period at the marsh edge, which falls between an approximate range of 70% to 80% of the time.

Nonetheless, some inaccuracies can also be pointed out by the results, such as that the modelled wave heights can be slightly overestimated at lower probabilities of occurrence. However the larger wave heights measured at both locations, which are found at the lower probabilities of occurrence, are modelled with a slight variability. These results show that the approach used to model the occurrence of wave heights in both water systems (consisting of wind speed and wind direction time series; water level time series generation by means of triangular interpolation; and wave growth limitation at the output location by 40% of the water depth) can fairly well represent actually occurring wave attack at each location.

B

Case studies: Marsh edge points

The analysis conducted regarding the habitat suitability analysis in this thesis is based on data retrieved from the salt marsh edge (with the exception of the flow velocity analysis). Such location was defined as the seaward limit at each study site where a distinction can be made between salt marsh vegetation and the mud flat fronting it (transition zone). In order to account for some of the spatial variability of this transition zone, several observation points along the marsh edge at each mature salt marsh site were selected from Google Earth satellite imagery, and are presented in the following Appendix.

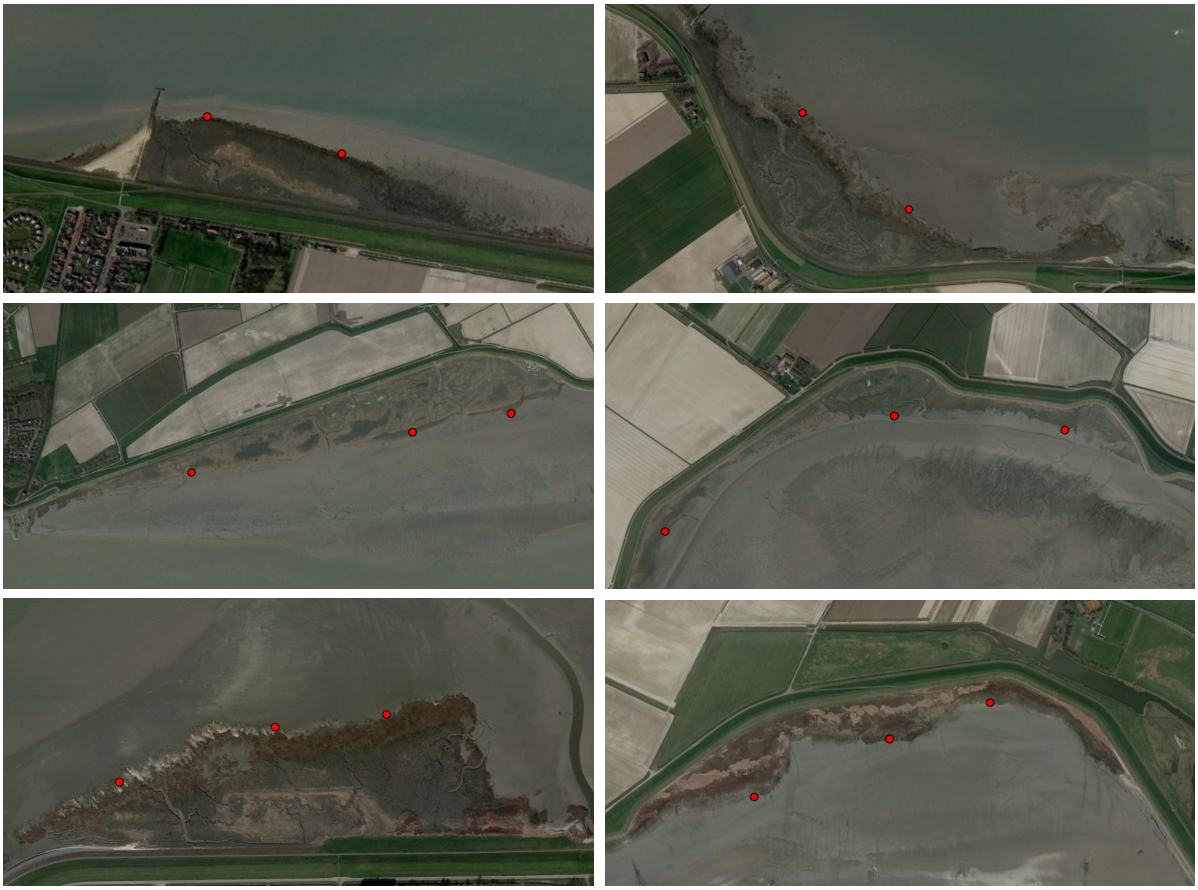

Figure B.1: Marsh edge points selected at mature salt marsh locations in the Western Scheldt. Computations of the inundation-free period were performed with respect to these points.

Figure B.2: Marsh edge points selected at mature salt marsh locations in the Wadden Sea. Computations of the inundation-free period were performed with respect to these points.